Manipulating aqueous chemistry environments in extractive metallurgy

Thesis presented for the Degree of

Master of Science

in the Department of Chemical Engineering

UNIVERSITY OF CAPE TOWN

by

Premesh Govan

May 2010

Crystallization & Precipitation Unit

Acknowledgements

I acknowledge the staff and students of the Department of Chemical Engineering at the University of Cape Town, for their assistance and guidance throughout the duration of my postgraduate studies. In particular, I would like to thank Professor A.E. Lewis for her enthusiasm, assistance and supervision, as well as Mr. Jeeten Nathoo for co-supervising this project.

I acknowledge the staff and students of the Crystallisation and Precipitation Unit of the Department of Chemical Engineering for their valuable assistance, support and constructive advice.

A special thanks to Anglo Research for the opportunity to be a part of their novel and innovative process.

On a personal note, to my parents and sister for their encouragement and moral support, as well as all my friends who have been understanding, patient and a source of inspiration over the past few years.

Synopsis

The Anglo Research Nickel (ArNi) process is a novel extractive metallurgical process that arose out of the need to develop a processing route for the recovery of nickel from lateritic ore deposits that is both economical and environmentally acceptable. Kieserite ($MgSO_4 \cdot H_2O$) crystallisation is a critical step in the process which leads to the regeneration of reagents (HCl, H_2SO_4 and MgO). Hence, the regeneration of reagents is dependent on the amount of magnesium sulphate that precipitates out within the limits of the operating conditions. These conditions include temperature and the ion-interactions of the background aqueous environment. Hence, by manipulating these parameters the optimal region and hence, operating conditions where the minimum solubility of the solute lies can be identified.

This novel ArNi process demonstrates the power of manipulating aqueous chemical environments in order to regenerate reagents and hence, develop more sustainable processes. Thus, the ArNi process has provided the building blocks to reinventing the way mining processes are designed, implemented and perceived. Therefore, in order to develop a broader understanding of how aqueous environments can be manipulated in order to process different types of ores, the solubility of NaCl in hypersaline brines was also investigated as a 2nd model system.

Temperature and ion interactions are the most important factors affecting both the solubility of slightly soluble magnesium sulphate, and highly soluble sodium chloride salts, as well as for the type of hydrate formed. However, there is a lack of data for the thermodynamic properties of these salts in multi-component systems, especially their solubilites at high temperatures. Thus, there is scope for the development of a better understanding of the ion interactions in multi-component systems under different aqueous environments and temperature conditions, and how these affect the precipitated solute.

To achieve the objectives of the study, experiments were conducted in 450 ml glass reactors. The desired operating temperatures were attained using heating bands and maintained with temperature controllers. Spiral reflux condensers were fitted to condense any vapour that evolved and ensure that the volume of solvent remained constant. Face-centred central composite designs and central composite factorial

designs were adopted for the $FeCl_3$-$MgCl_2$-HCl-$MgSO_4$-H_2O and $ZnCl_2$-HCl-NaCl-H_2O systems respectively. The factors that were varied were the concentrations of $FeCl_3$, $MgCl_2$ and HCl for the $FeCl_3$-$MgCl_2$-HCl-$MgSO_4$-H_2O system at 105˚C and the concentrations of $ZnCl_2$ and HCl at temperatures of 40˚C, 80˚C and 107˚C for the $ZnCl_2$-HCl-NaCl-H_2O system. The measured responses were the solubility of $MgSO_4$ and NaCl. Characterisations of the hydrates of $MgSO_4$ that formed under different aqueous environments were also established for the $FeCl_3$-$MgCl_2$-HCl-$MgSO_4$-H_2O system.

$FeCl_3$-$MgCl_2$-HCl-$MgSO_4$-H_2O system

Statistical analysis of each of the factorial phases established that a second order model best fits the experimental data and accounts for 98.3%, 96.1% and 98.3% of the variation in the solubility of $MgSO_4$. Within each phase, $MgCl_2$ concentration had the most significant effect on the solubility of $MgSO_4$ of all the varied factors. $MgCl_2$ suppressed the solubility of $MgSO_4$ due to the presence of the common Mg^{2+} ion. HCl had the opposite effect on the solubility of $MgSO_4$ i.e. increasing the concentration of HCl resulted in an increase in the solubility of $MgSO_4$ due to an increase in ionic strength. At low concentrations of $MgCl_2$ and HCl, increasing the concentration of $FeCl_3$ decreased the solubility of $MgSO_4$ due to the bond formation between SO_4^{2-} ions and ferric hydroxyl complexes. At high concentrations of $MgCl_2$ and HCl, increasing the concentration of $FeCl_3$ had a minimal effect on the solubility of $MgSO_4$.

$MgSO_4 \cdot H_2O$ precipitated independently or with a combination of $MgSO_4 \cdot 1.25H_2O$ or $MgSO_4 \cdot 6H_2O$ at each of the different concentration limits of $MgCl_2$, $FeCl_3$ and HCl. The $FeCl_3$ factor did not have an influence on the hydrate or hydrates that formed. However, the presence of $MgCl_2$ and HCl had a dehydrating action on the formation of the hydrates with HCl having a more pronounced effect.

$ZnCl_2$-HCl-NaCl-H_2O system

Statistical analysis of the central composite factorial designs at each of the temperatures investigated, found that a linear order model best fits the experimental data and accounted for 69.1%, 62.7% and 55.1% of the variation in the solubility of NaCl. The concentration of $ZnCl_2$ had the most pronounced influence on the solubility of NaCl. An increase in the concentration of $ZnCl_2$ increased the solubility of NaCl on account of the

formation of homo-polar bonds which decreases the ionization of the solution. The increase in the concentration of HCl decreased the solubility of NaCl. The effect of temperature did not have a significant effect on the solubility of NaCl because of the flat solubility line.

The findings in this study have shown that ion interactions play a crucial role in the solubility of salts in hypersaline brines. In addition, each ion has a different effect (common ion effect, ionic strength effects or complex formation) on the solubility of a specific salt and is unique to its individual system. Thermodynamic modelling can predict salt solubility trends. However, in order to gain a fundamental understanding of a system, especially complex systems, experimental measurements are a necessity.

The experimental measurements provide an in-depth understanding of specific systems which can lead to the manipulation of aqueous environments towards the development of more sustainable processes and hence, a whole new approach to extractive metallurgy.

Table of Content

List of Figures

List of Tables

Chapter 1. Introduction

1.1 Background Information

Minerals constitute a small but essential part of world production and trade, hence their supply is critical for infrastructural development within emerging markets as well as for the sustainable development of modern economies. Nickel ranks as the 6th (Dalvi *et al.*, 2004) most sought after mineral as it is one of the key components in steel. The demand for nickel has increased since the 1950's at an average rate of 4% per year. It is expected to rise to 51% by 2012 due to the expansion of emerging markets, especially China which accounts for 70% of the growth in demand worldwide.

The majority of nickel production, in the past, has come from sulfidic ores and accounts for 58% of primary nickel production. However, the demand of nickel has exceeded the replenishment rate of sulfide reserves. Thus, the future growth of nickel production is expected to come from laterite ores of nickel which account for 70% of world land based nickel reserves. However, due to technological challenges and low purity levels they have not been seen as sustainable and economically viable. The demand over the past decade, Figure 1.1, has seen nickel stocks being depleted, leading to a nickel price increase. The projected nickel price in the future is predicted to be adequate to provide a reasonable rate of return. Thus, overcoming major economic hurdles and providing the impetus for the development of technologically innovative ways of processing low grade lateritic ores.

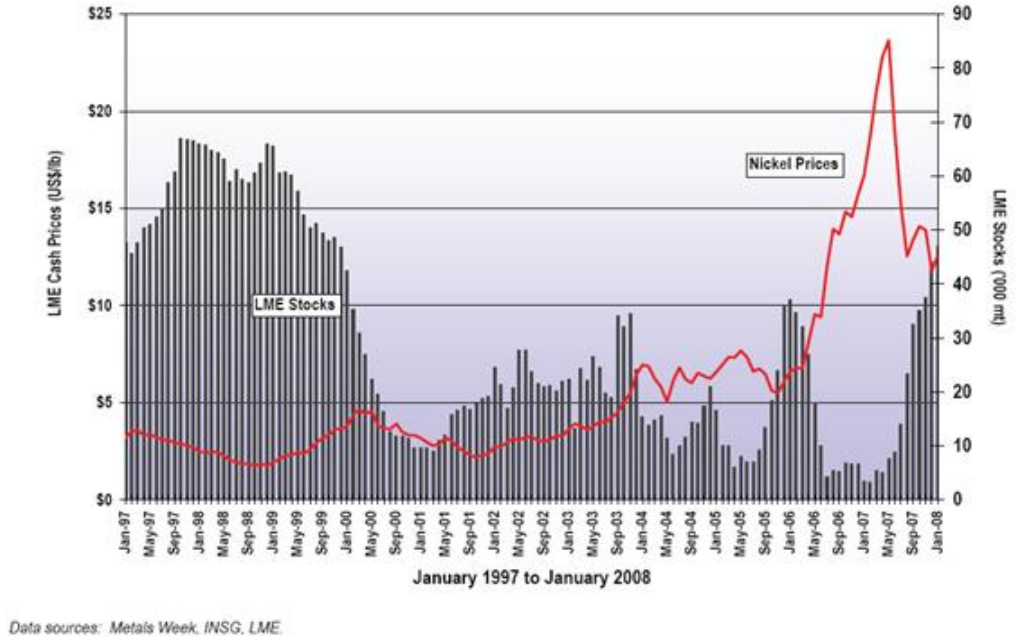

Figure 1.1: LME cash nickel prices and LME stocks, 1997-2008 (adopted from Metals week, INSG, LME)

1.2 Environmental concerns within the mining industry

The major environmental problems that concern post-mining base-metal production are solid waste production, gaseous emissions and high energy use. Most present solutions for environmental problems are available. However, in practice, they are scarcely implemented because the established production technology in the base metals industry is made up of mature technologies that are hard to change. Hence, the environmental performance of the minerals processing industry is driven strongly by technology design and operation.

Currently laterite processing routes, high pressure acid leaching (HPAL), carbon and smelting processes, incur large energy requirements as well as using reagents inefficiently. The existing laterite processes are bottlenecked with respect to brown field projects due to technological constraints and large power requirements for processing low grade ores.

The demand for nickel as well as the environmental concerns have motivated for the development of a process route for the recovery of nickel from lateritic ore deposits that

is both economical and environmentally acceptable. In the light of these concerns the ArNi – Anglo Research Nickel Process was developed.

1.3 Process description

The process, shown in Figure 1.2, introduces a new generic approach in optimising reagent and energy use where the crystallization step forms the heart of the process. The crystallization is carried out using sulphuric acid to precipitate magnesium sulphate according to equation [1-1].

$$MgCl_{2(aq)} + H_2SO_{4(aq)} + xH_2O \rightarrow MgSO_4.xH_2O + 2HCl_{(aq)} \quad [1\text{-}1]$$

The regenerated acid is recycled and used to leach the ore in the leaching step. The precipitated salt is thermally decomposed as shown in equation [1-2]. The metal oxide is used as the neutralising agent in the neutralisation step, while the SO_2 gas that is evolved is sent to acid regeneration and recycled back to the crystalliser.

$$MgSO_4.xH_2O_{(s)} \rightarrow MgO_{(s)} + SO_{2(g)} + xH_2O_{(g)} \quad [1\text{-}2]$$

The regeneration of reagents is dependent on the amount of magnesium sulphate that has precipitated out. Thus, it is important to maximise the yield of magnesium sulphate formed. Therefore, the minimum solubility needs to be determined within the limits of the given operational conditions. These conditions include temperature and the ion-interactions of the background aqueous environment.

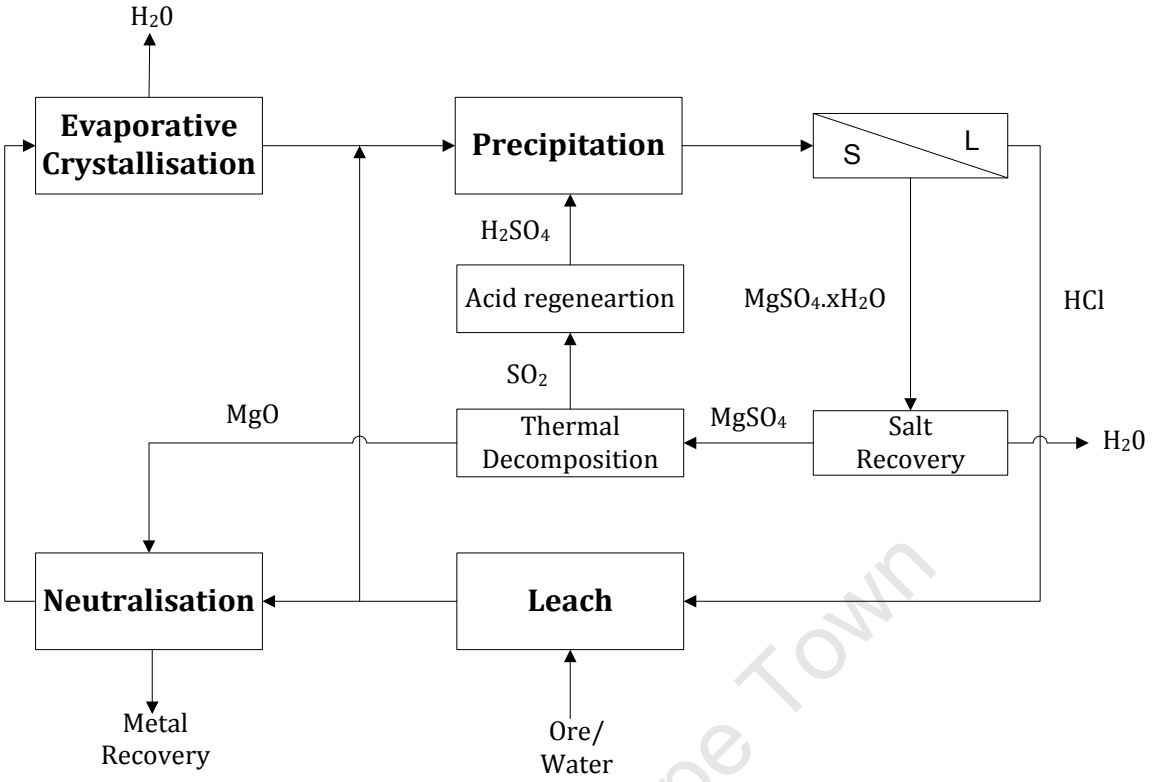

Figure 1.2: Simplified block flow diagram of the ArNi process

The ArNi process has addressed major problems within the mining industry by providing the building blocks to reinventing the way mining processes are designed, implemented and perceived. This may lead to the investigation of different ways of processing various ores. This can be promoted by finding innovative ways of manipulating the aqueous chemical environment to regenerate reagents and develop more sustainable extractive metallurgical processes. Hence, the solubility of NaCl in hypersaline brines was investigated as a 2nd model system.

1.4 Solubility

Solubility studies focus mainly on the effects of temperature and ion-interactions on the thermodynamic properties of the substance involved. These properties include the activity and ionic strength of the solutes, the Gibbs Free Energy, chemical potential and solubility products. Thermodynamics provide a basis for these properties which allow solubilites to be calculated, as well as providing valuable relationships between thermodynamic properties and other measurable properties of the substance involved.

In many cases, the problem of the solubility of salts in ternary and multi-component systems is that there is insufficient data to evaluate the thermodynamic properties.

1.4.1 Solubility of Magnesium Sulphate

There is a lack of data for the thermodynamic properties of magnesium sulphate, especially in multi-component systems. Experimental data is thus needed to evaluate the thermodynamic properties to determine the solubility of the salt as a function of temperature as well as in the presences of other solutes in solution. The hydrates of magnesium sulphate are one of the most important minerals formed as a result of sediment formation (Hardie, 1991). Magnesium sulphate exists in the form $MgSO_4 \cdot nH_2O$ where n has values (1, 2, 3, 4, 5, 6, 7, and 11) (Archer and Rard, 1998; Genceli *et al.*, 2007). Studies conducted by Apelblat and Manzurola (2003) reported that the stable hydrates of magnesium sulphate are $MgSO_4 \cdot 6H_2O$ and $MgSO_4 \cdot 7H_2O$ with the transition temperature being approximately 48˚C, above which $MgSO_4 \cdot H_2O$ is the stable hydrate. It is thus important to determine which conditions (temperature, ionic strength and the aqueous composition of the bulk solution) will favour the formation of the preferred hydrate.

1.4.2 Solubility of Sodium Chloride

The NaCl-H_2O binary system has been extensively studied with over 100 investigations over the last century. Although it has been studied over a wide range of temperatures and pressures, the studies have predominantly been carried out at atmospheric pressure. Earlier studies at elevated pressures exceeding 50 MPa were conducted by Möller (1862), Cohen (1910) and Sill (1916). A consolidated piece of work by Sawamura *et al.* (2007) provides a global overview of the solubility of the NaCl-H_2O binary system at elevated pressures. Figure 1.3 below summaries the work that has been conducted over the past 100 years.

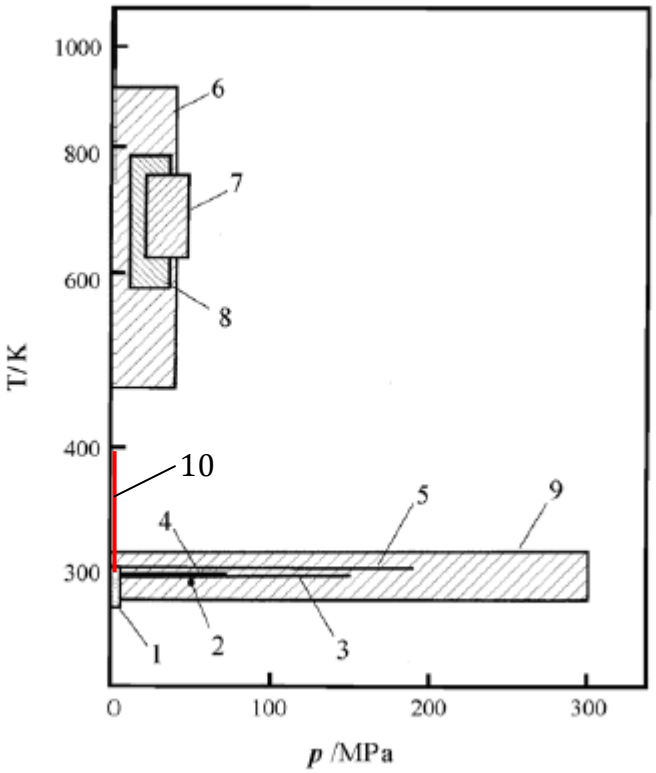

Figure 1.3: Diagram of current solubility data for sodium chloride in water. (1) Möller (1862); (2) Von Stackelberg (1896); (3) Cohen and Sinnige (1910); (4) Sill (1910); (5) Adams and Hall (1931); (6) Keevil (1942); (7) Olander and Liander (1950); (8) Bischoff et al. (1986); (9)Sawamura et al. (2007)

It is nonetheless important to note that, whilst the system under investigation is not a binary system, it falls within a region where limited studies on the binary system have been carried out, marked as (10) in Figure 1.3.

1.5 Problem statement

Temperature and ion interaction are the most important factors affecting both the solubility of slightly soluble magnesium sulphate, and highly soluble sodium chloride, salts as well as for the type of hydrate formed. However, there is a lack of data for the thermodynamic properties of these salts in multi-component systems, especially their solubilites at high temperatures. Thus, it is required to develop a better understanding of the ion interactions in multi-component systems, under different aqueous environments and temperature conditions, and how they affect the precipitated solute.

1.6 Objectives

In this study the main objectives are:

- To investigate the solubility of magnesium sulphate and sodium chloride in multi-component systems as a function of temperature;
- To characterise which hydrates of magnesium sulphate are formed under certain conditions;
- To characterise all crystallising salts.

References

Apelblat, A., Manzurola, E. (2003). Solubilities and vapour pressures of saturated aqueous solutions of sodium tetraborate, sodium carbonate, and magnesium sulfate and freezing-temperature lowerings of sodium tetraborate and sodium carbonate solutions , J. Chem. Thermodynamics, 35, p221–238.

Archer, D., Rard, G. Joseph, A. (1998). Isopiestic Investigation of the Osmotic and Activity Coefficients of Aqueous $MgSO_4$ and the Solubility of $MgSO_4 \cdot 7H_2O$ at 298.15K: Thermodynamic properties of the $MgSO_4 + H_2O$ System to 440K. Journal of Chemical Engineering Data 43(5), p791-806.

Cohen, E., Inouye, K., Euwen, C.Z. (1910). Physical Chem. 75. 257.

Dalvi, A.D., Bacon, W.G., Osborne, R.C. (2004). The Past and the Future of Nickel Laterites. In: Inco limited, The Prospectors and Developers Association of Canada PDAC 2004 International Convention.Toronto, Canada March 7-10, 2004.

Hardie, L.A. (1991). On the significance of evaporates, Annual Review Earth Planet Science, 19, p131-168.

Genceli, F.E., Lutz, M., Spek, A.L., Witkamp, G., (2007). Crystallization and characterization of a new Magnesium Sulfate hydrate-MgSO4·11H2O. Journal of Crystal Growth and Design. 7(12), p2460-2466.

Möller, K. (1862). The influence of the presence on the solubility of some salts. Ann. Physical Chem.117. 386.

Sawamura, S., Egoshi, N., Setoguchi, Y., Matsuo, H. (2007). Solubility of sodium chloride in water under high pressure. Fluid Phase Equilibria, 254. p158-162.

Sill, H. (1916). The influence of Pressure on Solubility. J Am Chem. Soc. 38. 2632.

Chapter 2. Theory and Literature Review

2.1 Thermodynamic of Crystallization

2.1.1 Basic relationships

An ideal solution is assumed when all interacting components, all dissolved substances as well as the solvent, do not influence each other. Thus, the activities of the components are equal to their concentration. However, this is not the case when considering a real solution due to the interaction between the components. Hence, the activity of each component is expressed as a product of the concentration and the activity coefficient (γ_m). The activity coefficient represents the deviation from ideality at a given concentration.

$$a_m = m\gamma_m \quad [2\text{-}1]$$

where m is the molality. Assuming that the dissolved components are electrolytes that dissociates in a single solvent into cations and anion, equation [2.1] is then represented by the relationship between the mean ionic activity ($a_\pm$) and the mean ionic activity coefficient ($\gamma_\pm$), as shown in equation [2.2].

$$a_m = a_{\pm.m}^{v} = (Qm\gamma_{\pm.m})^{v} \quad [2\text{-}2]$$

Where

$$Q = (v_+^{v+} v_-^{v-})^{\frac{1}{v}} \quad [2\text{-}3]$$

And

$$v = v_+ + v_- \quad [2\text{-}4]$$

where ν is the number of moles of ions in 1 mole of electrolyte. For non-electrolyte, ν=1 (Mullin, 2001).

The activity coefficients of individual ions cannot be independently determined. Thus, the notion that an electrolyte in solution is composed of ions which all pose the same average mean ionic coefficient ($y_\pm$) or mean activity ($a_\pm$) is introduced.

$$\gamma_\pm = (\gamma_+^{v+} \gamma_-^{v-})^{\frac{1}{v}}$$

$$a_{\pm} = (a_{+}^{v+} a_{-}^{v-})^{\frac{1}{v}} \quad [2\text{-}5]$$

2.1.2 Chemical potential

The chemical potential of a system, where the volume and entropy are fixed, is a measure of the change in energy to the system if an additional particle were introduced. If the system contains more than one component the chemical potential on the ith component is represented by equation [2-6]:

$$\mu_i = \mu_i^o + RTlna_i \quad [2\text{-}6]$$

where μ_i^o is the chemical potential of the ith component in the standard state and a_i represents the activity of the ith component. Representing the chemical potential as a measure of the mean activity, equation [2-2] is introduced into equation [2-6] to obtain equation [2-7].

$$u_{i,m} = u_{i,m}^o + vRTln(Qm\gamma_{\pm,m}) \quad [2\text{-}7]$$

To accurately determine the chemical potential of the ith component with respect to equation [2-7] a suitable standard state has to be defined. The standard state for the solvent is usually chosen as the state of the pure substance at the temperature and pressure of the system. Unit concentration is chosen for the dissolved substance where is has a unit activity coefficient at all pressures and temperatures. It can now be established that for the activity coefficient, partial molar heat capacity, partial molar enthalpy and partial molar volume of the substance in the standard solution, that the values of these quantities are the same in an infinitely dilute solution.

The activity coefficients reported in literature are based on the assumption that the substance dissociates completely in the solutions, giving v ions. These activity coefficients are called stoichiometric coefficients. However, if the electrolyte in the solution is only partially dissociated then equation [2-2] becomes:

$$(Qm\gamma_{\pm})^v = (Qm\gamma'_{\pm}\alpha')^v = \gamma' mK_m(1-\alpha') \quad [2\text{-}8]$$

where α' is the degree of dissociation, $\gamma'_{\pm}$ the mean ionic activity coefficient which takes dissociation into account, γ' is the activity of the molecules that did not dissociate, m is

the overall molality of the solution and K_m is the equilibrium dissociation constant (Sohnel and Garside, 1992).

2.1.3 Osmotic coefficient

The osmotic coefficient, represented in equation [2-9], is introduced as a more sensitive function of the concentration than the activity coefficient. The activity coefficient of the solvent only deviates slightly, from unity in non-ideal solutions.

$$\varphi = -\frac{1000}{vmM_1} lna_1 \qquad [2\text{-}9]$$

where M is the molar mass of solvent. The Gibbs-Duhem equation, for a binary solution, gives the relationship between the osmotic coefficient of the solution and the activity coefficient of the dissolved substance and is shown in equation [2-10]:

$$\left(\frac{1000}{M_1}\right) dlna_1 + vmdln\left(Qm\gamma_{\pm,m}\right) = 0 \qquad [2\text{-}10]$$

Substituting equation [2-9] into equation [2-10] and integrating, equation [2-11] is obtained.

$$\varphi = 1 + \frac{1}{m}\int_0^m mdln\gamma_{\pm,m} \qquad [2\text{-}11]$$

2.1.4 The effect of temperature on the activity coefficient and osmotic coefficient

The temperature dependence of the activity coefficient is determined by dividing equation [2-7] by temperature and then differentiating with respect to temperature at constant pressure.

$$\left(\frac{\partial ln\gamma_{\pm,m}}{\partial T}\right)_{P.m_{j\neq i}} = -\frac{\overline{H_i} - \overline{H_i^{\infty}}}{RT^2} \qquad [2\text{-}12]$$

And for the solvent

$$\left(\frac{\partial lna_1}{\partial T}\right)_{P.m_1} = -\frac{\overline{H_1} - H_1^o}{RT^2} \qquad [2\text{-}13]$$

The temperature dependence of the osmotic coefficient is obtained by differentiating equation [2-9] and combining equation [2-13].

$$\left(\frac{\partial \varphi}{\partial T}\right)_{P.m_1} = \frac{\overline{H_1} - H_1^o}{RT^2}\frac{1000}{\nu m M_1} \qquad [2\text{-}14]$$

2.1.5 The effect of concentration on the activity coefficient

The dissolved substances can be expressed using different concentration profiles with respect to their respective activities and activity coefficients. As the chemical potential of the components in solution is independent of the concentration unit, it is shown that:

$$\mu = \mu_c^o + RTlna_c = \mu_x^o + RTlna_x = \mu_m^o + RTlna_m \qquad [2\text{-}15]$$

where c, x and m represent the molar concentration, mole fraction and molalities respectively. The associated activities of the dissolved components with respect to these concentration scales are developed according to equation [2-2]:

$$\begin{aligned} a_c &= a_{\pm.c}^{\nu} = (Qc\gamma_{\pm.c})^{\nu} \\ a_x &= a_{\pm.x}^{\nu} = (Qx\gamma_{\pm.x})^{\nu} \\ a_m &= a_{\pm.m}^{\nu} = (Qm\gamma_{\pm.m})^{\nu} \end{aligned} \qquad [2\text{-}16]$$

Considering infinite dilution, i.e. when $\gamma_{\pm} \to 1$ as the concentration $\to$ 0, and substituting equations [2-16] into equation [2-15], the relationship between the activity coefficients in different concentration units and the standard chemical potential is established.

$$\mu_c^o = \mu_m^o - RT\mu ln\rho_w$$

$$\mu_x^o = \mu_m^o + RTln55.51 \qquad [2\text{-}17]$$

And

$$\gamma_{\pm,c} = \gamma_{\pm,m}(1 + 0.001mM)\left(\frac{\rho_w}{\rho_r}\right)$$

$$\gamma_{\pm,x} = \gamma_{\pm,m}(1 + \frac{mv}{55.51}) \quad [2\text{-}18]$$

The above equations are based on the assumption that water is the solvent. It should also be noted that the activity coefficients in the various concentration units are only regarded to be equal to each other in infinite dilute solutions.

2.1.6 Activity and osmotic coefficients in concentrated solutions

It is essential to know the activity coefficients of the dissolved substance and the osmotic coefficients of the solvent in saturated and supersaturated solutions when calculating the solubilities, as well as determining the thermodynamic driving force.

The activity coefficients associated with soluble substances are easily determined from a vast literature data bases or by direct experimental measurements. However, reliable thermodynamic correlations have been developed by Pitzer and Mayorga (1973) and Kusik and Meissner (1973) which can predict the thermodynamic data accurately, within certain solutions. However, solutions that contain sparingly soluble electrolytes, within highly supersaturated solutions, are pragmatic. Experimental determinations are made difficult as supersaturated solutions are highly unstable. Under these conditions, theoretical estimates and appropriate correlations are used. However, each correlation has specific assumptions associated with the model of which the ionic strength of the solution plays an important role. The ionic strength of a solution is defined as:

$$I = 0.5 \sum_i c_i z_i^2 \quad [2\text{-}19]$$

When considering a binary solution of low ionic strength the expanded Debye-Huckel relationship is used.

$$log\gamma_{\pm} = -A|z_+ z_-|\sqrt{I}/(1 + \bar{a}B\sqrt{I}) \quad [2\text{-}20]$$

where $\bar{a}$ represents an effective ionic radius and holds for $I \leq 10^2$ molm^{-3}. When considering high ionic strength solutions up to 6×10^3 molm^{-3}, the activity coefficient of sparingly soluble electrolytes at 25˚C can be estimated using the Bromley correlation. As

was mentioned, there are many different correlations with specific assumptions associated with each one. When using a specific correlation it should be noted that choosing a correlation that suits the specific system is essential to predict the correct thermodynamic data.

2.2 Solubility

Solubility is a measure of the maximum amount of solute that can dissolve, under constant temperature, pressure and system composition, in a solvent at equilibrium, which results in a saturated solution. The main factors which affect solubility are temperature and the ion-interactions. Thus, solubility studies focus on the effects these 2 factors have on the thermodynamic properties of the substances involved. These properties include the activities and ionic strengths of the solutes, the Gibbs free energies, chemical potentials and solubility products. However, experimental data on the thermodynamic properties is very scarce, particularly the solubility of salts in ternary and multi-component systems. Hence, simulation models, such as the Pitzer ion-interaction model, are used to predict these thermodynamic properties.

2.2.1 The effect of temperature on solubility

The solubility of a solute in a solvent is determined by the balance of intermolecular forces between the ions in solution and the entropy change that accompanies the attraction and association of the molecules of a solvent with the molecules or ions of a solute. Temperature alters this balance thus, decreasing or increasing the solubility of a solute in a solvent. The heat supplied to the system, in the form of temperature, breaks the bonds that hold the solid together and subsequently releases the latent heat of fusion from the solid. Energy is also liberated during the formation of bonds being formed between the solute and the solvent. If the heat required to break the bonds holding the solid together is less than the heat given off during the dissolving process, the net dissolving reaction is exothermic. Thus, the addition of more heat, in the form of temperature, inhibits the dissolving reaction as excess heat is already being liberated by the reaction. This situation, as is the case with $MgSO_4$ at high temperatures, results in a decrease in solubility with an increase in temperature. Alternatively, if the heat required to break the bonds holding the solid together is greater than the heat given off during the dissolving process, the net dissolving reaction is endothermic. Thus, the addition of

heat inhibits the dissolution process due to the excess heat already being liberated by the reaction. This is the case for about 95% of solutes, including NaCl (Hill and Petrucci, 1999).

2.2.1.1 The effect of temperature on the solubility of $MgSO_4$

Figure 2.1 represents the solubility of $MgSO_4$, as a function of temperature. Linke and Siedell (1965) showed that the solubility of $MgSO_4$ increased with increasing temperature, until a temperature of 70˚C. Thereafter, the solubility of $MgSO_4$ decreased with increasing temperature.

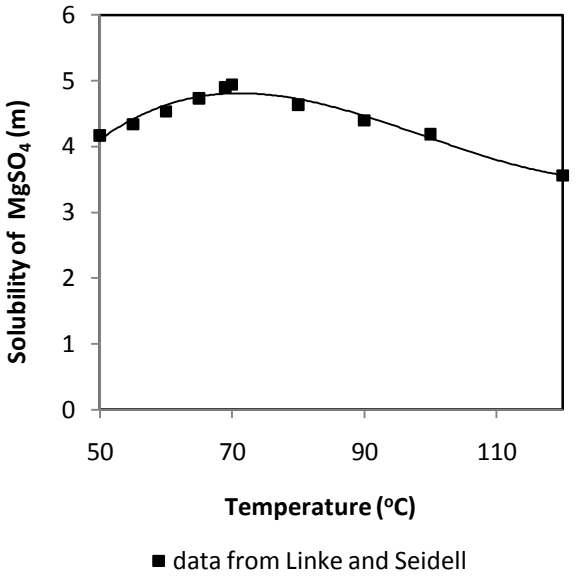

Figure 2.1: The effect of temperature on the solubility of $MgSO_4$ (adopted from Linke and Seidell, 1965)

Work conducted by El Guendouzi *et al*. (2002); Abdelfatah *et al*. (2002); El Guendouzi *et al*. (2003) on the solubility of $MgSO_4$ at constant temperature measured the activity and osmotic coefficients for binary systems. Whereas Apelblat and Manzurola (2003) and Pillay *et al*., (2005) did extensive research to determine the influence of temperature on the thermodynamic properties in fairly complex systems.

2.2.1.2 The effect of temperature on the solubility of NaCl

Figure 2.2 shows the solubility of NaCl, as a function of temperature. As can be seen, the solubility of NaCl increases only slightly with temperature thus, indicating that its solubility is relatively independent of temperature.

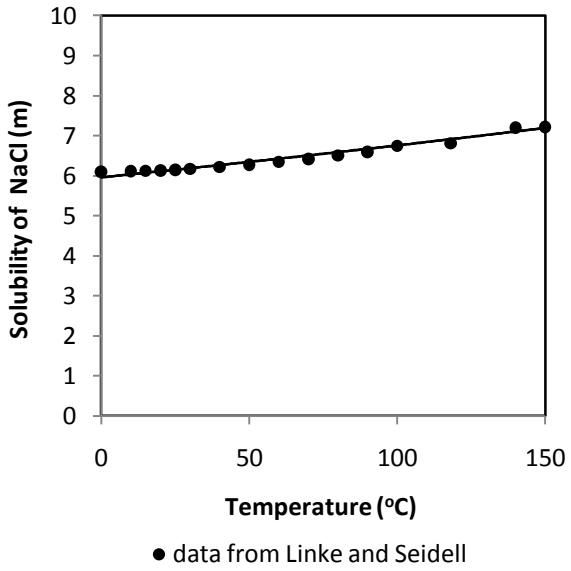

Figure 2.2: The effect of temperature on the solubility of a NaCl (adopted from Linke and Seidell, 1965)

Work conducted by Hubert *et al.* (1996) determined the activity coefficients for the NaCl-H_2O binary system within the 25 - 100˚C temperature range, using a calorimetric measurement technique. Using these calorimetric measurements, the parameters for the Pitzer model were established and subsequently were verified experimentally. The experimental and calculated values for the water activities were found to be in agreement, indicating that the Pitzer model accurately described the binary system.

2.2.2 The effect of impurities on solubility

The impurities present in saturated solutions can have considerable and varying effects on the solubility characteristics of systems. The presence of impurities can result in three different conditions:

- The impurities may combine or react with the solute forming complexes or compounds which can alter the whole nature of the system;
- The solution may become undersaturated or supersaturated. If the solution becomes undersaturated, the solute will dissolve in the solution, whereas the solute will precipitate out if the solution becomes supersaturated;
- The system remains in its original saturated state and the solubility of the solute remains unchanged.

2.2.2.1 Ion-interaction effects

The solubility of a sparingly soluble electrolyte in water is often expressed in terms of the concentrated solubility product K_c. The solubility product, for saturated solutions, is expressed according to equation [2-21]:

$$K_c = constant = (c_+)^x (c_-)^y \quad [2\text{-}21]$$

where c_+ and c_- are the ionic concentrations expressed as $molL^{-1}$. However, the simple solubility product principle is extremely limited and is restricted to solutions of very sparingly soluble salts. For concentrated solutions the fundamental approach using the concept of activity is adopted. Hence, the activity solubility product K_a, is defined by the following equation:

$$K_c = constant = (a_+)^x (a_-)^y \quad [2\text{-}22]$$

where a_+ and a_- are the ionic activities. As the activity of an ion may be expressed in terms of the ionic concentration (c) and the ionic activity coefficient (γ), equation [2.22] can be expressed as:

$$K_a = \left(c_+ \gamma_+\right)^x \left(c_- \gamma_-\right)^y \quad [2\text{-}23]$$

The activity of an ion depends on the concentration of all other ions in solution. Thus, the presence of a dissolved foreign electrolyte can greatly influence the activity coefficient of a sparingly soluble salt. The presence, in solution, of an ion in common with a sparingly soluble salt will significantly decrease the salt solubility (the common ion effect). The presence of an ion not in common with any of those of the solute can increase the solute solubility on account of the increase in ionic strength. (Mullin, 2001).

2.2.2.2 The effect of temperature and ion-interactions on solubility of $MgSO_4$

As discussed, both the temperature and the ion-interactions affect solubility. Marion and Farren (1999) focused their studies on both the influence of temperature and ion-interaction in a multi-component system. Marion and Farren used the Pitzer-equation parametization method, within the temperature range of -60 – 25°C, to investigate the effect that Na^+, K^+, Ca^+ and Cl^- had on the solubility of $MgSO_4$. The mathematical equation

used to define the Pitzer-equation parameter used to calculate the solubility product as a function of temperature is shown in equation [2-24]:

$$P(T)_j = a_{1j} + a_{2j}T + a_{3j}T^2 + a_{4j}T^3 + \frac{a_{5j}}{T} + \frac{a_{ij}}{T^2} + a_{6j}\ln T \qquad [2\text{-}24]$$

where j is the jth Pitzer-equation parameter or solubility product and a_{ij} is the parameter coefficient. The results obtained from the model estimates, were in good agreement with experimental measurements and of the three hydrates, $MgSO_4 \cdot 6H_2O$, $MgSO_4 \cdot 7H_2O$ and $MgSO_4 \cdot 12H_2O$. Epsomite had the highest solubility product. In the study it was also found that the hydrates of $MgSO_4$ can persist in metastable equilibrium over a wide temperature range. This complicates interpretations of experimental measurements and theoretical calculations.

Pillay *et al*. (2005) also studied the effect of temperature and ion-interaction on thermodynamic model parameters in the K-Na-Mg-Cl-SO_4 system. The results showed that further investigation into the effect that cations with high charge to radius ratios have on the solubility of $MgSO_4$ was needed.

Studies conducted by Abdelfetah *et al*. (2002) on binary systems, used a hydrometric method to determine the thermodynamic properties for the $MgSO_4$-$MnSO_4$-H_2O system. El Guendouzi *et al*. (2003) also studied the thermodynamic properties (water activity, osmotic and activity coefficients) for the $MgSO_4$-$NaSO_4$-H_2O system at 25˚C. The interaction of ions was used to explain the model coefficients when determining the osmotic coefficients of aqueous $MgSO_4$ in the presences of $NaCl_{(aq)}$ and $KCl_{(aq)}$ (Archer *et al*., 1998).

There is a lack of thermodynamic data for ternary and multi-component systems containing cations with high charge to radius ratio, such as Fe^{2+}, Fe^{3+} and Mg^{2+}, in a mixture with other ions. However, work conducted by Christov (2004) used the Pitzer ion-interaction model for the Na-K-Mg-Cl-SO_4-H_2O system at 25˚C to determine the effect Fe^{2+} and Fe^{3+} had on the component activities and standard potentials. Christov used the Pitzer ion-interaction model to calculate the solubility equilibria in the systems containing the Fe^{2+} and Fe^{3+} and showed that the mixed $(Mg,Fe)SO_4 \cdot 7H_2O$ and

$(Fe,Mg)SO_4 \cdot 7H_2O$ crystals deviated slightly from the ideal mixed crystals. Christov (2004) also reported that in the construction of the model for the multi-component system, $Na+K+Mg+Fe(II)+Fe(III)+Cl+SO_4+H_2O$, did not take certain factors such as: (a) the lack of solubility data for the ternary systems; (b) the lack of activity data and (c) the assumption on the composition and nature of the crystallising solid phase, into account.

2.2.2.3 The effect of temperature and ion interactions on the solubility of NaCl

2.2.2.3.1 Dilute systems

Harned and Owen (1958) and Robinson and Stokes (1970) have contributed a substantial amount of experimental data for ternary aqueous electrolyte systems. Despite this, there are only a few studies that have focused on correlating the activity coefficients for these types of systems in the concentrated regions. The activity coefficients of electrolytes in dilute solutions change only slightly with compositions at constant total molality. However, this change is apparent in concentrated solutions with studies in these concentrated regions having been discussed previously by Meissner *et al*. (1972). Robinson and Stokes (1970) focused their studies on the HCl-NaCl-H_2O system and its constituent binaries from very low molalities, up to highly concentration solutions.

There are difficulties in accurately describing the activity coefficients for the HCl-NaCl-H_2O system from low concentrations to highly concentrated or saturated solutions. The Brönsted-Guggenheim theory (Harned and Robinson, 1968) describes systems below 0.2 m concentrations. The equations used in this theory are derived using the excess Gibbs energy where the excess Gibbs energy is defined by two parts. The first leads to the Debye-Hückel limiting law and the second is the correction to the Debye-Hückel theory. Considering a ternary aqueous solution of j, k, and common ion i, the excess Gibbs energy (g^E) is:

$$g^E = g^E(\text{Debye}-\text{Hückel}) + 2A_{ij}x_i x_j + 2A_{ik}x_i k_k \qquad [2\text{-}25]$$

where ion j belongs to electrolyte 2 and k to electrolyte 3. X_i is the ionic mole fraction of ion i, and the parameters A_{ij}, A_{ik} characterise the interaction between pairs of ions. The ionic activity coefficients are calculated by differentiating equation [2-25] to form the Brönsted-Guggenheim equations for two 1-1 electrolytes with a common ion.

$$\ln \gamma_2 = -\frac{d\sqrt{I}}{\left(1+\sqrt{I}\right)} + 2A_{ij}m_2 + (A_{ij} + A_{ik})m_3 \quad [2\text{-}26]$$

$$\ln \gamma_3 = -\frac{d\sqrt{I}}{\left(1+\sqrt{I}\right)} + 2A_{ik}m_3 + (A_{ij} + A_{ik})m_2 \quad [2\text{-}27]$$

where d represents the Debye – Hückel constant, m_2 and m_3 are the molalities of the electrolytes, and I is the ionic strength. Equations [2-26] and [2-27] are limited to molalites below 0.2 m, as mentioned above.

2.2.2.3.2 Concentrated systems

In 1938, Bruauner *et al.* introduced a concept that was an extension of the Langmuir theory, which gives the relationship of the absorption of gas molecules on a solid surface and developed the Brunauer Emmett Teller (BET) model. Stokes and Robinson (1948) conceptually adapted the theory of gas adsorption on solid surfaces and related it to the absorption theory of electrolytes. The BET equation was modified for a two component electrolyte-water system giving the water activity a_w, as a function of the water mole fraction, shown in equation [2-28].

$$\frac{a_w(1-x_w)}{x_w(1-a_w)} = \frac{1}{Fr} + \frac{(F-1)}{Fr} \quad [2\text{-}28]$$

where both F, an energetic parameter, and r, a structural parameter, are independent of x_w.

The energetic parameter, F, is given by

$$F = \exp\left(\frac{\varepsilon_i}{RT}\right) \quad [2\text{-}29]$$

In which: $$\varepsilon_i = E_L - E \quad [2\text{-}30]$$

where E is the molar binding energy of water sites close to the ions. E_L is the molar binding energy of water in pure water; R is the gas constant and T the temperature. The parameter R is expressed as:

$$R = \frac{N_A}{N_S} \quad [2\text{-}31]$$

where N_s is the number of available sites with the binding energy E, for the water molecules, per mole of electrolyte and N_A is the Avogadro constant. Ally and Braunstein (1998) extended the BET model and used statistical mechanics, a probability model that is based on systems with high populations where the motions of particles or objects are subjected to forces, to represent the activities for two-salt and single solvent mixtures in highly concentrated solutions. The extended BET model is shown in equation [2-32]

$$\alpha_{A\iota} = \frac{A}{A+B}\left(\frac{r_i A - D_i}{r_i A}\right)^{r_i} \qquad [2\text{-}32]$$

where *A* and *B* are the numbers of particles of the respective salts and *D* is the total amount of water adsorbed on *A*. Ally and Braunstein (1998) made 2 basic assumptions in their BET model. Firstly, in a multi-component system the mixing of salts follows the rule of an ideal solution as the change in the internal energy is due only to water adsorption. Secondly, the parameters r_i and ε_i relate only to the electrolyte i and thus are independent of any other electrolyte. Since these assumptions are not always true in real aqueous systems, Clegg and Simons (2001) derived a new set of BET equations based on the framework of Ally and Braunstein (1998). Based upon the Gibbs free energy, given by Ally and Braunstein (1998), of a mixed solution, equations were proposed for ion and solvent activites in a single-solvent and multi-ion mixture. With a regular model approximation Abraham and Abraham (2000) proposed a mixing term for the non-ideality of the salt-salt interaction. The model was used to predict salt solubilities in ternary mixtures and the water activities in common ion systems as well as in reciprocal systems. Work conducted by Zeng *et al*. (2007) used the extended BET model ,proposed by Ally and Braustein, together with the mixing term ,proposed by Abraham and Abraham, to represent the salt-salt interaction in describing the solubility behaviour and components activities for the HCl-$MgCl_2$-H_2O system over the 0 – 140˚C temperature range. The model reproduced isotherms using only binary model parameters that were in agreement with experimental data from Dahnee (1969). The model also predicted that the amount of precipitated $MgCl_2 \cdot 6H_2O$ salt increased with an increase in the concentration of HCl, over the whole temperature range. $MgCl_2 \cdot 6H_2O$

crystallised out with a decrease in temperature. However, a double salt $HCl.MgCl_2 \cdot 7H_2O$ started to precipitate out when the concentration of HCl reached 9-11 m.

Harned's rule (Harned and Owen, 1958) is commonly used for concentrated systems where, for a ternary solution at constant total molality, the logarithm of the activity coefficient of each electrolyte is proportional to the molality of the other electrolyte. The activity coefficients are expressed as:

$$\log \gamma_2 = \log \gamma_{2(o)} - \alpha_{23} m_3 \qquad [2\text{-}33]$$

$$\log \gamma_3 = \log \gamma_{3(o)} - \alpha_{32} m_2 \qquad [2\text{-}34]$$

where the subscripts 2 and 3 refer to HCl and NaCl respectively. α_{23} and α_{32} characterise the interactions occurring between the two electrolytes, HCl and NaCl. Although Harneds rule is used to describe concentrated systems, the ternary parameter within the Harned rule expression, depends on both temperature and total molality.

Studies conducted by Funk (1974) used the Harned rule to develop equations that accurately describe the activity coefficients of the electrolytes for the HCl-NaCl-H_2O system. The study showed that the equations were in agreement with the system for the temperature range of 0 - 50˚C and in the total concentration range of 0.2 m to approximately 10 m. The proposed equations can be extrapolated to new conditions of temperature and composition, as well as to systems with more than two electrolytes. However, although the equations describe the HCl-NaCl-H_2O system well, more work is required for them to have general applications to other systems.

Studies conducted by Deyhimi *et al*. (2007) investigated the thermodynamic properties for the ternary NaCl-$MgCl_2$-H_2O system using potentiometric measurements at a constant temperature of 25˚C. The ternary electrolyte system was also modelled based on the Pitzer ion-interaction and semi-empirical theory for mixed salts within the ionic strength range of 0.05 - 4.3 m. The effect of varying the molality of NaCl, at a constant ionic strength, showed a decrease in the excess Gibbs free energy, as well as a decrease in the water activity.

Berger and Winand (1970) studied the effect of chlorides, iron, zinc, sodium and hydrogen, on the solubility, density and electrical conductivities of aqueous Cu^{+} and Cu^{2+} chlorides. Increasing the $FeCl_2$ concentration decreased the solubility of $CuCl_2$ to less of a degree when compared to the effect of increasing the $ZnCl_2$ concentration. Increasing the total Cl^- concentration decreased the $CuCl_2$ solubility if the Cl^- ions were added as $ZnCl_2$. However, the solubility of NaCl increased with the addition of $ZnCl_2$. The results were qualitatively interpreted when taking the relative Cl^- donor or acceptor characters of the separate salts into account.

In summary, the literature review conducted showed that temperature and ion interactions are important parameters influencing the solubility of both $MgSO_4$ and NaCl. Although much work has been done on the solubility of both compounds, each system is unique both in terms of composition and the conditions under which they were investigated. Consequently, the literature review focussed on a more fundamental level, where the effects of different ions on the solubility have been explained using thermodynamic properties. These properties are described by ion interaction theories, such as Brönsted-Guggenheim and Debye-Hückel limiting law, to develop thermodynamic models, such as the Pitzer ion interaction model, to try and accurately describe these complex systems. However, the lack of thermodynamic data especially in multi-component systems and at certain temperatures does not give an accurate or reliable source of information.

References

Abdelfetah, M., El Guendouzi, M., Abderrahim, D. (2002). Hygrometric determination of the thermodynamic properties of the system $MgSO_4$-Na_2SO_4-H_2O at 298.15K (2002). Fluid Phase Equilibria, 201(2), p233-244.

Abdelfetah, M., El Guendouzi, M., Abderrahim, D. (2002). Thermodynamic properties of the system $MgSO_4$-$MnSO_4$-H_2O at 298.15K. Fluid Phase Equilibria, 202(2), p221-231.

Abraham, M., Abraham, M.C., (2000). Electrolyte and water activities in very concentrated solutions. Electrochimica. 46. p137-142.

Archer, D., Rard, G. Joseph, A. (1998). Isopiestic Investigation of the Osmotic and Activity Coefficients of Aqueous $MgSO_4$ and the Solubility of $MgSO_4 \cdot 7H_2O$ at 298.15K: Thermodynamic properties of the $MgSO_4 + H_2O$ System to 440K. Journal of Chemical Engineering Data 43(5), p791-806.

Ally, M.R., Braunstein, J. (1998). Statistical mechanics of multilayer adsorption: electrolyte and water activities in concentrated solutions. J. Chem. Thermodyn. 30, p49-58.

Apelblat, A., Manzurola, E. (2003). Solubilities and vapour pressures of saturated aqueous solutions of sodium tetraborate, sodium carbonate, and magnesium sulfate and freezing-temperature lowerings of sodium tetraborate and sodium carbonate solutions. J. Chem. Thermodynamics, 35, p221-238.

Berger, J.M., Winand, R. (1970). Solubilities, densities and electrical conductivities of aqueous copper(I) and copper(II) chlorides in solutions containing other chlorides such as iron, zinc, sodium and hydrogen chlorides Electrochimica Acta, 15(5), p757-767.

Brunauer S., Emmet, P.M., E. Teller, P.M.(1938).Adsorption of Gases in Multi-molecular Layers J. Am. Chem. Soc.60, p309-319.

Clegg, S.L., Simonson, J.M., (2001). A BET model of the thermodynamics of aqueous multi-component solutions of extreme concentrations. J. Chem. Thermodynamics. 33, p1457-1472.

Cristov, C. (2004). Pitzer ion-interaction parameters for Fe(II) and Fe(III) in the quinary {Na+K+ Mg + Cl +SO_4 +H_2O} system at T=298.15K. Journal of Chemical thermodynamics. 36(3), p223-235.

Dähne, C., 1969. Bestimmung der Löslichsisothermen des Systems HCl–MgCl2–H2O zwischen −55 und +80 °C. Z. Anorg. Allg. Chem. 371, p59–73.

Deyhimi, F., Karimzadeh, Z., Salamt-Ahangari, R,. (2007), Thermodynamic investigation of a ternary mixed electrolyte (NaCl/MgCl2/H_2O) system using Na+ solvent polmeric membrane ion-selective electrode. Fluid Phase Equilibria 254. p18-27.

El Guenodouzi, M., Mounir, A., Dinane, A. (2003). Water activity, osmotic and activity coefficients of aqueous solutions of Li_2SO_4, Na_2SO_4, K_2SO_4, $(NH_4)2SO_4$, $MgSO_4$, $MnSO_4$, $NiSO_4$, $CuSO_4$ and $ZnSO_4$ at T=298.15K. Journal of Chemical Thermodynamics, 35(2), p209-220.

Funk, E.W. (1974). Activity Coefficients at High Concentrations in the Hydrochloric Acid-Sodium Chloride-Water System. Ind. Eng. Chem., Process Des. Develop., Vol. 13, No 4.

Harned, H.S., Owen, B.B. (1958). The physical chemistry of electrolyte solutions. 3rd edition. Chapter 14 Amer. Chem. Soc Monogr. 137 Reinhold.

Harned, H.S., Robinson, R.A., (1968). Multicomponent Electrolyte Solutions, Pergamon, London.

Handbook of Chemistry and Physics.(1943), 27th edition, Chemical Rubber Publishing Co., Cleveland, Ohio.

Hubert, N., Solimando, R., Pere, A., Schuffenecker, L. (1996). Dissolution enthalpy of NaCl in water at 25 oC, 45 oC and 60 oC. Determination of the Pitzer's parmaters of the {H2O-NaCl} system and the molar dissolution enthalpy at infinite dilution of NaCl in water between 25 oC and 100 oC. Thermochimica Acta 294. p157-163.

John W. Hill, Ralph H. Petrucci, (1999) *General Chemistry*, 2nd edition, Prentice Hall, 1999.

Kusik, C.L. and Meissner, H.P. (1973). I&EC proc. Des. Develop., 12, 112.

Linke, W.F. and Seidell, A., 1965. In: *Solubilities of Inorganic and Metal-Organic Compounds* Vol. II, D. van Nostrand Co., Princeton. Riddance.

Marion, G.M. and Farrren, R.E. (1999). Mineral solubilities in the Na-K-Mg-Ca-Cl-SO_4-H_2O system: a re-evaluation of the sulphate chemistry in the Spencer-Moller-Weare model, Geochimica et Cosmochimica Acta, 63(9), p1305-1318.

Meissner, H.P., Kusik, C.L. (1972). Activity Coefficients of Strong Electrolytes in Multicomponent Aqueous Solutions. AlCheJ., 18(2), p294-248.

Meissner, H.P., Tester, J. W. (1972). Activity Coefficients of Strong Electrolytes in Aqueous solution. Ind. Eng. Chem. Proc. Dev., p128-133.

Mullin, J.W. (2001). Crytallization 4th edition, London: Reed Education and Professional Publishing .

Pillay, V., Gaertner, R.S., Himawan, C., Seckler, M.M., Lewis, A.E., witkamp, Geert-Jan.(2005), $MgSO_4$ + H_2O system at Eutectic Conditions and thermodynamic Solubility Products of $MgSO_4 \cdot 12H_2O$(s) and $MgSO_4 \cdot 7H_2O$(s). Journal of Chemical and Engineering Data, 50(2), p551-555.

Pitzer, K. S. and Mayorga, G. (1973) Thermodynamics of electrolytes. II. Activity and osmotic coefficients for strong electrolytes with one or both ions univalent. *J. Phys. Chem*. 77, p2300–2308.

Robinson, R.A., Stokes, R.H. (1970). Electrolyte Solutions, 2nd edition. Appendix 1, London, Butterworths p457.

Robinson, R.A., Stokes, R.H. (1970). Electrolyte Solutions. 2nd ed, Chapter 15. London. Butterworths.

Sohnel, O. and Garside, J. (1992). *Precipitation: Basic Principles and industrial applications.* Butterworth-Heinemann Ltd, Oxford.

Stokes, R.H., Robinson, R.A. (1948).Ionic Hydration and Activity in Electrolyte Solutions. J. Am. Chem. Soc. 70(5), p1870-1878.

Zeng, D., Liu, H., Chen, Q., (2007). Simulation and prediction of solubility phase diagram for the separation of MgCl2 from LiCl brine using HCl as a salting out agent. Hydrometallurgy. 89, p21-31.

Chapter 3. Response Surface Methodology

3.1 Introduction

Response surface methodology (RSM) is a combination of statistical and mathematical techniques that are used for building models that are useful for the analysis of problems. A response is influenced by several variables and the objective is to optimize the response. The measure of the performance of the response, y, depends on the controllable independent input variables $(\xi_1, \xi_2, \ldots . \xi_k)$. The relationship is represented by equation [3-1]:

$$y = f(\xi_1, \xi_2, \ldots \xi_k) + \varepsilon \qquad [3\text{-}1]$$

Equation [3-1] is an empirical model, a response surface model, where ε is the associated error term which represents the variability that is not accounted for e.g. background noise, analytical error etc. Treating ε as the statistical error, it is assumed to have a normal distribution with mean zero and variance σ^2. If the mean is zero the response is reduced to equation [3-3]:

$$E(y) = \eta = E[f(\xi_1, \xi_2, \ldots ., \xi_k)] + E(\varepsilon) \qquad [3\text{-}2]$$

$$\eta = f(x_1, x_2, \ldots x_k) \qquad [3\text{-}3]$$

where the natural variables, $(\xi_1, \xi_2, \ldots . \xi_k)$,are transformed to coded variables, $(x_1, x_2, \ldots x_k)$. The coded variables are usually defined by dimensionless variables with mean zero and the same spread or standard deviation. The coded variables are calculated according to equation [3-4]:

$$x_i = \frac{\xi_i - [\max(\xi_i) + \min(\xi_i)]/2}{[\max(\xi_i) - \min(\xi_i)]/2} \qquad [3\text{-}4]$$

3.2 Building empirical models

The unknown function f is approximated using a first, second or higher order model. Given a case for two independent variables, the first order model is represented by equation [3-5]:

$$\eta = \beta_0 + \beta_1 x_1 + \beta_2 x_2 \qquad [3\text{-}5]$$

where the β's are a set of unknown parameters and can be estimated by analysing data collected from the system using, linear regression (Myers and Montogomery, 1995). The response surface generated from the two variables x_1 and x_2 is a plane lying above the x_1, x_2 space. In the case where the true response shows curvature a first order model is inadequate. Hence, a second order model may be required. A second order model, for two variables, is represented by equation [3-6]:

$$\eta = \beta_0 + \beta_1 x_1 + \beta_2 x_2 + \beta_{11} x_1^2 + \beta_{22} x_2^2 + \beta_{12} x_1 x_2 \qquad [3\text{-}6]$$

In general for k variables a first order model is given by:

$$\eta = \beta_0 + \beta_1 x_1 + \beta_2 x_2 + \cdots + \beta_k x_k \qquad [3\text{-}7]$$

and the second order model is given by:

$$\eta = \beta_0 + \sum_{j=1}^{k} \beta_j x_j + \sum_{j=1}^{k} \beta_{jj} x_j^2 + \sum \sum_{i<j} \beta_{ij} x_i x_j \qquad [3\text{-}8]$$

3.2.1 Estimation of the parameters in empirical models

An empirical model represents a model that approximates the observed response. If the number of experimental runs is greater than the number of variables then the response (y) may be related to the regressor variables k, as:

$$y_i = \beta_0 + \sum_{j=1}^{k} \beta_j x_{ij} + e_i, \qquad i = 1,2, \ldots \ldots, n \qquad [3\text{-}9]$$

Where β_1, β_2….β_k are the regression coefficients.

The simplest way to solve for the regression coefficients is in a matrix notation (Myers and Montogomery, 1995). Each observed response (y_i) will have an observation on each regressor variable where, the regressor variable x_{ij} denotes the i^{th} observation or level of variable x_j. The data collected can then be represented in a matrix notation as:

$$\boldsymbol{y} = \boldsymbol{X}\beta + \boldsymbol{e} \qquad [3\text{-}10]$$

Where, $\boldsymbol{y} = \begin{bmatrix} y_1 \\ y_2 \\ \vdots \\ y_n \end{bmatrix}$, $\boldsymbol{X} = \begin{bmatrix} 1 & x_{11} & x_{12} & \ldots & x_{1k} \\ 1 & x_{21} & x_{22} & \ldots & x_{2k} \\ \vdots & \vdots & \vdots & \cdots & \vdots \\ 1 & x_{n1} & x_{n2} & \cdots & x_{nk} \end{bmatrix}$, $= \begin{bmatrix} \beta_o \\ \beta_1 \\ \vdots \\ \beta_k \end{bmatrix}$, $\boldsymbol{e} = \begin{bmatrix} e_o \\ e_1 \\ \vdots \\ e_n \end{bmatrix}$

When estimating the regressions parameters in multiple regression models the least square method is used. The method of least squares chooses the β's so that the sum of

the squares of the errors are minimised (Myers and Montogomery, 1995). The least square function is represented by equation [3-11] and in order to find the vectors of least square estimates equation [3-11] needs to be minimised.

$$L = \sum_{i=1}^{n} e_i^2 \qquad [3\text{-}11]$$

To find the vector of least squares estimators b, equation [3-12] needs to be minimised and hence through simplification the least square estimator of β is represented by equation [3-13].

$$L = \sum_{i=1}^{n} e_i^2 = e'e = (y - X\beta)'(y - X\beta) \qquad [3\text{-}12]$$

$$\boldsymbol{b} = (\boldsymbol{X}'\boldsymbol{X})^{-1}\boldsymbol{X}'\boldsymbol{y} \qquad [3\text{-}13]$$

The fitted regression model is thus represented by:

$$\hat{y} = XB \qquad [3\text{-}14]$$

In scalar notation, the fitted model is:

$$\hat{y_i} = b_0 + \sum_{j=1}^{k} b_j x_{ij}, \qquad i = 1,2, \ldots \ldots, n \qquad [3\text{-}15]$$

The difference between the observation y_i and the fitted value $\hat{y_i}$ is a residual $e_i = y_i - \hat{y_i}$, and in vector notation:

$$\boldsymbol{e} = \boldsymbol{y} - \hat{\boldsymbol{y}} \qquad [3\text{-}16]$$

3.2.2 Estimating the variance σ^2

The sum of squares, of the residuals, is represented by equation [3-17].

$$SS_E = \sum_{i=1}^{n} (y_i - \hat{y_i})^2 = \sum_{i=1}^{n} e_i^2 \qquad [3\text{-}17]$$

An unbiased estimator of the variance σ^2, is given by:

$$\widehat{\sigma^2} = \frac{SS_E}{n - p} \qquad [3\text{-}18]$$

where n is the number of independent values and p is the number of model parameters. It should be noted that σ^2 depends on the form of the model that is fit to the data (Myers and Montogomery, 1995).

3.2.3 Analysis of variance

The test for significance of a regression is to determine if there is a linear relationship between the response variable y and the subset of the regressor variables (Myers and Montogomery, 1995). The appropriate hypotheses are:

$$H_o: \beta_1 = \beta_2 = \cdots = \beta_k = 0 \qquad [3\text{-}19]$$

$H_1: \beta_j \neq 0$ for at least one j

Rejection of H_0 means that at least one of the regressor variables X_1, X_2,... X_k contributes significantly to the model. This test is commonly called an analysis of variance (ANOVA). The total sum of the squares (S_{yy}) is divided into the sum of squares due to the model, (SS_R) and the sum of squares due to error SS_E, as seen in equation [3-20].

$$S_{yy} = SS_R + SS_E \qquad [3\text{-}20]$$

The total sum of squares is given by:

$$S_{yy} = \sum_{i=1}^{n} y_i^2 - \frac{(\sum_{i=1}^{n} y_i)^2}{n} \qquad [3\text{-}21]$$

The sum of squares due to the model can be calculated as:

$$SS_R = b'X'y - \frac{(\sum_{i=1}^{n} y_i)^2}{n} \qquad [3\text{-}22]$$

The test procedure for H_o is to compute

$$F_o = \frac{SS_R/k}{SS_E/(n-k-1)} = \frac{MS_R}{MS_E}$$

[3-23]

and if F_o exceeds $F_{a,k,n-k-1}$ H_o is rejected. H_o can also be rejected if the p-values for the statistic of F_o is less than α. One could make the error by rejecting H_o, when in fact H_o is true. The probability of such an error occurring is called the level of significance and is denoted by α (Walpole and Myers, 1995). Table 3.1 is a general layout of an ANOVA.

Table 3.1: Analysis of Variance for significance of regression in multiple regressions

Source of variance	Sum of Squares	Degree of freedom	Mean Square	F_o
Regression	SS_R	k	MS_R	MS_R/MS_E
Residual	SS_E	n-k-1	MS_E	
Total	S_{yy}	n-1		

If the F_o value is greater than those in the appropriate statistical tables the response is significant and there is a linear relationship. It is also possible to test for the significance of individual variables or interaction parameters.

R^2 is the coefficient of multiple determination and is defined by:

$$R^2 = \frac{SS_R}{S_{yy}} \quad where\ 0 \leq R^2 \leq 1$$

[3-24]

R^2 is a measure of the amount of reduction in the variability of y obtained by the regressor variables in the model. In general, the R^2 gives an indication of how well the fit of the regression model is for a given number of regressors.

3.3 Two-level factorial design

Factorial designs are used to investigate the joint effects of several factors on a response variable. A 2^k factorial design is a special case where each of the factor k, has only two levels. The class of 2^k factorial designs are very important in response surface work and their application is important in three main areas:

- To identify the process variables for the specific system at the start of the response surface study.
- To fit a first-order response surface model, to generate the factor effect estimates required to perform the method of steepest ascent.
- To provide the basic building blocks used to create other surface designs.

3.3.1 The 2^2 factorial design

The simplest case is the 2^2 factorial design for a process with two variables. The levels of factors that are varied are called low, (-), or high, (+). Figure 4.1 shows the experiments required when varying factors, A and B, for a 2^2 factorial design.

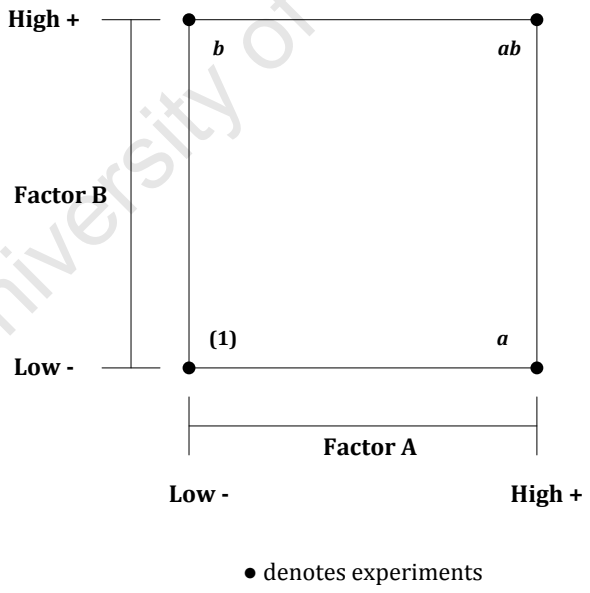

Figure 3.1: The 2^2 factorial design

3.3.2 The 2^3 factorial design

A 2^3 factorial design is implemented when three factors, A, B and C, each at 2 levels are of interest. There are eight treatment combinations, shown in Figure 3.2, where the high level of any factor at a point in the design is denoted by the corresponding lowercase letter. The lower level of a factor is denoted by the absence of the corresponding letter.

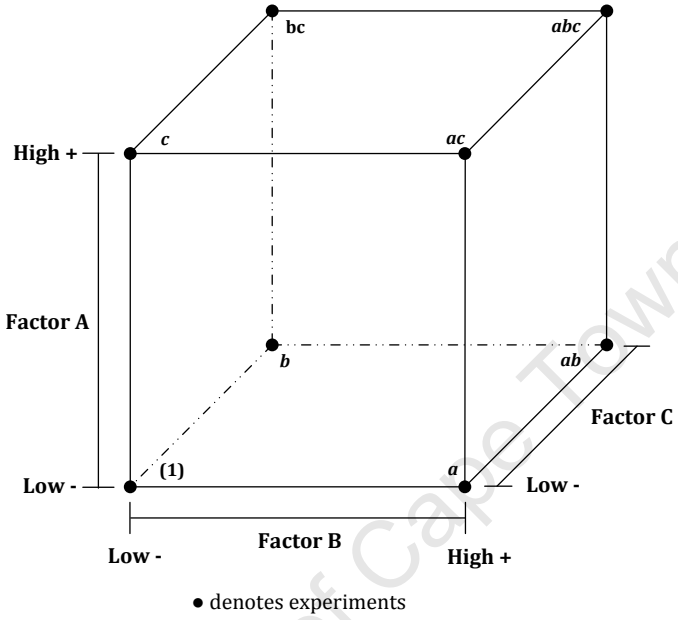

Figure 3.2: The 2^3 factorial design

In 2^k factorial designs there is no repetition of experiments to determine experimental errors. Hence, it is important to carry out experiments at the centre points that would allow finding an estimate of the error.

3.4 Design for fitting second order models

3.4.1 Central composite design

The most popular class of fitting second order designs are centre composite designs (CCD). The CCD is a very efficient design in situations that call for a non-sequential batch response surface experiment. The three components of the design, graphically represented in Figure 3.3, comprise of:

- The factorial points, representing the experiments at upper and lower levels, contribute in estimating the linear terms and the two factor interactions;

- The axial points, representing the experiments at an upper or lower level in combination with the centre points, contribute in a large way to estimation of the quadratic terms;
- The centre points provide an internal estimation of the error, as well as contributing towards the estimation of the quadratic terms.

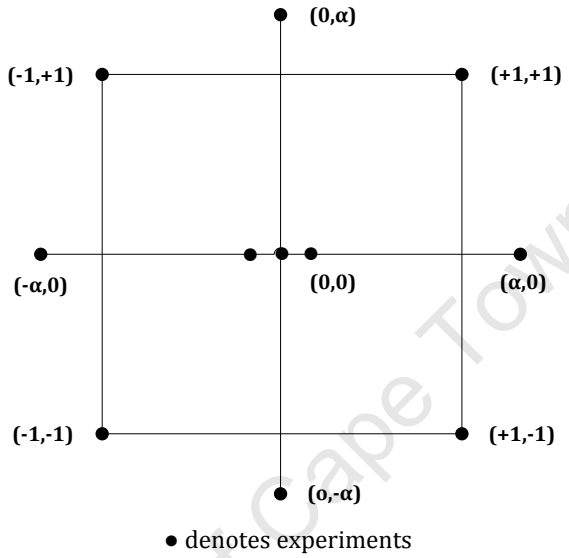

Figure 3.3: A Central composite design for k=2

3.4.2 Face centred design

In the case of a cubical design, when the experiment falls outside the region of interest, a variation of the CCD, called the face centred cube, is an effective second order design. This design locates the axial points on the centres of the faces of the cube as shown in Figure 3.4. The variation of the CCD is sometimes used as it requires three levels of each factor.

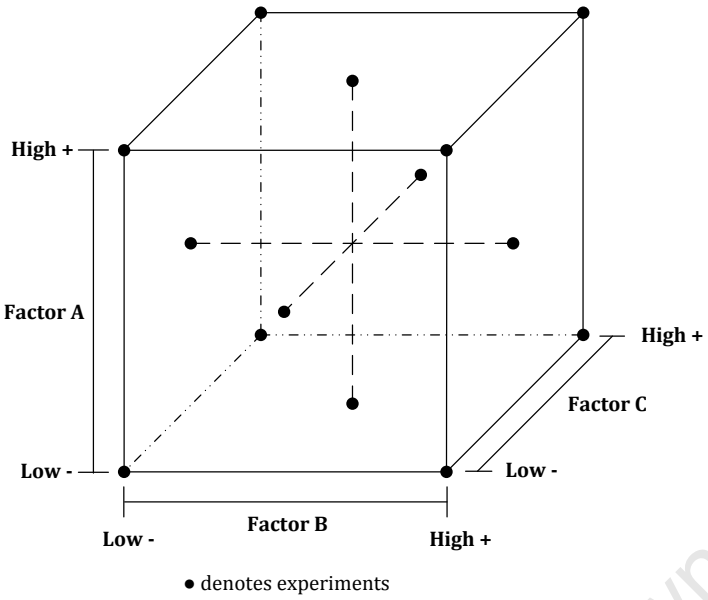

Figure 3.4: A face-centred central composite design for k=3

3.4.3 The ridge analysis

If a stationary point lies outside the experimental area it is often not possible to operate the system at this point and the fitted model is not reliable outside the region of the experiment. The analysis is to anchor the stationary points inside or on the perimeter of the experimental region, to determine the nature of the system. The ridge analysis produces a locus of points, each of which is a point of maximum response with the constraint that lies on a sphere of a certain radius. The output of this analysis is the set of co-ordinates of the maxima or minima along with the predicted response, $\hat{y}$, at each computed point on the path.

References

Myers, R.H. and Montgomery, D.C. (1995). Response Surface Methodology. John Wiley and Sons, New York.

Walpole, R.E. amd Myers, R.E. (1985). Probability and statistics for engineers. Collier MAcmillian, New York.

Chapter 4. Experimental and Methodology

4.1 Modelling methodology

The aqueous thermodynamic modelling was carried out using OLI Stream Analyser's (OLI Systems Inc., 2009) Mixed Solvent Electrolyte (MSE) model. The MSE model incorporates interaction parameters between specific species pairs from its database which was developed from the interactions between species within binary, ternary and quaternary systems. These parameters are used in equations such as the Pitzer-Debye-Huckel and UNIQUAC equations to predict the thermodynamic behaviour within specific aqueous systems.

Within this investigation the OLI Stream Analyser Version (OLI Systems Inc., 2009) was used to model the precipitation point of the salts that would be saturated, either $MgSO_4$ or NaCl, under the conditions specified in Table 4.4 and Table 4.7 respectively. The data generated by the model was used to observe the effect temperature and the background aqueous environment had on the solubility of $MgSO_4$ and NaCl.

4.2 Experimental Methodology

Factorial designs are used to investigate the interactive effects of several factors on a response variable. However, deciding on the type of experimental design that best fits the system under investigation is a sequential process, as shown in Figure 4.1.

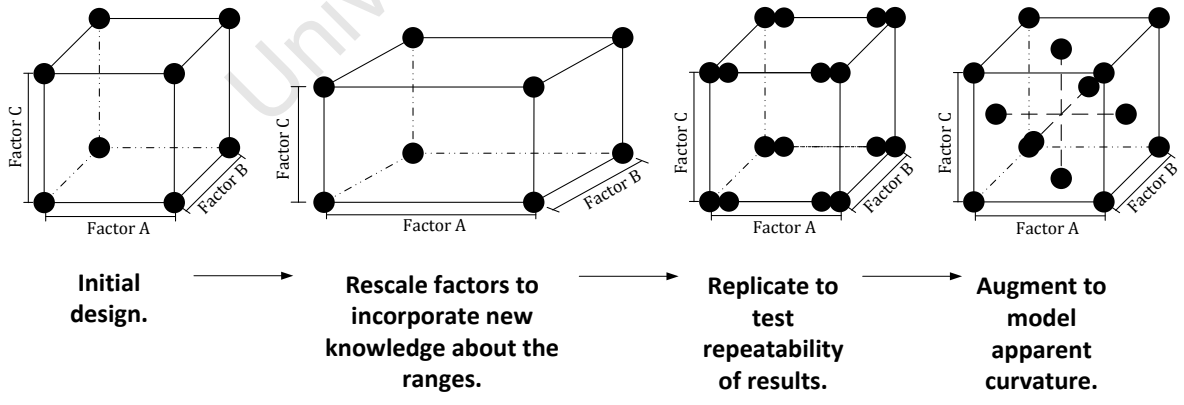

where • denotes each experiment in the factorial design.

•• denotes experiments that were repeated at the same experimental conditions.

Figure 4.1: Sequential experimental design methodology

The initial step begins by screening the factors that are to be used and adjusting the range of the factors to fit within physical constraints. Replicating experimental runs gives an indication of the error. When deciding the final experimental model, consideration of interactions and curvature need to be established. Designing and fitting a first order model gives an estimation of certain potentially important interactions. The design should also allow some information regarding model curvature. Once an indication of how the variable affects the response, a final experimental design can be established.

4.2.1 Screening and rescaling factors

Table 4.1 and Table 4.2 show the proposed concentration limits and temperature ranges for the $FeCl_3$-$MgCl_2$-HCl-$MgSO_4$-H_2O and $ZnCl_2$-HCl-NaCl-H_2O systems, for which the investigation was conducted.

Table 4.1: Levels of aqueous electrolyte composition for solubility measurements for the $FeCl_3$-$MgCl_2$-HCl-$MgSO_4$-H_2O system

Species	Level
$FeCl_3$ [m]	0-2
$MgCl_2$ [m]	1-6
HCl [m]	0-6
Temperature (˚C)	105

where [m] denotes molality in moles of solute per kg of solvent.

Table 4.2: Levels of aqueous electrolyte composition for solubility measurements for the $ZnCl_2$-HCl-NaCl-H_2O system

Species	Level
$ZnCl_2$ [m]	1 - 6
HCl [m]	0.25 - 0.50
Temperature (˚C)	40, 80, 120

where [m] denotes molality in moles of solute per kg of solvent.

Screening and rescaling the concentration and temperature ranges, within each specific system is explained in sections 4.2.1.1 and 4.2.1.2.

4.2.1.1 Rescaling factors for the $FeCl_3$-$MgCl_2$-HCl-$MgSO_4$-H_2O system

The concentration limits initially proposed could not be attained due to the solubility limit of HCl being exceeded, for the $FeCl_3$-$MgCl_2$-HCl-H_2O system, at high temperatures. Figure 4.2 and Figure 4.3 show the effect $FeCl_3$ has on the solubility of HCl at different $MgCl_2$ concentrations at a temperature of 105˚C using OLI Stream Analyser (OLI Systems Inc., 2009).

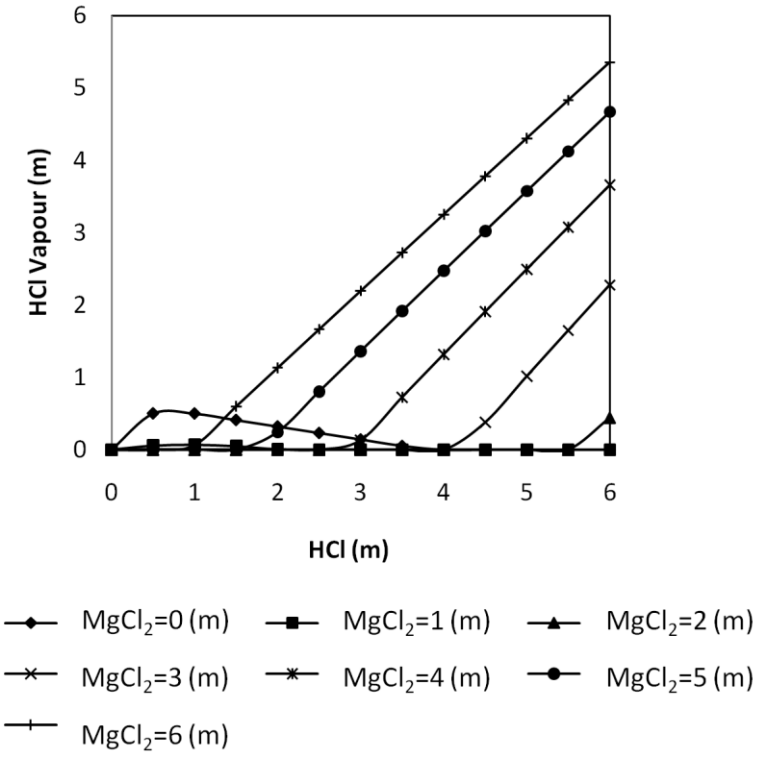

Figure 4.2: The effect of $MgCl_2$ on the solubility of HCl at an Om $FeCl_3$ concentration

The results showed that increasing the concentration of $FeCl_3$ had a slight effect on the solubility of HCl. However, at concentrations above 2 m of $MgCl_2$, within the 0 - 6 m HCl concentration range, HCl vapour evolved thus, exceeding the solubility limit of HCl. Increasing the concentration above 2 m of $MgCl_2$ lead to an increase in the amount of HCl vapour evolved at high concentrations of HCl. The solubility limit was not exceeded at concentrations below 1 m of HCl across the $MgCl_2$ concentration range.

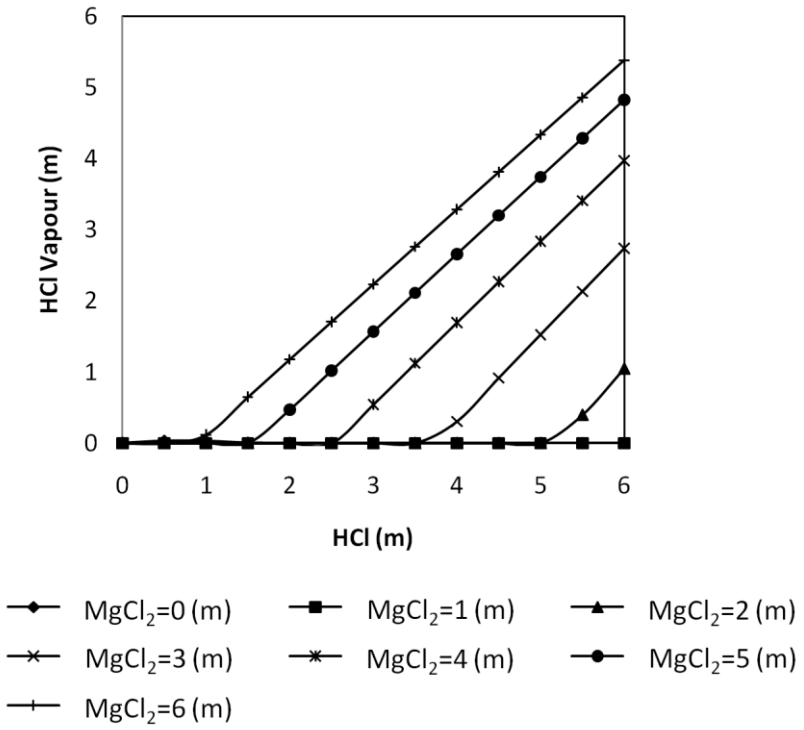

Figure 4.3: The effect of $MgCl_2$ on the solubility of HCl at a 2m $FeCl_3$ concentration

The presence of $MgCl_2$ increases the proton activity in chloride solutions, hence, reducing the acid requirements in the leaching stage of the process as well as increasing the precipitation of $MgSO_4$. Therefore, the initial concentration range of $MgCl_2$ was kept constant and hence, the concentration of HCl was adjusted accordingly, so as not to exceed the solubility limit at specific $MgCl_2$ concentrations.

4.2.1.2 Rescaling factors for the $ZnCl_2$-HCl-NaCl-H_2O system

The 120˚C upper temperature limit initially proposed could not be reached as it exceeded the boiling point of the system. Table 4.3 shows the variation in boiling points over a range of $ZnCl_2$ concentrations. The results showed that the initial estimate of the boiling point (120˚C) were significantly higher than that observed experimentally. The boiling point increased with increasing concentrations of ions in solution as well as after the addition of NaCl.

Table 4.3: Experimentally determined boiling points for various ranges of $ZnCl_2$ and NaCl concentrations

		Boiling point temperature(˚C)	
Experiment	**$ZnCl_2$ [m]**	**Undersaturated with NaCl**	**Saturated with NaCl**
1	1	101.8	109.6
2	4	107.5	114.0
3	6	108.0	117.2

It was found that, within the given concentration ranges of each reagent, the highest temperature that could be attained without exceeding the boiling point was 107˚C. Hence, the upper limit was correspondingly adjusted.

4.2.2 Experimental designs

Experiments aimed at fitting 1st and 2nd order models were carried out using the factorial designs shown below within each specific system. Experiments conditions were conducted at levels given in Table 4.4 and Table 4.7.

4.2.2.1 Experimental designs for the $FeCl_3$-$MgCl_2$-HCl-$MgSO_4$-H_2O system

Table 4.4: Levels of factors varied for solubility measurements for the $FeCl_3$-$MgCl_2$-HCl-$MgSO_4$-H_2O system at a temperature of 105˚C

		Factors/levels			
		-2	**-1**	**0**	**2**
Phase 1	**$FeCl_3$ [m]**	0.000	-	1.000	2.000
	$MgCl_2$ [m]	1.000	-	3.500	6.000
	HCl [m]	0.000	1.750	3.500	6.000
Phase 2	**$FeCl_3$ [m]**	0.500	-	1.250	2.000
	$MgCl_2$ [m]	2.250	-	4.125	6.000
	HCl [m]	0.000	-	1.750	3.500
Phase 3	**$FeCl_3$ [m]**	1.000	-	1.500	2.000
	$MgCl_2$ [m]	3.500	-	4.750	6.000
	HCl [m]	0.000	-	1.750	3.500

The experimental design, model building procedure, and sequential experimentation that were used in identifying the region of minimum solubility involved sequential movement from one region to another. Once the interaction between the factors were established, three level factorial designs for fitting the response surfaces were chosen. A face-centred central composite design or face-centred cubes, shown in Figure 4.4, was chosen, as the region of interest which would fit a cuboidal surface rather than a spherical one. This design locates the axial or star points on the centre of the faces of the cube for three variable factors. This model requires only three levels of each factor which would fit a model to give an overall picture of the effect each variable, $FeCl_3$, $MgCl_2$ and HCl, has on the response, solubility of $MgSO_4$.

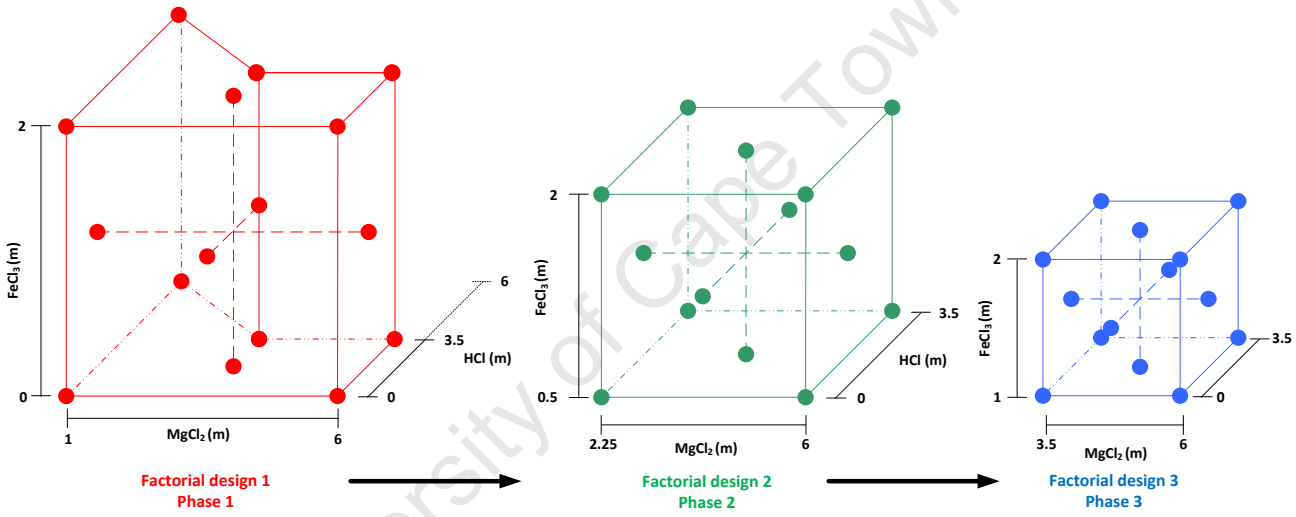

where • denotes each experiment in the factorial design.

Figure 4.4: Sequential face-centred central composite designs used in the process improvement with steepest ascent

Table 4.5 gives the full face-centred central composite designs that were executed. The factorial designs were implemented at each of the 3 levels at a temperature of 105˚C aimed at fitting 1st and 2nd order models. In these cases +1, ½, 0 or -1 levels were used over the concentration ranges listed in Table 4.4 and shown graphically in Figure 4.4.

Table 4.5: Face-centred central composite factorial designs, used for solubility measurements for the $FeCl_3$-$MgCl_2$-HCl-$MgSO_4$-H_2O system at a temperature of 105˚C

		Factors\Levels		
Experiment numbers for Phase 1	**Experiment numbers for Phase 2 and Phase 3**	**$FeCl_3$**	**$MgCl_2$**	**HCl**
P1.1	**P2/P3.1**	-2	-2	-2
P1.2	**P2/P3.2**	2	2	-2
P1.3	**P2/P3.3**	2	0	0
P1.4	**P2/P3.4**	2	-2	-2
P1.5	**P2/P3.5**	-1	2	-2
P1.6	**P2/P3.6**	0	0	-2
P1.7	**P2/P3.7**	-2	-2	2
P1.8	**P2/P3.8**	-2	0	0
P1.9	**P2/P3.9**	2	-2	2
P1.10	**P2/P3.10**	0	0	0
P1.11	**-**	0	-2	-1
P1.12	**-**	0	0	-1
P1.13	**-**	2	2	0
P1.14	**-**	0	0	-1
P1.15	**-**	0	2	-1
P1.16	**-**	2	0	-1
P1.17	**-**	0	0	-1
P1.18	**-**	-2	0	-1
P1.19	**-**	-2	2	0
-	**P2/P3.11**	0	0	0
-	**P2/P3.12**	0	-2	0
-	**P2/P3.13**	0	0	0
-	**P2/P3.14**	0	2	0
-	**P2/P3.15**	2	2	2
-	**P2/P3.16**	0	0	2
-	**P2/P3.17**	-2	2	2

4.2.2.2 Experimental design for hydrate determination

A 2^3 factorial design was used in determining the hydrates that precipitate out at the various concentration levels, shown in Figure 4.5, as well as identifying if any other salts precipitate out.

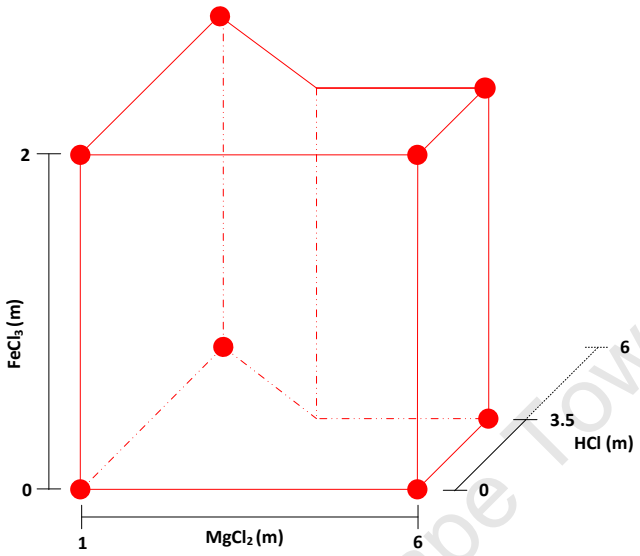

where • denotes each experiment in the factorial design.

Figure 4.5: A 2^3 factorial design used for the $FeCl_3$-$MgCl_2$-HCl-$MgSO_4$-H_2O system in determining the hydrates that are formed

Table 4.6 lists the levels of the factors in the experiments carried out for the 2^3 factorial designs, in determining the hydrates that are formed for the $FeCl_3$-$MgCl_2$-HCl-$MgSO_4$-H_2O system.

Table 4.6: The2^3 factorial design used to determine the hydrates formed in the $FeCl_3$-$MgCl_2$-HCl-$MgSO_4$-H_2O system

	Factors\Levels		
Experiment number	**$FeCl_3$**	**$MgCl_2$**	**HCl**
H1	-1	-1	-1
H2	-1	-1	1
H3	1	1	0
H4	1	-1	1
H5	-1	1	0
H6	1	-1	-1
H7	-1	1	-1
H8	1	1	-1

4.2.2.3 Experimental designs for the $ZnCl_2$-HCl-NaCl-H_2O system

The central composite factorial design, shown in Figure 4.6 was used to evaluate the effect $ZnCl_2$ and HCl has on the solubility of NaCl at each specific temperature, 40˚C, 80˚C and 107˚C at the concentrations shown in Table 4.7.

Table 4.7: Levels of factors varied for solubility measurements for the $ZnCl_2$-HCl-NaCl-H_2O system

	Factor/levels				
	$-\sqrt{2}$	**-1**	**0**	**1**	**$\sqrt{2}$**
$ZnCl_2$ [m]	0.000	1.000	3.500	6.000	7.036
HCl [m]	0.198	0.250	0.375	0.500	0.552
Temperature (^oC)	-	40	80	107	-

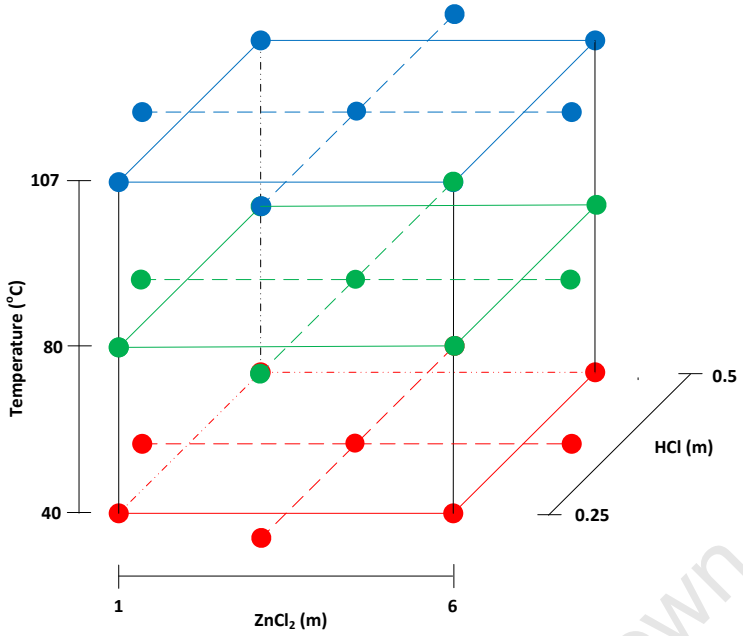

where • denotes each experiment in the factorial design.

Figure 4.6: Central composite factorial designs used for solubility measurements for the $ZnCl_2$-HCl-NaCl-H_2O system at 3 levels

Some levels were not feasible due to negative values. The value -0.355 m for $ZnCl_2$ is impossible for -√2 level. In this case a concentration of 0 m for $ZnCl_2$ was used for the -√2 level. Table 4.8 lists the levels of the factors in the experiments carried out for the central composite factorial design for the $ZnCl_2$-HCl-NaCl-H_2O system

Table 4.8: Centred composite factorial designs used for solubility measurements for the $ZnCl_2$-HCl-NaCl-H_2O system

	Factors\Levels	
Experiment number	**$ZnCl_2$**	**HCl**
N1	1	1
N2	0	0
N3	-1	1
N4	1	-1
N5	-1	-1
N6	0	$\sqrt{2}$
N7	0	0
N8	0	$-\sqrt{2}$
N9	0	0
N10	$\sqrt{2}$	0
N11	$-\sqrt{2}$	0

4.3 Experimental setup

All the experiments were carried out in 450 ml glass sealed reactors illustrated in Figure 4.7. The reactors were fitted with three equally spaced built in glass baffles to ensure complete mixing. The solutions in the reactors were mixed using magnetic stirrers. The top of the reactors were sealed with glass lids with ports for sample collection, spiral reflux condensers to condense any vapour that evolved and thermocouples to measure the temperature in the reactors. The operating temperatures for the experiments were reached using Mica heating bands and maintained to ±0.1˚C of the desired operating temperatures using Gefran 600 temperature controllers, for the duration of the experiment. Due to the acidic nature of the brines, the thermocouples were placed in glass tubes, which were filled with silicone gel and placed in the reactors. The Spiral Reflux condensers were attached to MRC BL-30 refrigerated bath circulators with 96% ethylene glycol that circulated at a temperature of -4˚C.

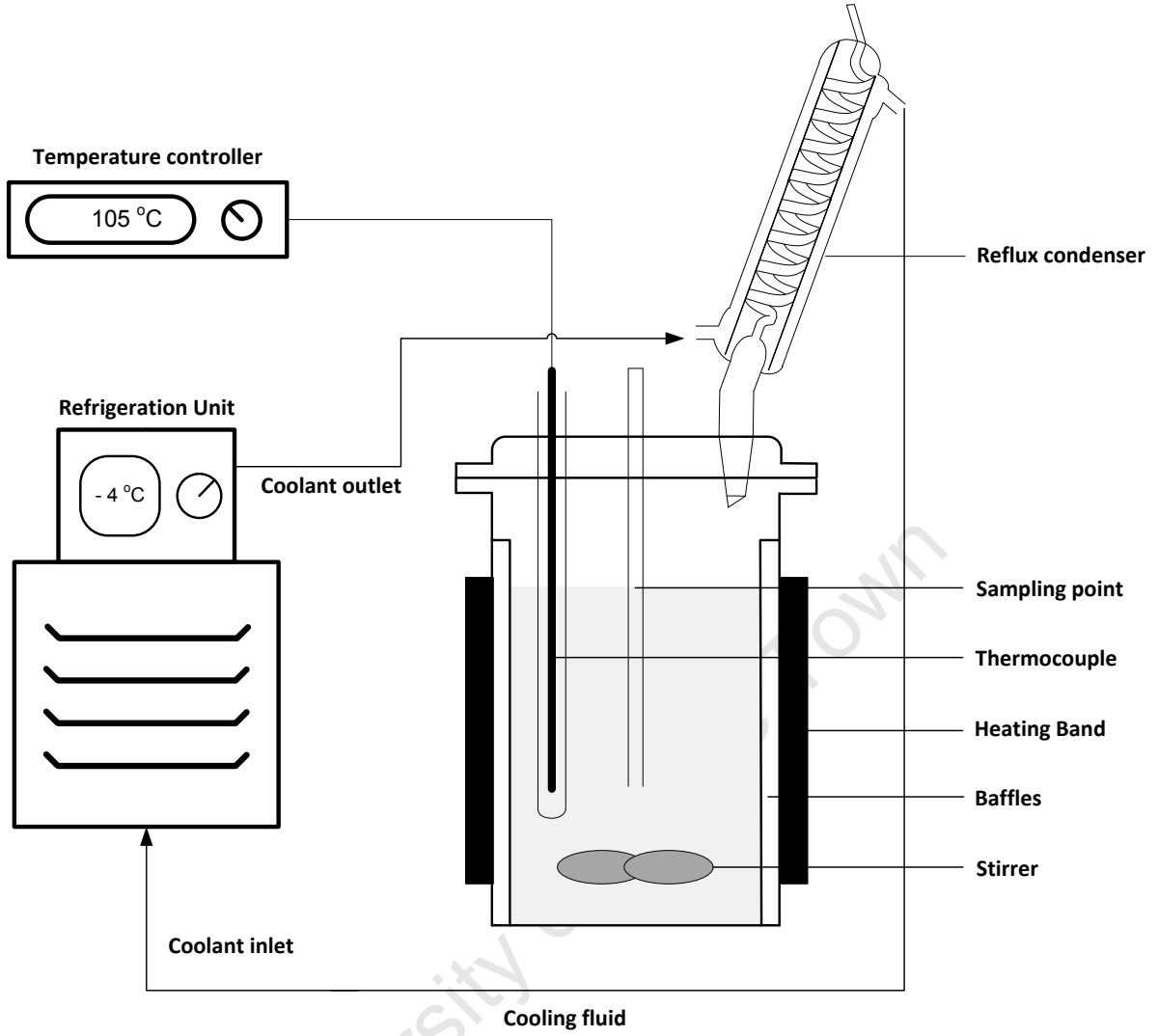

Figure 4.7: Experimental set up

4.4 Experimental procedure

4.4.1 Solubility measurements

The reaction vessels were filled with solutions, as described in Table 4.4 and Table 4.7, with all the background salts except the ones that would be at saturation, either $MgSO_4$ or NaCl. The solutions were heated and once the desired operating temperature had been reached the equilibrium components were added in excess to saturate the solution. The experiments were run for 4 ½ hrs once the supersaturated solutions reached thermal equilibrium. This duration is the residence time for the industrial precipitation reactors.

4.4.2 Hydrates

To characterise which hydrates precipitated out at various background aqueous environments as well as identifying any other salts that precipitate out experiments were repeated at the solubility limit, of the saturated salt, determined in experiments P1. The experimental procedure was repeated according to section 4.4.1 with the exception of not saturating the solution with $MgSO_4$. The amount of $MgSO_4$ added to the solution was determined from experiments P1.

4.5 Sampling and analysis

4.5.1 Solubility Sampling

Samples were collected at predetermined time intervals using a preheated syringe. A 5 ml sample solution was taken and immediately filtered using a Millipore 0.45 µm filter into a glass bottle, preheated at the operating temperature.

4.5.1.1 Solubility analysis

4.5.1.1.1 Solubility analysis for the $FeCl_3$-$MgCl_2$-HCl-$MgSO_4$-H_2O

The filtrate was diluted and sent for analysis to determine the concentration of ions in solution. For the $FeCl_3$-$MgCl_2$-HCl-$MgSO_4$-H_2O system, a brown precipitate formed when the mother liquor was diluted with pure deionised water. Analysis of the precipitate, using X-ray fluorescence (XRF), showed that the main elements were iron and sulphur. Babacan (1971) represented the phase diagram for the conditions for the precipitation of different iron phases from a ferric sulphate solution. His finding showed that basic iron sulphate salts precipitated out between the pH range of 2 - 3. Thereafter, the increase in pH resulted in the precipitation of iron oxy-hydroxides. Hence, it was assumed that the brown precipitate was likely to be $Fe(OH)_3$ or an iron sulphate precipitate.

The 2 m $FeCl_3$ and 0.5 m $MgSO_4$ system was monitored over a 24 hr period. This was to investigate the effect of ageing on the precipitate, as well as observing the change in the concentration of SO_4^{-2}, in the form of solid $BaSO_4$. The diluted system was analysed for the change in concentration of SO_4^{2-} using a turbidity measurement. This measurement measured the concentration of suspended particles in solution, before and after the addition of $BaCl_2$. The absorbance measurement before the addition of $BaCl_2$, was a

measure of the solids formed as a result of the system being diluted. The measurement after the addition of $BaCl_2$, was a combination of the solids formed, upon dilution, and the insoluble $BaSO_4$ precipitate. The curve representing the solids in the sample solution, shown in Figure 4.8, was a measure of how the precipitates aged over time. It can be seen that there was an increase in absorbance over time, indicating an increase in solid formation. The curve represented by the solids present before and after the $BaCl_2$, was a measure of the combination of the brown precipitate and the $BaSO_4$ precipitate. The difference between the 2 curves is the formation of the $BaSO_4$ precipitate and is a measure of the concentration of SO_4^{2-} ions in solution. The concentration of SO_4^{2-} decreased over time as the difference between the two curves decreased, indicating that the SO_4^{2-} ions are absorbed onto the brown precipitate. Work conducted by Jonsson (2003) showed that the precipitate formed is most likely a ferric hydroxyl complex where the SO_4^{2-} ions are absorbed onto the precipitate surface.

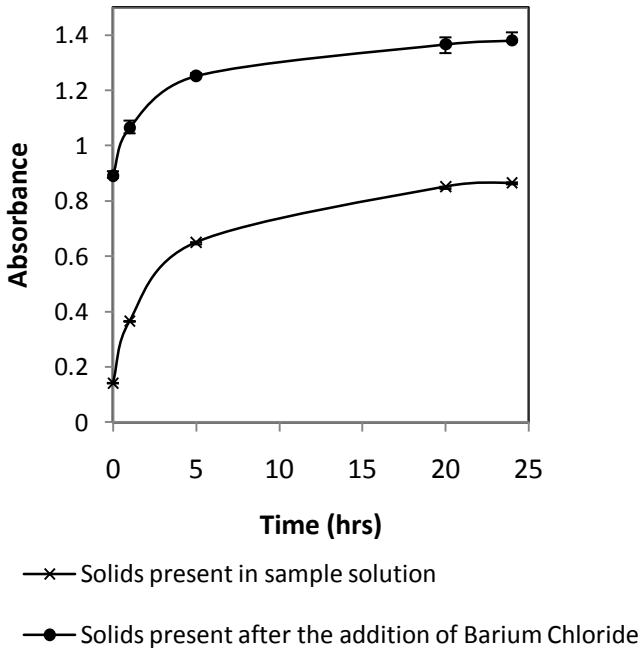

Figure 4.8: The ageing effect of solids formed before and after the addition of barium chloride for a pure water system

The formation of the brown precipitate is a result of the change in pH. Sandenbergh (2007) showed the conditions, temperature and pH, for the precipitation of different iron phases. To prevent the formation of any iron precipitating, the pH has to be kept below 2. Figure 4.9 shows the same system, with 2 m $FeCl_3$ and 0.5 m $MgSO_4$, at a pH

that was adjusted below 2. It can be seen that adjusting the pH prevents the formation of the ferric precipitate and prevents the absorbance of SO_4^{2-} ions as both curves are relatively stable.

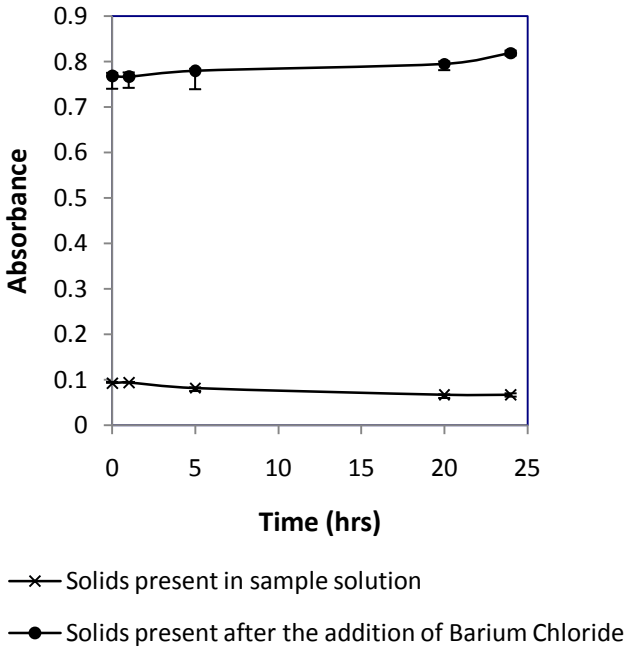

Figure 4.9: The ageing effect of solids formed before and after the addition of barium chloride for an acidified water system

To prevent the precipitation for the $FeCl_3$-$MgCl_2$-HCl-$MgSO_4$–H_2O system the filtrate was diluted using acidified water at a pH of 1.5. To acidify the water, 36% nitric acid was used. The $ZnCl_2$-HCl-NaCl-H_2O system was diluted with deionised water.

Work conducted by Reisman *et al.* (2006) investigated the effects of sample dilution, filter pore size and acidification on sulphate quantification using different analytical methods, a turbidimetric method (TM), ion chromatography (IC) and inductively coupled plasma optical spectrometry (ICP-OES). Results showed that ICP-AES provided the best sulphate recoveries within all factors. Hence, for the $FeCl_3$-$MgCl_2$-HCl-$MgSO_4$–H_2O system ICP-AES was used to measure the concentration of SO_4^{2-} ions as well as the concentration of Mg^{2+} ,Fe^{3+} and Cl^- ions.

4.5.2 Hydrate sampling and analysis

Samples were taken at 4 ½ hour time intervals using preheated syringes. The samples were taken and immediately filtered, under vacuum, in a heated filtration system shown in Figure 4.10. Silicon oil, at the operating temperature of the experiment, was circulated through the glass filter to ensure the solution was maintained, at the operating temperature, while the solution was filtered. The filtered solid was washed using 99% methanol to remove as much of the entrained mother liquor. The washed solid was placed on X-ray diffraction (XRD) sample holders and sealed using parafilm, to ensure the solid did not hydrate, before it was sent for analysis using XRD. Scanning electron microscopy (SEM) was used to identify the morphology of the precipitates that formed.

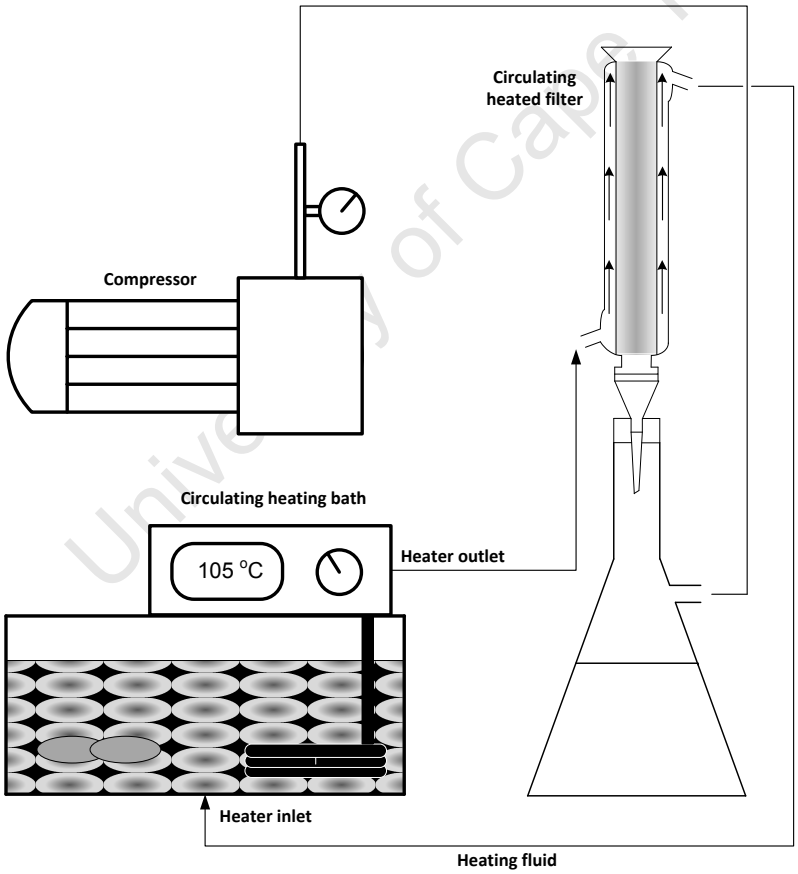

Figure 4.10: Heated filtration system used to filter the precipitated solid at elevated temperatures

References

Jonsson, J. (2003), Phase transformation and surface chemistry of secondary iron minerals formed from acid mine drainage. PhD Thesis, Umea University. Umea.

Babcan, J., 1971. Synthesis of jarosite—KFe3(SO4)2(OH)6. Geol. Zb.22 (2), p299–304.

OLI Systems Inc, 2009. Stream Analyser version 3.0.1.0, Morris Plains, New Jersey.

Reisman, D.J., Sundaram, V., Al-Aded, S., Allen, D. (2007) Statistical validation of sulfate quantification methods used for analysis of acid mine drainage. Talanta, vol. 71, p303-311.

Sandenderg, R.F. (2007), Influence of temperature and pH on the quality of metastable iron phases produced in zinc-rich solutions. Hydrometallurgy, vol. 86, p178-190.

Chapter 5. Results and Discussion

5.1 $FeCl_3$-$MgCl_2$-HCl-$MgSO_4$-H_20 system

5.1.1 Aqueous thermodynamic modelling of the $FeCl_3$-$MgCl_2$-HCl-$MgSO_4$-H_20 system

Using OLI System Inc Stream Analyser (OLI Systems Inc., 2009) the system was modelled using the conditions specified in Table 5.4 to predict the precipitation point of $MgSO_4 \cdot H_20$ as well as to investigate the effect each species, $FeCl_3$, $MgCl_2$ and HCl, has on the solubility of $MgSO_4$ at 105˚C.

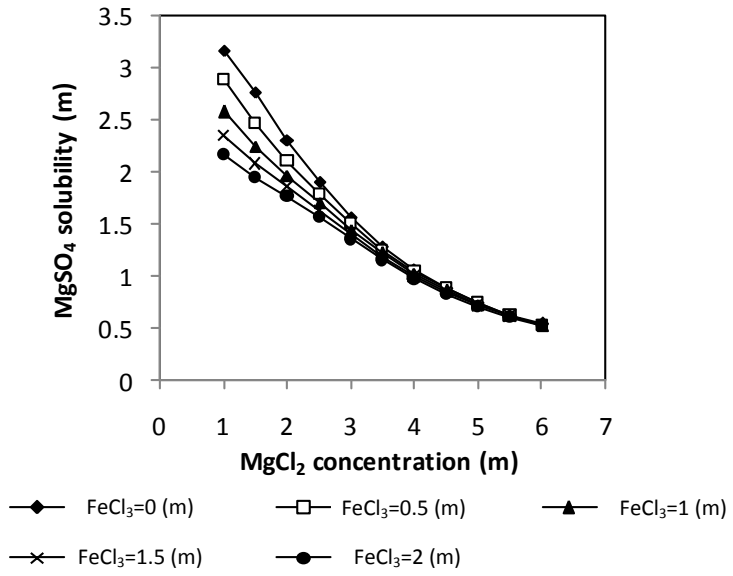

Figure 5.1: Thermodynamic modelled $MgSO_4$ solubility for the $FeCl_3$-$MgCl_2$-$MgSO_4$-H_20 system at varying concentrations of $FeCl_3$ and $MgCl_2$ at a temperature 105°C

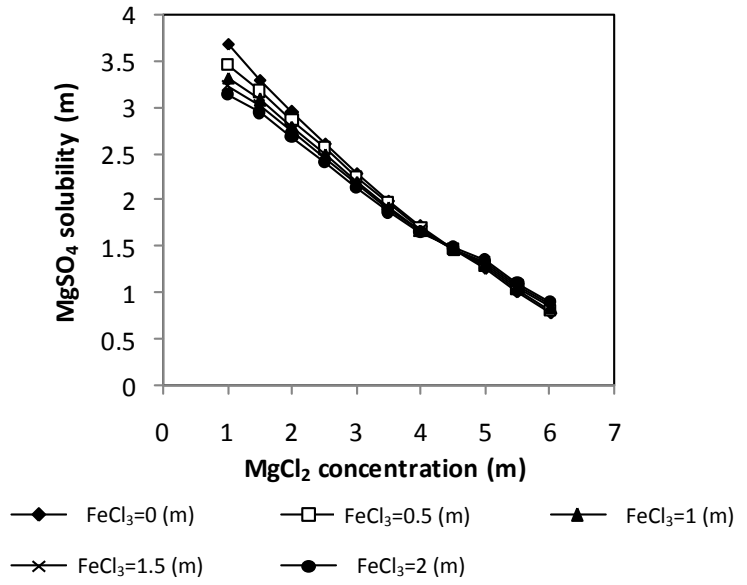

Figure 5.2: Thermodynamic modelled $MgSO_4$ solubility for the $FeCl_3$-$MgCl_2$-HCl-$MgSO_4$-H_20 system at varying concentrations of $FeCl_3$ and $MgCl_2$ at an HCl concentration of 1.75 m and temperature 105°C

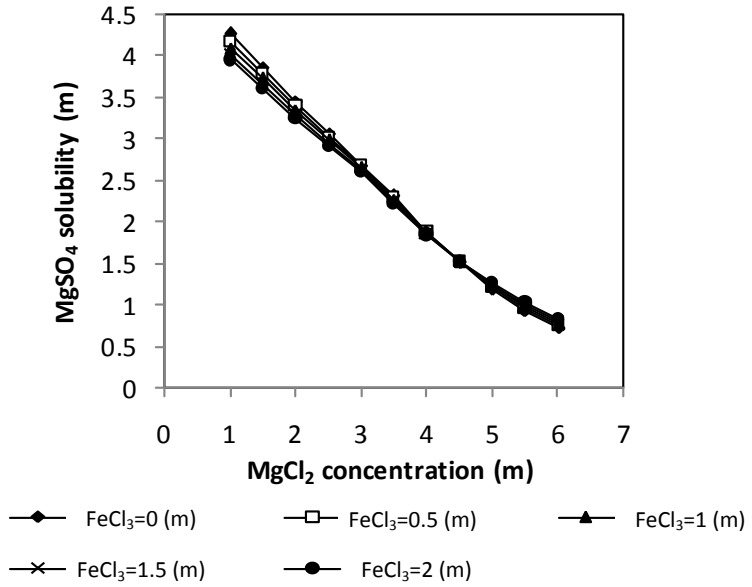

Figure 5.3: Thermodynamic modelled $MgSO_4$ solubility for the $FeCl_3$-$MgCl_2$-HCl-$MgSO_4$-H_20 system at varying concentrations of $FeCl_3$ and $MgCl_2$ at an HCl concentration of 3.5 m and temperature 105°C

The results presented in Figures 5.1, 5.2 and 5.3 show similar trends. An increase in the concentration of $MgCl_2$ results in a decrease in the solubility of $MgSO_4$ with an increase in the concentration of $FeCl_3$, and an increase in solubility of $MgSO_4$ with an increase in the concentration of HCl.

The change in the solubility of $MgSO_4$ for the $FeCl_3$-$MgCl_2$-$MgSO_4$-H_2O system is shown in Figure 5.1. It can be seen that at fixed low concentrations of $MgCl_2$ an increase in $FeCl_3$ results in the largest difference in the $MgSO_4$ solubility. However, this change in $MgSO_4$ solubility is minimised with an increase in $MgCl_2$ concentration until an $MgCl_2$ concentration of 4m, after which $FeCl_3$ has no influence on the $MgSO_4$ solubility.

With the introduction of HCl, the solubility of $MgSO_4$ increases at fixed concentrations of $MgCl_2$ as shown in Figure 5.2. As the concentration of HCl increases, there is a further increase in the $MgSO_4$ solubility at the same fixed $MgCl_2$ and $FeCl_3$ concentrations as shown in Figure 5.3. The introduction of HCl also minimises the change in the solubility of $MgSO_4$ at fixed low concentrations of $MgCl_2$, as a result of an increase in $FeCl_3$, as seen in Figure 5.1. A further increase in the HCl concentration results in a smaller difference between the $MgSO_4$ solubility. Therefore, increasing the concentration of $FeCl_3$ has minimal influence on the solubility of $MgSO_4$ with an increase in the HCl across the $MgCl_2$ concentration range. The aqueous thermodynamic modelling results have shown that the concentration of $MgCl_2$ has the most pronounced effect on the solubility of $MgSO_4$ in the specified system.

5.1.2 Experimentally determined solubilities for the $FeCl_3$-$MgCl_2$-HCl-$MgSO_4$-H_20 system

Figures 5.4, 5.5 and 5.6 illustrate the surface responses generated using a quadratic model. The model is used to illustrate the effect of varying the concentrations of $MgCl_2$ and $FeCl_3$. This modelling work was in accordance with the concentration ranges specified in Table 5.4, on the solubility of $MgSO_4$ at HCl concentrations of 0 m, 1.75 m and 3 m respectively at a temperature of 105˚C.

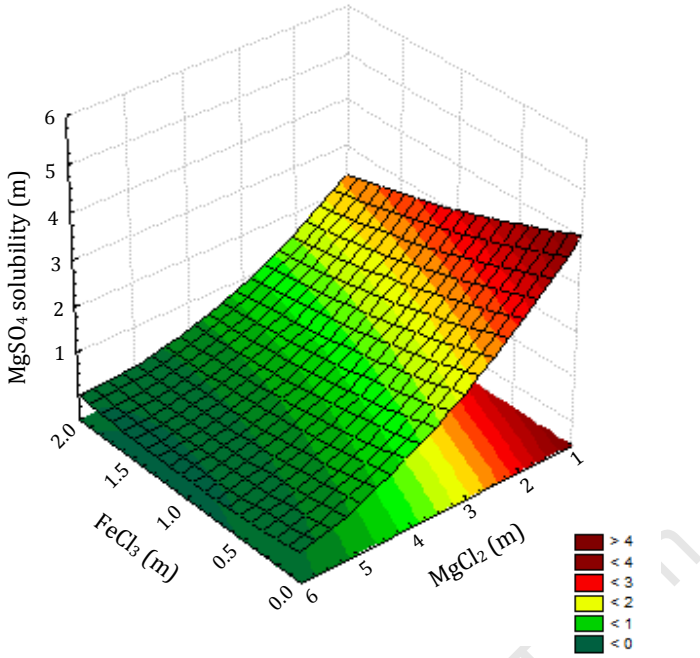

Figure 5.4: A surface plot of experimentally obtained solubility data for $MgSO_4$ as a function of varying $FeCl_3$ and $MgCl_2$ concentrations at an HCl concentration of 0 m at a temperature of 105°C generated using a quadratic model

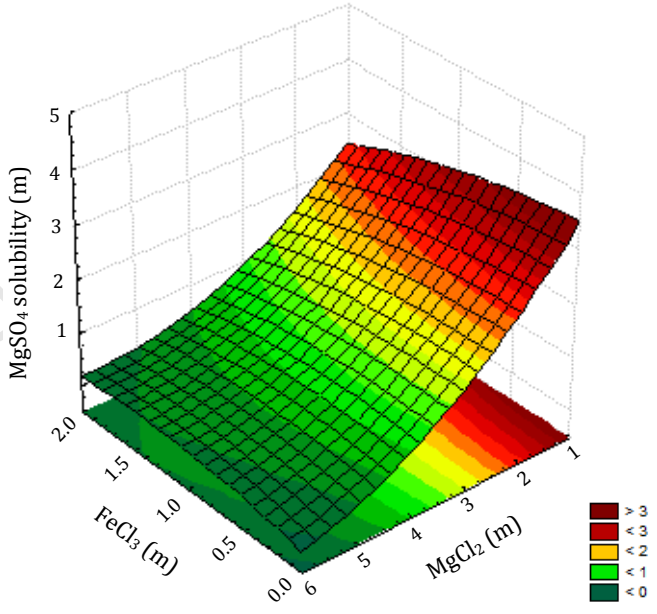

Figure 5.5: A surface plot of experimentally obtained solubility data for $MgSO_4$ as a function of varying $FeCl_3$ and $MgCl_2$ concentrations at an HCl concentration of 1.75 m at a temperature of 105°C generated using a quadratic model

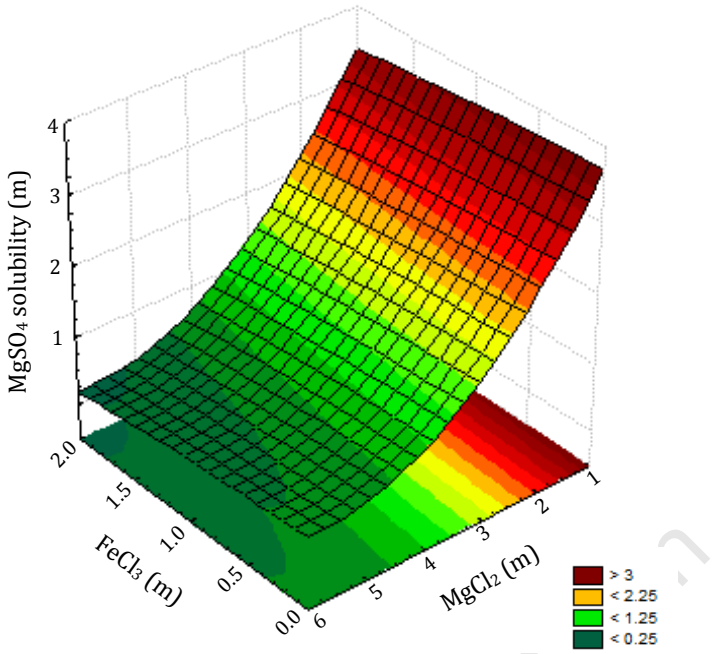

Figure 5.6: A surface plot of experimentally obtained solubility data for $MgSO_4$ as a function of varying $FeCl_3$ and $MgCl_2$ concentrations at an HCl concentration of 3.5 m at a temperature of 105°C generated using a quadratic model

5.1.2.1 The effect of $FeCl_3$ on the solubility of $MgSO_4$

The surface plots that are generated in Figures 5.4, 5.5 and 5.6 illustrate similar trends i.e. it can be seen that, at low concentrations of $MgCl_2$, increasing the concentration of $FeCl_3$ decreases the solubility of $MgSO_4$. As the $MgCl_2$ concentration increases the effect of $FeCl_3$ is minimised, showing that at high concentrations of $MgCl_2$, $FeCl_3$ does not have a significant influence on the solubility of $MgSO_4$. The same result is observed at different concentrations of HCl.

When iron hydrolyses in aqueous solution, as is the case with most metal ions, the metal cations form hexa-coordination aqua complexes at low pH (Jolivet *et al.*, 2004). An increase in the pH leads to the deprotonation of these metal complexes through polymerisation reactions. This polymerisation can proceed through two different condensation mechanisms, olation and oxilation. The formation of hydroxo bridges in aquohydroxo complexes through the condensation of the hydroxo complexes is called olation. The condensation polymerisation of oxohydroxo complexes leads to the formation of oxo-dimers is called oxolation which results in the displacement of a water molecule (Jolivet *et al.*, 2004). However, any ferric complex whose anion moiety is a

weaker ligand will be replaced by ligands which form stronger coordination bonds with the metal cation. In the presence of sulphate anions, the sulphur atom is highly electronegative and will replace the water molecules attached to the iron cation to form water soluble iron complexes (Brown *et al.*, 1992).

Work conducted by Lister and Rivington (1955) investigated the effect of varying acidity and ferric concentrations at high and low sulphate concentrations on the formation of ferric sulphate complexes. Their finding showed that, at low sulphate concentrations (0.001 m) the following equilibria exist:

$$Fe^{3+} + SO_4^{2-} \leftrightarrow FeSO_4^{+},$$

$$Fe^{3+} + HSO_4^{-} \leftrightarrow FeHSO_4^{2+},$$

$$H^{+} + SO_4^{2-} \leftrightarrow HSO_4^{-}.$$

The effect of varying the acid concentration was shown to remove absorbing ions, presumably $FeSO_4^{+}$, or to introduce other ions, presumably $FeHSO_4^{2+}$, or both. However, at higher sulphate concentrations (0.05 m) $Fe(SO_4)^{2-}$ and $FeSO_4 \cdot HSO_4$ are formed.

The interactions and bond formations between metal ions and sulphate ligands lead to the formation of water-soluble iron complexes. The increase in iron concentration thus increases complex formation which in turn leads to an increase in the solubility of $MgSO_4$.

5.1.2.2 The effect of $MgCl_2$ on the solubility of $MgSO_4$

The surface plots that are generated in Figures 5.4, 5.5 and 5.6 show that an increase in $MgCl_2$ concentration results in a decrease in the $MgSO_4$ solubility. The solubility slope changes from a relatively steep slope to a shallower slope as the concentration of $MgCl_2$ increases. Thus, an increase in the concentration of $MgCl_2$ has a smaller effect on the solubility of $MgSO_4$ at concentrations higher than 4 m. The depressing effect of magnesium ions on the $MgSO_4$ solubility is due to the common ion effect where the presence of the common ion drives the dissociation equilibrium of $MgSO_4$ to form more of the solid $MgSO_4$. The experimental data generated by Campbell *et al*. (1934) and Bousmina *et al*. (2003) presented solubility results of the $MgSO_4$-$MgCl_2$-H_20 system as a

function of temperature at three different $MgCl_2$ concentrations. Results concur with the findings in this study.

5.1.2.3 The effect of HCl on the solubility of $MgSO_4$

In general the solubility of $MgSO_4 \cdot H_2O$ is directly proportional to the concentration of HCl. The presence of non-common ions increases the solute solubility on an account of an increase in ionic strength. The increase in the concentration of HCl increases the number of protons which form bonds between the free sulphate ions, resulting in the formation of bisulphate complexes. The formation of bisulphate complexes thus reduces the free sulphates in the solution and allowing the system to dissolve more $MgSO_4$ solute. Hence, the increase in HCl levels increases the formation of bisulphate complexes, in the presences of acids, and increases the solubility of $MgSO_4$, as shown in Figures 5.4, 5.5 and 5.6.

5.1.3 Characterisation of the hydrates of $MgSO_4$ that form under varying background aqueous environments

5.1.3.1 XRD results

Five monoclinic hydrates of $MgSO_4$ (hexa, pent-, tetra-, five-forths and mono-hydrates) exist when in contact with aqueous solutions of the salt at the temperatures near their boiling points. The hexa-hydrate is the most stable phase in the temperature range between 48 and 68˚C and could under certain conditions, remain stable up to a temperature of 100˚C. Van't Hoff *et al*. (1901) identified that the transition from the hexa-hydrate to the mono-hydrate occurs at a temperature of 68˚C. The mono-hydrate remains the stable phase up to a temperature of 240˚C. However, between the temperatures of 68 and 72˚C, a transition of the hexa-hydrate into the five-fourths hydrate occurs. A transition of the penta-hydrate into the tetra-hydrate occurs close to a temperature of 77.5˚C.

Magnesium is one of the alkali earth metals found in the third period and second group of the periodic table. Having a high charge to radius ratio, it has a tendency to be hydrated instead of polarised in solutions. The Mg^{2+} ion exists predominantly as the hexa-aqua complex $[Mg(H_2O)_6]^{2+}$ where the six water molecules bond with the inner sphere of the hydrated Mg^{2+} ion. The sulphate ions in the complex form hydrogen bonds with the water molecules. These water molecules are considered to define the structure

of the complex it bonds to. Hence, both $Mg^{2+}$and SO_4^{2-} readily hydrate, especially in dilute aqueous solutions. Within mixed halide-sulphate solutions, the most stable complex is the hexa-aqua complex. However other complexes can exist in under different aqueous environments.

Due to the low levels of supersaturation required for the nucleation of the hexa-hydrate complexes, these hexa-hydrate complexes have the fastest crystallisation rates. The formation of the lower hydrates requires a partial dehydration of the hexa-aqua complex and the building of more complex, interconnected, co-ordination polyhedral structures. The structure of the penta and tetra-hydrate complexes consists of mixed tetrahedral SO_4^{2-} and mixed magnesium $[Mg(H_20)_4O_2]^{2+}$ complexes. The presence of free hydrogen bonded water molecules in the penta-hydrate structure and the bonding of the polyhedral distinguishes between the penta and tetra-hydrates. The penta-hydrate forms a chain structure, which has non-coordinated hydrogen bonded H_2O molecules between the two oxygen atoms of the same SO_4^{2-} tetrahedron and the coordination of two neighbouring Mg^{2+} ions. The tetra-hydrate structure consists of a ring formed by two SO_4^{2-} tetrahedrals with four oxygen atoms forming bridge bonds with two of the magnesium octahedrals. The formation of a ring within the $MgSO_4{\cdot}4H_2O$ structure is thus more stable than the chain structure of $MgSO_4{\cdot}5H_2O$. The monohydrate structure forms at the slowest crystallisation rate as it forms the most complicated coordination pattern. The $MgSO_4{\cdot}H_2O$ is a chain-bonded structure consisting of a mixed $[Mg(H_20)_2O_4]^{2+}$ octahedral. The octahedral is formed by the four oxygen atoms from the four SO_4^{2-} tetrahedrals and the two H_2O molecules. Each of the H2O molecules are common with the two Mg^{2+}octahedrals (Balarew *et al.*, 2001).

Work conducted by Robson (1927) investigated the solubility curves of $MgSO_4{\cdot}6H_2O$, $MgSO_4{\cdot}5H_2O$, $MgSO_4{\cdot}4H_2O$ and $MgSO_4{\cdot}H_2O$ over the temperature range of 68 to 240˚C His findings are summarised in Figure 5.7.

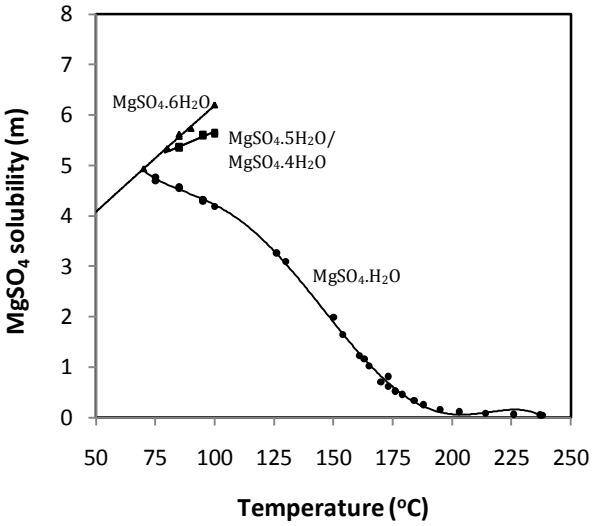

Figure 5.7: The solubility of $MgSO_4$ with the corresponding hydrates formed as a function of temperature (adapted from Robson (1927))

Results showed that the solubility curves for $MgSO_4 \cdot 5H_2O$ and $MgSO_4 \cdot 4H_2O$ lie marginally above the curve for the $MgSO_4 \cdot H_2O$ at 95˚C. It was observed that the solubility curves of $MgSO_4 \cdot 6H_2O$ and $MgSO_4 \cdot 4H_2O$ were close together in the aqueous solution at 100°C. However, upon further stirring, the $MgSO_4 \cdot 6H_2O$ disappeared resulting in a slight decrease in the solubility. Thus it was assumed that the $MgSO_4 \cdot 6H_2O$ curve lies slightly above that of the $MgSO_4 \cdot 4H_2O$. The solubility curve for $MgSO_4 \cdot H_2O$ was found to decrease rapidly with the increase in temperature from 68 to 200˚C. It then decreases slowly up to a temperature of 238˚C. Equilibrium was reached slower at temperatures below 200˚C and faster at temperatures above 200˚C. Hence between the temperature ranges of 70-110˚C the precipitation of a specific hydrate or hydrates cannot be established.

Figure 5.8 shows the effect of changing the background aqueous environment has on the formation of the different hydrates of magnesium sulphate. The background aqueous environment was varied according to the experimental design represented in Table 4.6. Due to the hydrophilic nature of $MgSO_4$, during the XRD analysis the precipitates were covered with a polyvinylidene chloride sheet, commonly known as "cling wrap", which provided a barrier for water absorption. However, it was observed that the presence of the cling wrap produced a specific diffraction pattern, represented by the grey curves within each XRD plot in Figure 5.8, located over 2θ ranges of 24-28

and 39-41. As a result of this, the peaks found over these ranges were difficult to distinguish.

It can be seen that keeping the $MgCl_2$ and HCl concentrations constant while varying the concentration of $FeCl_3$ has no effect on the hydrate or hydrates that form within each position A, B, C and D as shown in Figure 5.8. Within each of the respective positions, the $MgSO_4 \cdot H_2O$ precipitates out independently or with a combination of the $MgSO_4 \cdot 1.25H_2O$ or the $MgSO_4 \cdot 6H_20$ hydrate. At position A, a combination of the $MgSO_4 \cdot H_2O$ and the $MgSO_4 \cdot 6H_2O$ forms. However, by increasing the concentration of $MgCl_2$ from 1m to 6m while keeping the concentration of HCl fixed at 0 m, the result shows the formation of the $MgSO_4 \cdot H_2O$ and $MgSO_4 \cdot 1.25H_2O$ at position B. Increasing the concentration of HCl from 0 m to 3.5 m whilst maintaining the concentration of $MgCl_2$ at 6 m results in the precipitation of only $MgSO_4 \cdot H_2O$ as shown at position C. The same result is observed when increasing the concentration of HCl from 0 m to 6 m at a constant $MgCl_2$ concentration of 1m, as seen at position D.

Thus, an increase in $MgCl_2$ and HCl concentrations has a dehydrating effect on the formation of the hydrates, with HCl having a more pronounced effect. Balarew *et al.* (2001) investigated the formation of $MgSO_4$ hydrates within a $MgCl_2$-$MgSO_4$-H_20 system at temperatures of 50 and 75˚C. At a temperature of 50˚C, their findings showed the presences of four crystallisation fields, $MgCl_2 \cdot 6H_2O$, $MgSO_4 \cdot 6H_20$, $MgSO_4 \cdot 4H_2O$ and $MgSO_4 \cdot H_2O$, which formed within the metastable fields of $MgSO_4 \cdot 7H_20$, $MgSO_4 \cdot 6H_20$ and $MgSO_4 \cdot 4H_20$ respectively. At 75˚C, $MgSO_4 \cdot H_20$ formed a stable crystallisation hydrate within the $MgSO_4 \cdot 6H_20$ and $MgSO_4 \cdot 4H_2O$ metastable fields. At both temperatures the increase in the concentration of $MgCl_2$ resulted in the dehydration of the hydrated magnesium sulphate. The $MgCl_2$-$MgSO_4$-H_2O system was also studied by Campbell *et al.* (1934) at 100˚C. Their results confirmed the dehydration effect of the $MgCl_2$ solution and the precipitation of the $MgSO_4 \cdot H_2O$ at the high temperatures.

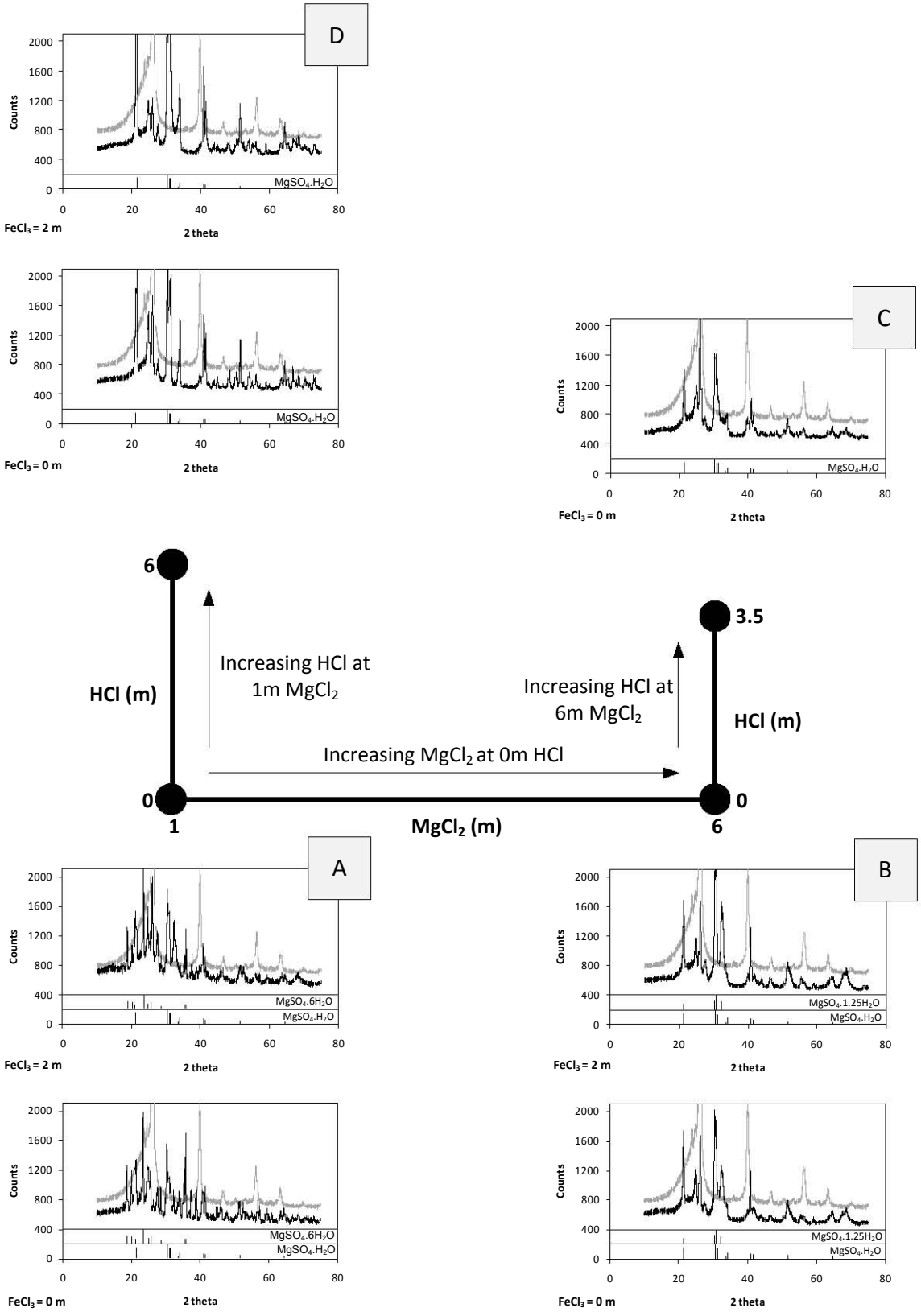

Figure 5.8: XRD scans identifying the hydrates of $MgSO_4$ that form under different background aqueous environments at a temperature of 105°C

5.1.3.2 SEM results

Figure 5.9 shows the morphology of the precipitation of the hydrates prepared at the experimental conditions specified in Table 4.6.

The precipitates that form at position A are at a varied concentration of 0 m and 2 m $FeCl_3$ and a constant concentration of 1 m $MgCl_2$. The increase in the concentration of $FeCl_3$ shows a change in the morphology of the precipitate that forms. At a concentration of 0m $FeCl_3$, the precipitate that forms does not have a definitive crystal structure. However, an increase in the concentration of $FeCl_3$ to 2 m results in a prism precipitate. It should be noted that the precipitate that forms is a mixture of $MgSO_4 \cdot 6H_2O$ and $MgSO_4 \cdot H_20$, as shown in Figure 5.9, and that the results obtained are qualitative rather than quantitative. Hence, the images obtained could be that of the $MgSO_4 \cdot 6H_2O$ or the $MgSO_4 \cdot H_2O$ or a mixture of the two. Thus, the observation in the change in morphology due to the increase in $FeCl_3$ concentration could be as a result of the different hydrates that form or a change in morphology of a single hydrate.

The results show that by increasing the concentration of $MgCl_2$ to 6 m, at position B, the precipitates have no definitive crystal structure at $FeCl_3$ concentrations of 0m and 2m. The same result is observed at position C and D.

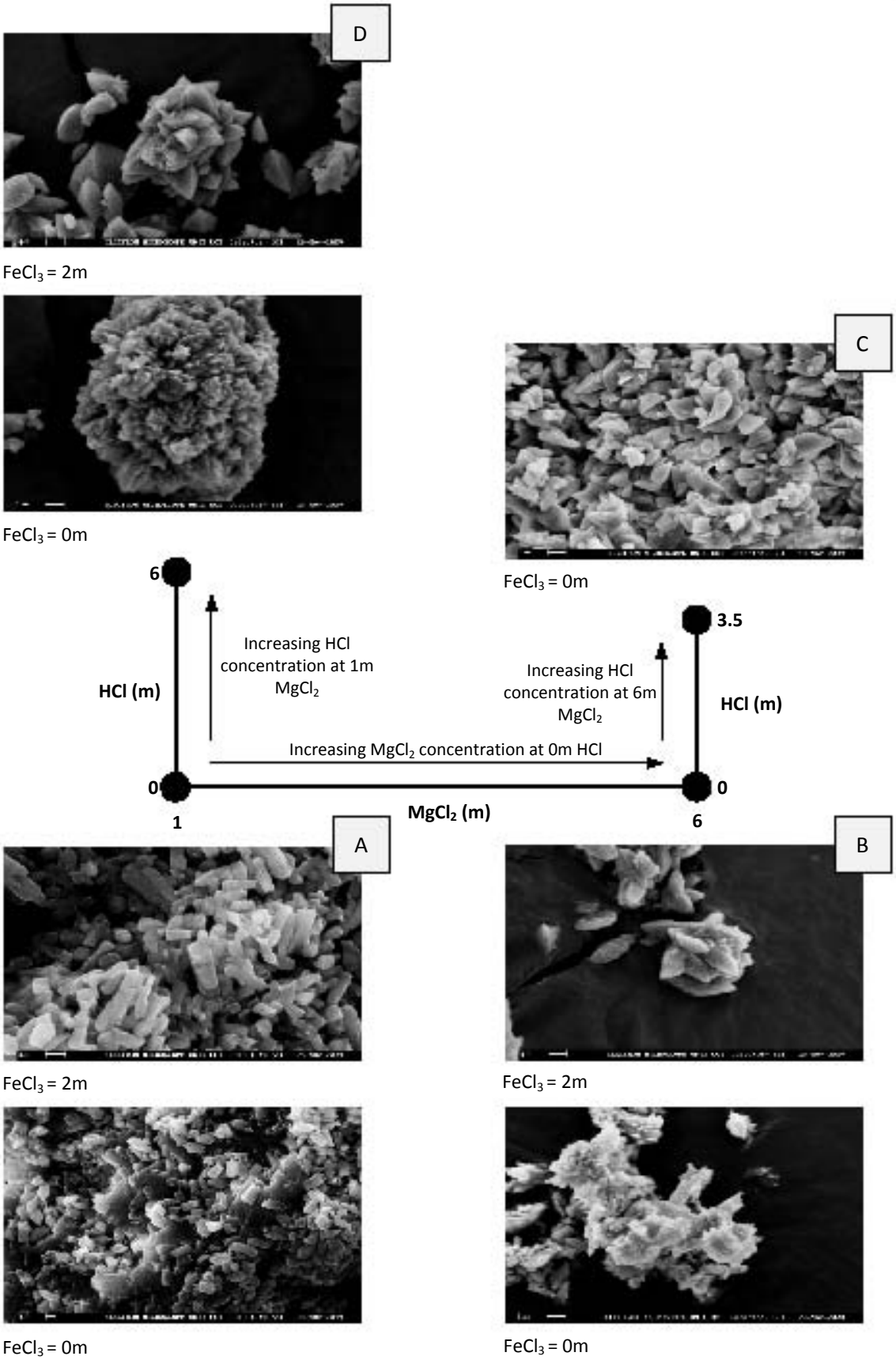

Figure 5.9: SEM pictures of the effect the background aqueous environment has on the morphology of the precipitated hydrates of $MgSO_4$ at a temperature of 105°C

5.1.4 Statistical analysis of the experimental results for the $FeCl_3$-$MgCl_2$-HCl-$MgSO_4$-H_2O system

The main objective of the statistical analysis of the experimental data is to identify the factor/s that have the greatest impact on the solubility of $MgSO_4$ within each factorial phase. The analysis also determines the most applicable model based on how accurately it describes the system. The analysis of the experimental data was analysed by Design Expert Version 8 (Stat Ease Inc, 2009). Table 5.1 and 5.2 shows the notation and units of the response and factors used in the models.

Table 5.1: Notations and units of the responses used in the experimental models for the $FeCl_3$-$MgCl_2$-HCl-$MgSO_4$-H_2O system

Response	Notation	Unit
$MgSO_4$ solubility , Phase 1	$MgSO_{4Phase1}$	mol/kg solvent
$MgSO_4$ solubility , Phase 2	$MgSO_{4Phase2}$	mol/kg solvent
$MgSO_4$ solubility , Phase 3	$MgSO_{4Phase3}$	mol/kg solvent

Table 5.2: Notations and units of the factors used in the experimental models for the $FeCl_3$-$MgCl_2$-HCl-$MgSO_4$-H_2O system

Factors	Notation	unit
$FeCl_3$ concentration	X_{FeCl_3}	mol/kg solvent
$MgCl_2$ concentration	X_{MgCl_2}	mol/kg solvent
HCl concentration	X_{HCl}	mol/kg solvent

5.1.4.1 Summary of the models fitted for the 3 factorial phases

Tables 5.3, 5.4 and 5.5 below shows the type of function used to best fit the data, p-values and R^2 values, that were used to determine which model best fits the experimental data to accurately describe the solubility of $MgSO_4$ at a temperature of 105˚C within the three factorial phases.

Table 5.3: Summary of statistical parameters used to fit the data for phase 1 for the $FeCl_3$-$MgCl_2$-HCl-$MgSO_4$-H_20 system at 105°C

Model	Model P-value	Lack of fit P-value	Adjusted R^2	
Linear	< 0.0001	0.0084	0.8209	
2FI	0.5160	0.0076	0.8132	
Quadratic	**< 0.0001**	**0.0768**	**0.9834**	**Suggested**
Cubic	0.0768		0.9982	

Table 5.4: Summary of statistical parameters used to fit the data for phase 2 for the $FeCl_3$-$MgCl_2$-HCl-$MgSO_4$-H_20 system at 105°C

Model	Model P-value	Lack of fit P-value	Adjusted R^2	
Linear	< 0.0001	0.0001	0.8851	
2FI	0.9260	0.0001	0.8541	
Quadratic	**0.0120**	**0.0003**	**0.9605**	**Suggested**
Cubic	0.0003		1.0000	

Table 5.5: Summary of statistical parameters used to fit the data for phase 3 for the $FeCl_3$-$MgCl_2$-HCl-$MgSO_4$-H_20 system at 105°C

Model	Model P-value	Lack of fit P-value	Adjusted R^2	
Linear	< 0.0001	0.0191	0.9074	
2FI	0.2693	0.0202	0.9185	
Quadratic	**0.0052**	**0.0840**	**0.9834**	**Suggested**
Cubic	0.0840		0.9979	

The null hypothesis represents the hypothesis of no change or no effect. The p-values are a measure of testing whether the null hypothesis is true or should be rejected. Small probability values, values less than 0.05, call for the rejection of the null hypothesis**.** The R^2 value is a measure of the amount of variation around the mean, explained by the model, adjusted for the number of terms in the model. The R^2 value decreases as the number of terms in the model increases if those additional terms do not add value to the model. Considering the p-values and R^2 values the quadratic model was chosen, for each response at the three factorial phases, to best describe how the background aqueous environment affects the solubility of $MgSO_4$.

5.1.4.2 Second order models

The statistical analysis results obtained for the second order models is given in Appendix C1.

5.1.4.2.1 Fitting a second order model to the $MgSO_4$ solubility data from the factorial study

The fitted quadratic regression models for the solubility of $MgSO_4$ as a function of the process parameters at a temperature of 105˚C within each of the different factorial phases is shown in Tables 5.6, 5.7 and 5.8 respectively. The standard errors (SE) and p-values are also given.

Table 5.6: 2nd order model for the solubility of $MgSO_4$ within factorial phase 1

Factors	Coefficient Estimate	SE	P-value
Intercept	1.0701	0.0635	
(X_{FeCl_3})	-0.1391	0.0500	0.0239
(X_{MgCl_2})	-1.0958	0.1014	< 0.0001
(X_{HCl})	0.2330	0.1163	0.0801
$(X_{FeCl_3})(X_{MgCl_2})$	0.4348	0.0642	0.0001
$(X_{FeCl_3})(X_{HCl})$	0.3612	0.0650	0.0005
$(X_{MgCl_2})(X_{HCl})$	0.4484	0.1241	0.0068
$(X_{FeCl_3})^2$	-0.0338	0.0820	0.6912
$(X_{MgCl_2})^2$	0.8283	0.0885	< 0.0001
$(X_{HCl})^2$	-0.0867	0.1689	0.6216

Table 5.7: 2nd order model for the solubility of $MgSO_4$ within factorial phase 2

Factors	Coefficient Estimate	SE	P-value
Intercept	0.7104	0.0691	
(X_{FeCl_3})	-0.1087	0.0616	0.1282
(X_{MgCl_2})	-0.9220	0.0616	< 0.0001
(X_{HCl})	0.1057	0.0616	0.1371
$(X_{FeCl_3})(X_{MgCl_2})$	0.1194	0.0717	0.1469
$(X_{FeCl_3})(X_{HCl})$	0.0263	0.0717	0.7262
$(X_{MgCl_2})(X_{HCl})$	0.1118	0.0717	0.1698
$(X_{FeCl_3})^2$	0.0578	0.0992	0.5814
$(X_{MgCl_2})^2$	0.4289	0.0992	0.0050
$(X_{HCl})^2$	-0.0220	0.0992	0.8316

Table 5.8: 2nd order model for the solubility of $MgSO_4$ within factorial phase 3

Factors	Coefficient Estimate	SE	P-value
Intercept	0.3834	0.0175	
(X_{FeCl_3})	-0.0624	0.0156	0.0072
(X_{MgCl_2})	-0.3051	0.0156	< 0.0001
(X_{HCl})	0.1906	0.0156	< 0.0001
$(X_{FeCl_3})(X_{MgCl_2})$	0.0861	0.0182	0.0032
$(X_{FeCl_3})(X_{HCl})$	0.0346	0.0182	0.1053
$(X_{MgCl_2})(X_{HCl})$	-0.0092	0.0182	0.6305
$(X_{FeCl_3})^2$	0.0381	0.0251	0.1803
$(X_{MgCl_2})^2$	0.1225	0.0251	0.0028
$(X_{HCl})^2$	-0.0202	0.0251	0.4516

The parameters defined for each variable in the models are called the partial regression coefficients. They measure the expected change of the response as a function of the variation of the specific variable while the other variables remain constant. Thus, the partial regression coefficient for a particular variable represents a measure of the influence that particular variable has on the overall response. Furthermore, the variable with the greatest absolute value coefficient is considered to be the most influential on the overall response. In all three regression models the concentration of $MgCl_2$ is found to be the most significant factor affecting the solubility of $MgSO_4$. A p-value less than 0.05, generated by the t-test, confirms that the $MgCl_2$ concentration has the most

significant influence on the solubility of $MgSO_4$. The quadratic model within the first phase also shows that besides the $MgCl_2$ concentration, the effect of the other 2 factors, $FeCl_3$ and HCl concentrations, is insignificant in terms of their influence on the solubility of $MgSO_4$. However, the interaction between each variable does have an effect on the solubility. The same observation can be seen in the third factorial phase. The variation in the solubility of $MgSO_4$ accounts for 98.3%, 96.1% and 98.3% within each of the respective factorial models as seen in Tables 5.6, 5.7 and 5.8.

5.2 $ZnCl_2$-HCl-NaCl-H_20 system

5.2.1 Aqueous thermodynamic modelling of the $ZnCl_2$-HCl-NaCl-H_20 system

The thermodynamically calculated solubility of NaCl was determined using OLI System Inc Stream Analyser (OLI Systems Inc., 2009) for the range of conditions specified in Table 5.7. A full factorial design was carried to investigate the effect that each individual component, $ZnCl_2$ and HCl, has on the solubility of NaCl at 3 temperature levels.

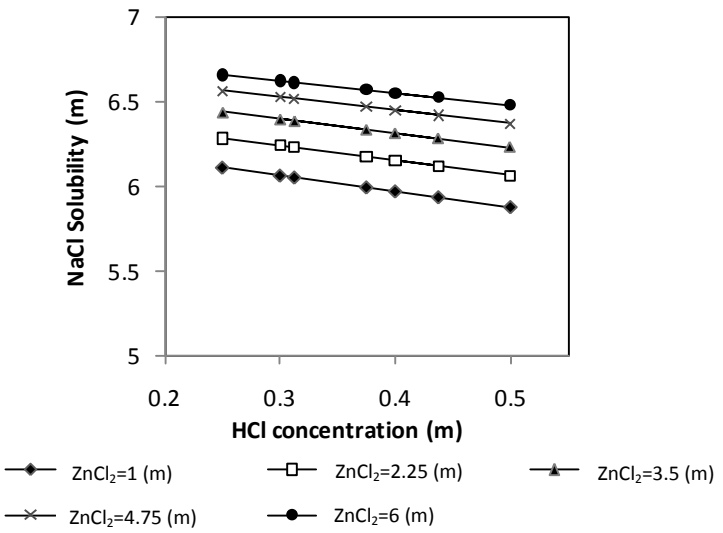

Figure 5.10: Thermodynamic modelled NaCl solubility for the $ZnCl_2$-HCl-NaCl-H_20 system at varying concentrations of $ZnCl_2$ and HCl at a temperature of 40˚C

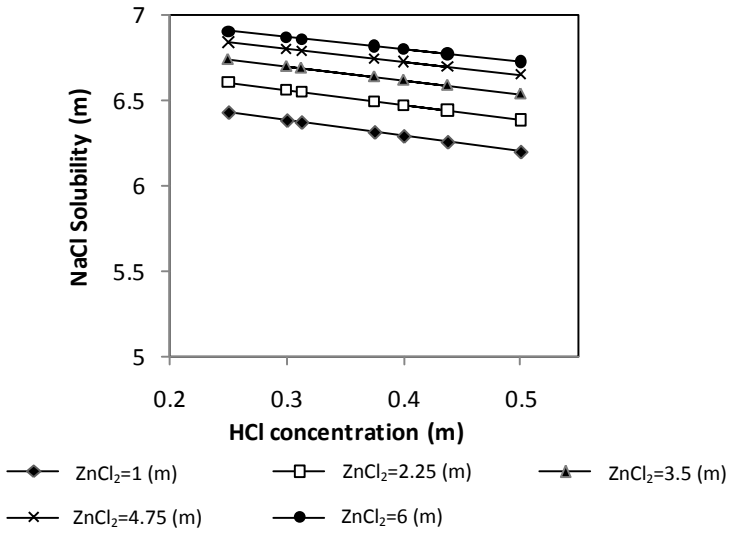

Figure 5.11: Thermodynamic modelled NaCl solubility for the $ZnCl_2$-HCl-NaCl-H_20 system at varying concentrations of $ZnCl_2$ and HCl at a temperature of 80°C

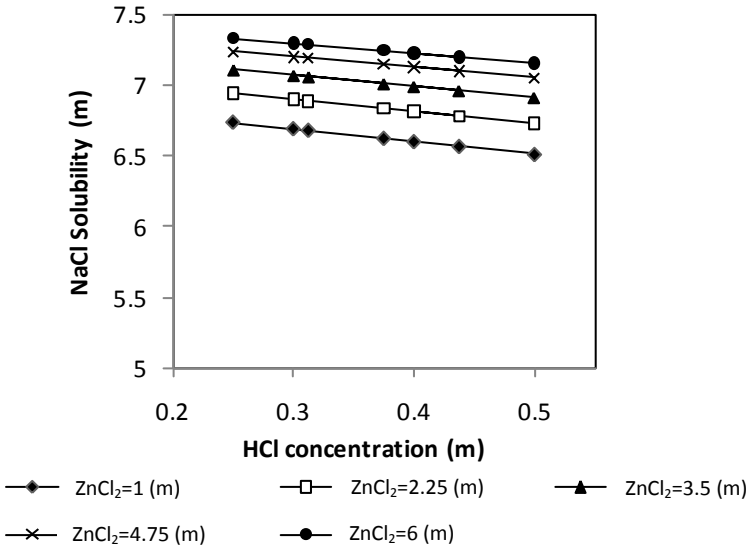

Figure 5.12: Thermodynamic modelled NaCl solubility for the $ZnCl_2$-HCl-NaCl-H_20 system at varying concentrations of $ZnCl_2$ and HCl at a temperature of 107°C

The results show that the trends observed in Figures 5.10, 5.11 and 5.12 are similar, with the only difference being that as the temperature increases the trend lines shifted upwards i.e. the higher the temperature the higher the solubility. The increase in the solubility as a result of the increase in the temperature is expected due to the increase in the excess Gibbs free energy. However, the solubility of NaCl increases only slightly

with an increase in the temperature, indicating that, within the specified system, the solubility is relatively independent of temperature as is shown in section 2.2.1.2.

From Figures 5.10, 5.11 and 5.12 it can be seen that as the concentration of HCl increases, the solubility of NaCl decreases. The opposite result is observed, for an increase in the concentration of $ZnCl_2$, which results in an increase in the solubility of NaCl. Within the HCl concentration range investigated, the change in the solubility of NaCl is not as large as the change in the solubility of NaCl within the investigated $ZnCl_2$ concentration range. Thus, within the concentration limits of this specific system, $ZnCl_2$ has a greater effect on the solubility of NaCl.

5.2.2 Experimentally determined solubilities for the $ZnCl_2$-HCl-NaCl-H_20 system

5.2.2.1 The effect of time on the solubility of NaCl within the $ZnCl_2$-NaCl-H_20 system

Figure 5.13 below shows the change in NaCl solubility and solution density with time for a 4 m $ZnCl_2$ solution at a temperature of 107˚C. The solution density is just an indication of the change in concentration within the system i.e. if the concentration were to change there would be a commensurate change in the density of the solution.

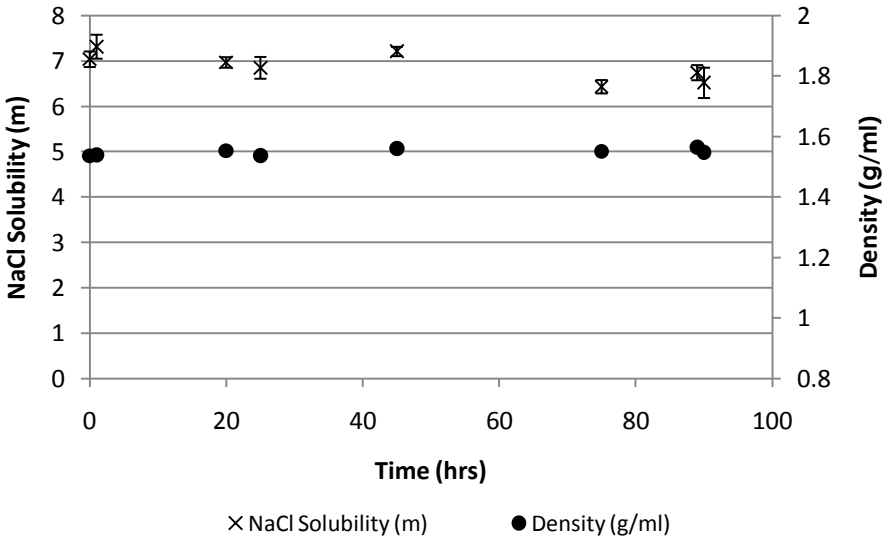

Figure 5.13: Experimentally determined NaCl solubility in a 4 m $ZnCl_2$-NaCl-H_20 system at a temperature of 107˚C

The solubility of NaCl remains reasonably constant for the entire period of the experiment as can be seen in Figure 5.13. This indicates the evidence of rapid kinetics as the system reaches equilibrium instantaneously.

5.2.2.2 The effect of concentration and temperature on the solubility of NaCl within the $ZnCl_2$-HCl-NaCl-H_20 system

Figure 5.14, 5.15 and 5.17 show the response surfaces, generated using a linear model. The response surfaces show the effect of varying the concentrations of $ZnCl_2$ and HCl, as specified in Table 5.7, has on the NaCl solubility at temperatures of 40˚C, 80˚C and 107˚C respectively.

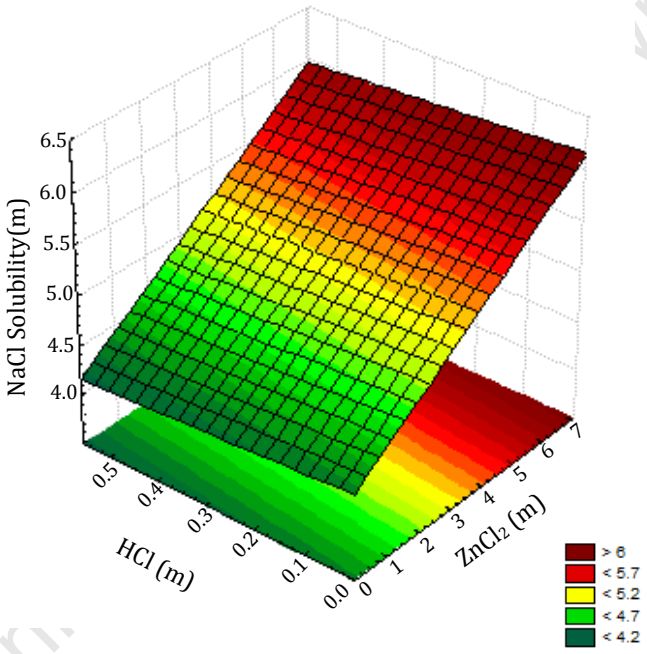

Figure 5.14: A surface plot of experimentally obtained solubility data for NaCl as a function of varying HCl and $ZnCl_2$ concentrations at a temperature of 40°C generated using a linear model

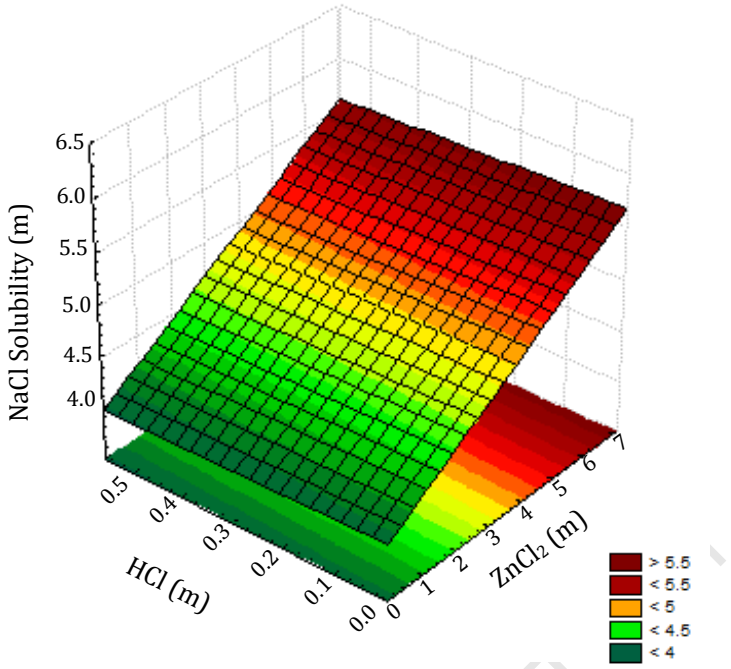

Figure 5.15: A surface plot of experimentally obtained solubility data for NaCl as a function of varying HCl and $ZnCl_2$ concentrations at a temperature of 80°C generated using a linear model

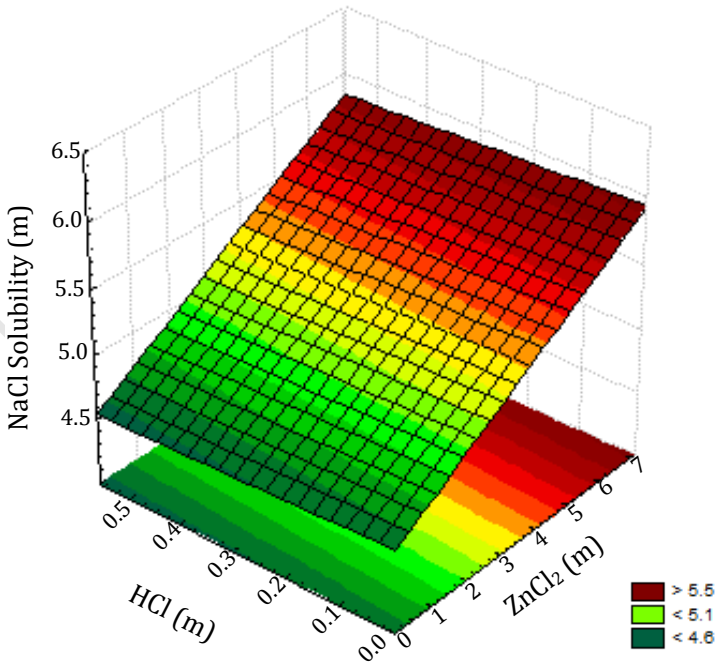

Figure 5.16: A surface plot of experimentally obtained solubility data for NaCl as a function of varying HCl and $ZnCl_2$ concentrations at a temperature of 107°C generated using a linear model

The surface plots generated in Figures 5.14, 5.15 and 5.16 shows similar trends. It can be seen that increasing the temperature does not have a significant effect on the solubility of NaCl within the background aqueous environment, as shown in section 2.2.1.2.

However, it can be seen that as the concentration of HCl increases, the solubility of NaCl decreases. This observation is explained by the common ion effect. Increasing the chloride ion concentration in solution drives the association equilibrium equation to shifting towards the formation of NaCl solid hence decreasing the amount of NaCl that can be dissolved in the system. This observation is consistent with the findings of Linke (1965) and Akhumov *et al.* (1954).

Increasing the concentration of $ZnCl_2$ resulted in an increase in the solubility of NaCl as observed in the surface plots generated in Figures 5.14, 5.15 and 5.16. Shevchuck and Moshinskii (1969) investigated the solubility of NaCl for the $ZnCl_2$-NaCl-H_20 system and constructed an isotherm at 25˚C. Their work showed that, within the $ZnCl_2$ concentration range investigated in this study, the results corresponded, i.e. an increase in concentration of $ZnCl_2$ results in an increase in the solubility of NaCl. However, a further increase in the $ZnCl_2$ concentration showed a decrease in concentration due to the precipitation of a double salt.

Hibben (1937) investigated the suppression of the ionization of $ZnCl_2$ in aqueous solutions by adding common chloride ions. The results showed that for the binary $ZnCl_2$-H_2O system, decreasing the concentration of $ZnCl_2$ from 1 m to ½ m resulted in a decrease in intensity faster than can be accounted for by the dilution effect alone. Thus, predicting that there is an increased ionization that occurs together with the dilution. This is explained by the binding between the zinc and chloride atoms which is homo-polar (a covalent bond whose total dipole moment is zero) in concentrated solutions and hetero-polar (a covalent bond whose total dipole moment is not zero) in dilute solutions. This implies that in concentrated solutions the bonds between the zinc atoms and chloride atoms are not broken thus, the solution is not completely ionized which gives rise to the formation of complexes or colloidal particles.

In the ternary $ZnCl_2$-NaCl-H_2O system, at a $ZnCl_2$ concentration of ¼ m the increase in the concentration of NaCl from 1 m to 2 m gives rise to a slight shift indicating that an

increase in the common ion resulted in a shift in the association equilibrium equation. The presence of the chloride ions shifts the equilibrium towards forming homo-polar bonds. An increase in $ZnCl_2$ concentration from ¼ m to ½ m whilst keeping the NaCl concentration constant at 2 m, gives an intensified shift verifying that the increased concentration of the common ion produces homo-polar bonds and decreases the ionization of the solution.

In addition to the common ion effect on the formation of homo-polar bonds there is a notable alteration in intensity of the water band which was attributed to the hindered translational motion of the water molecules. Within the binary $ZnCl_2$-H_2O system, the increase in concentration does not lead to a shift in intensity. However within the $ZnCl_2$-NaCl-H_2O ternary system, the shift was intensified by the presence of NaCl and diminished by the presence of $ZnCl_2$. The shift was a result of the displacement of the zinc ion-dipole bond with the lone pair of electrons from the oxygen atom of the water molecule and the formation of a new ion-dipole bond with the sodium ion and the lone pair of electrons on the oxygen atom. This is due to the sodium having an uncompleted 3s orbital which favours a greater attraction towards the lone pair of electrons associated with the oxygen atom unlike zinc which has a complete 4s orbital. This observation can be further illustrated by observing the activity of water within the $ZnCl_2$-NaCl-H_20 system shown in Figure 5.17.

5.2.2.2.1 Water activity within the $ZnCl_2$-NaCl-H_20 system

Water activity is a measure of the continuum energy status of the water in a specific system and is controlled by the colligative effects of dissolved species interacting with the water through hydrogen bonding, ionic bonding and dipole-dipole attractions. Water activity is also very dependent on temperature due to changes in water binding, dissociation of water or the solubility of solutes in water. These factors combined influence the energy of the system which in turn influences the ability of the solute to dissolve in a specific mixed electrolyte system.

Figure 5.13 illustrates the activity of water as a function of the total electrolyte concentration for the $ZnCl_2$-NaCl-H_2O system at 80˚C, where each line represents the ratio of $ZnCl_2$ to NaCl. The water activity decreases as the total concentration increases. The top trend line shows how the activity of water decreases in a binary $ZnCl_2$-H_2O

system. The bottom trend line shows the activity of water in the binary NaCl-H_2O system. The binary $ZnCl_2$-H_2O system shows the smallest deviation in the water activity from ideal behaviour. However, there is an increase in water activity with the addition of NaCl as explained above. The addition of pure NaCl into the system causes the largest deviation whilst the addition of pure $ZnCl_2$ results in the smallest deviation in the water activity from ideal behaviour.

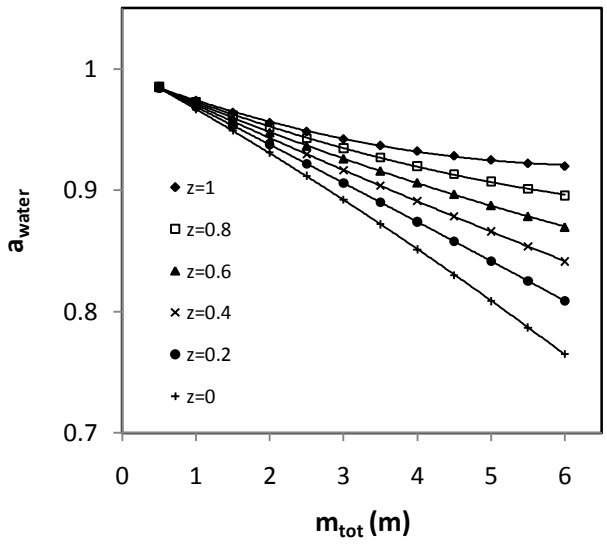

Figure 5.17: Water activity in the $ZnCl_2$-NaCl-H_20 system at 80°C. z is the molar ratio concentration (m) of $ZnCl_2$; (1-z) molar ratio concentration (m) of NaCl.

5.2.3 Comparison between experimental and modelled systems

The empirical models generated within this study used OLI system's mixed solvent electrolyte (MSE) model which incorporates the interactions between specific pairs of species. The OLI system is used to predict thermodynamic properties of both aqueous and mixed electrolyte systems ranging from relatively simple systems, binary and ternary, as well as certain multi-component systems for dilute solutions to solid saturations. The long-range interaction parameters are represented by the Pitzer-Debye-Huckel expression and the short range terms are expressed by the UNIQUAC model to predict thermodynamic properties in dilute as well as concentrated systems. The thermodynamic properties of the MSE are based on experimental data and comprise of the interaction terms within specific binary species. These binary species interaction terms are based on the assumption that within the aqueous phase other components do not affect the binary interactions. Thus within relatively simple systems

the model can predict thermodynamic properties accurately however fails within multi-component systems. The binary interactions between the specific species as well as the effect of other species for the $ZnCl_2$-HCl-NaCl-H_20 system has not been extensively studied, as shown in section 3.3.3, resulting in the empirical model not having the necessary information to accurately predict the solubility within the system. For this reason the empirical model does not accurately predict the solubility behaviour with Average Absolute Relative Deviations (AARD), shown in Table 5.9, that are extremely high.

Table 5.9: Average absolute relative deviations (AARD) between experimental and thermodynamic calculated results in the $ZnCl_2$-HCl-NaCl-H_2O systems

		AARD (%)		
$ZnCl_2$ (m)	**HCl (m)**	**40 (°C)**	**80 (°C)**	**107 (°C)**
7.0355	0.3750	12.6	35.5	37.6
6.0000	0.5000	9.2	11.1	14.8
6.0000	0.2500	10.9	26.5	23.4
3.5000	0.3750	26.1	41.6	37.4
3.5000	0.5518	31.1	35.4	30.8
3.5000	0.1982	30.9	38.3	32.7
1.0000	0.5000	21.3	53.6	40.7
1.0000	0.2500	28.1	39.6	38.1
0.0000	0.3750	47.1	59.4	39.0

$$* AARD = \left(\frac{100}{NP}\right)\sum_{i}^{NP}\left(\frac{|experimental\ value - modelled\ value|}{experimental\ value}\right)$$

where NP: no of experimental points.

5.2.4 Statistical analysis of experimental results for the $ZnCl_2$-HCl-NaCl-H_20 system

The main objective of the statistical analysis is to identify the best type of regression model that accurately fits the experimental data that was generated. Once the model has been identified it provides information on the interaction between parameters and identifies which factors have the greatest impact on the solubility of NaCl at each of the three temperatures. Analysis of the experimental data was carried out using Design

Expert Version 8 (Stat Ease Inc., 2009). Tables 5.10 and 5.11 shows the notation and units of the response variables and factors used in the statistical analysis.

Table 5.10: Notations and units of the responses used in the experimental models for the $ZnCl_2$-HCl-NaCl-H_20 system

Response	Notation	Unit
NaCl solubility at 40 ^oC	$NaCl_{40}$	mol/kg solvent
NaCl solubility at 80 ^oC	$NaCl_{80}$	mol/kg solvent
NaCl solubility at 107 ^oC	$NaCl_{107}$	mol/kg solvent

Table 5.11: Notations and units of the factors used in the experimental models for the $ZnCl_2$-HCl-NaCl-H_20 system

Factors	Notation	unit
$ZnCl_2$ concentration	X_{ZnCl_2}	mol/kg solvent
HCl concentration	X_{HCl}	mol/kg solvent

5.2.4.1 Summary of the model fitted for the three temperatures

Tables 5.12, 5.13 and 5.14 below show the types of functions used to fit the data, p-values and R^2 values. These values are used in determining which model best fits the experimental data to accurately describe the solubility of NaCl at temperatures of 40˚C, 80˚C and 107˚C respectively.

Table 5.12: Summary of statistical parameters used to fit the data for the $ZnCl_2$-HCl-NaCl-H_20 system at 40˚C

Model	Model P-value	Lack of fit P-value	Adjusted R^2	
Linear	**0.0037**	**0.8317**	**0.6910**	**Suggested**
2FI	0.8604	0.7757	0.6485	
Quadratic	0.9426	0.6040	0.5194	
Cubic	0.6040		0.4464	

Table 5.13: Summary of statistical parameters used to fit the data for the $ZnCl_2$-HCl-NaCl-H_20 system at 80˚C

Model	Model P-value	Lack of fit P-value	Adjusted R^2	
Linear	**0.0079**	**0.2108**	**0.6273**	**Suggested**
2FI	0.1220	0.2514	0.7046	
Quadratic	0.4554	0.2161	0.6981	
Cubic	0.2161		0.8869	

Table 5.14: Summary of statistical parameters used to fit the data for $ZnCl_2$-HCl-NaCl-H_20 system at 107˚C

Model	Model P-value	Lack of fit P-value	Adjusted R^2	
Linear	**0.0166**	**0.3808**	**0.5512**	**Suggested**
2FI	0.4627	0.3541	0.5277	
Quadratic	0.5310	0.2933	0.4868	
Cubic	0.2933		0.7349	

The null hypothesis represents the hypothesis of no change or no effect. The p-values are a measure of testing whether the null hypothesis is true or should be rejected. Small probability values, values less than 0.05, call for the rejection of the null hypothesis**.** The R^2 value is a measure of the amount of variation around the mean, explained by the model, adjusted for the number of terms in the model. The R^2 value decreases as the number of terms in the model increases if those additional terms do not add value to the model. Considering the p-values and R^2 values the linear model was chosen, for each response at the three factorial phases, to best describe how the background aqueous environment affects the solubility of NaCl.

5.2.4.2 First order models

The statistical analysis results obtained for the linear order models is given in Appendix C2.

5.2.4.2.1 Fitting linear models to the NaCl solubility data from at the 3 temperatures

The fitted linear regression models for the solubility of NaCl as a function of the process parameters at temperatures of 40˚C, 80˚C and 107˚C are shown in Tables 5.15, 5.16 and 5.17 respectively. The standard errors (SE) and p-values are also given.

Table 5.15: 1st order model for the solubility of NaCl at a temperature of 40˚C

$NaCl_{40}$ =	5.1131	+0.63004(X_{ZnCl_2})	-0.04153(X_{HCl})
SE	0.11	0.13	0.13
P-value		0.0011	0.7531

Table 5.16: 1st order model for the solubility of NaCl at a temperature of 80˚C

$NaCl_{80}$ =	4.80515	+4.80515(X_{ZnCl_2})	-0.01557(X_{HCl})
SE	0.11	0.13	0.13
P-value		0.0025	0.9087

Table 5.17: 1st order model for the solubility of NaCl at a temperature of 107˚C

$NaCl_{107}$ =	5.23678	+0.45451(X_{ZnCl_2})	-0.01935(X_{HCl})
SE	0.10	0.12	0.12
P-value		0.0054	0.8763

The parameters defined for each variable in the models are called the partial regression coefficients. They measure the expected change of the response as a function of the variation of the specific variable while the other variables remain constant. Thus, the partial regression coefficient for a particular variable represents a measure of the influence that particular variable has on the overall response. Furthermore, the variable with the greatest absolute value coefficient is considered to be the most influential on the overall response. In all three linear regression models the concentration of $ZnCl_2$ is found to be the most significant factor affecting the solubility of NaCl. A p-value less than 0.05, generated by the t-test, confirms that the $ZnCl_2$ concentration has the most significant influence on the solubility of NaCl. The variation in the solubility of NaCl accounts for 69.1%, 62.7% and 55.1% within each of the respective factorial models as seen in Tables 5.15, 5.16 and 5.17.

References

Akhumov, E.I., Spiro, N.S., 1954. Solubility of Chlorides in Hydrochloric acid. Journal of applied chemistry of the USSR, 27, p1103-1108.

Balarew, C., Tepavitcharova, S., Rabadjieva, D., Voigit., 2001. Solubility and Crystallization in the system $MgCl_2$-$MgSO_4$-H_2O at 50˚C and 75˚C. Journal of solution Chemistry, 30(9), p815-823.

Brown, R.A., Hills, C., Young, D.C., Fullerton, Miller, A.E., 1992, Iron complex synthesis. US Pat. 5,089,040.

Bousmina, F., Zayani, L., Hassen-Chehimi, D., Kbir-Ariguib, N., Trabelsi-Ayedi, M., (2003). Experimental determination of the isotherm at 15°C of the System Mg^{2+}/Cl^-, SO_4^{2-}–H_2O, Monatsh. Chem., 134, p763-768.

Campbell, A.N., Downes, K.W., Samis, C.S., 1937. The system $MgCl_2$-KCl-$MgSO_4$-K_2SO_4-H_2O at 100˚C. J. Am. Chem. Soc., 56(12), p 2507-2512.

Hibben, J.H., 1937. The common Ion effect on some aqueous solutions as shown by means of the Raman Effect. American Physical Society., Vol. 51, issue 7. p593-594.

Jolivet, J., Chaneac, C., Tronc, E. (2004), Iron oxide chemistry. From molecular clusters to extended solid networks, *Chemical Communications*, pp. 481 - 487.

Linke, W.F., Seidell, A., Solubilities of Inorganic and Metal-Organic Compounds, American Chemical Society, Washington, DC, vol. I: 1958, vol. II: 1965.

Lister, M.W., Rivington, D.E., 1955. Ferric Sulphate complexes and ternary complexes with thiocyanate ions. Canadian journal of Chemisty. Vol 33, p1591-1602

OLI Systems Inc, 2009. Stream Analyser version 3.0.1.0, Morris Plains, New Jersey.

Robson, H.L., 1927. The system $MgSO_4$-H_2O from 68 to 240˚C. J. Am. Chem. Soc., 49(11), p2772-2783.

Shevchuck, V.G., Moshinskii, A.S., 1969. The $ZnCl_2$-$ZnSO_4$-H_2O and NaCl-$ZnCl_2$-H_2O system at 25˚C. Russian journal of Inorganic Chemistry, 14(9), p1316-1318.

Stat Ease Inc, 2009, Design Expert version 8.0.1.0, Minneapolis.

Van't Hoff, Jacobus H.; Meyerhoffer, Wilhelm. Formation of oceanic salt deposits, particularly of the stassfurt beds. XXI. Formation of kainite at 25˚C Sitzungsberichte der Akademie der Wissenschaften in Berlin (1901), 420-7. CODEN: SAWBEB CAN 0:105661 AN 1906:105661 CAPLUS.

Chapter 6. Conclusions and Recommendations

6.1 Conclusions

The ArNi process has shown the importance of the ability to manipulate the aqueous environment in order to develop a sustainable metallurgical process. This process lead to investigations of applying the knowledge generated to other aqueous systems, as shown in the 2nd model system, for the development of other metallurgical processes. Therefore, the primary objective of this study was the investigation into the effect of temperature and ion interactions on the solubility of slightly soluble ($MgSO_4$) and highly soluble (NaCl) salts within multi-component systems and the following conclusions have been drawn:

$FeCl_3$-$MgCl_2$-HCl-$MgSO_4$-H_2O system

- The thermodynamically modelled system, at a temperature of 105˚C, showed that $MgCl_2$ has the greatest effect on the solubility of $MgSO_4$. The increase in the concentration of $MgCl_2$ resulted in a decrease in the solubility of $MgSO_4$. An increase in the concentration of HCl resulted in an increase in the solubility of $MgSO_4$ while an increase in the concentration of $FeCl_3$ decreased the solubility of $MgSO_4$ at low concentrations of $MgCl_2$ and HCl. However, the effect of $FeCl_3$ on the solubility of $MgSO_4$ was minimised as the concentrations of $MgCl_2$ and HCl were increased.
- The statistical analysis of the experimental data showed that $MgCl_2$ had the greatest effect on the solubility of $MgSO_4$ and with the given experimental data, the quadratic model was identified as the most accurate model to describe the system.
- The experimentally determined quadratic surface plots showed that:
    - Increasing the concentration of $MgCl_2$ decreased the solubility of $MgSO_4$ due to the common ion effect with respect to Mg^{2+} ions;
    - Increasing the concentration of HCl increased the solubility of $MgSO_4$ as a result of an increase in the ionic strength due to the presence of non-common chloride ions;

- Increasing the concentration of $FeCl_3$ decreased the solubility of $MgSO_4$ due to ferric hydroxyl complexes interacting with SO_4^{2-} ions in solution.

- $MgSO_4 \cdot H_2O$ was precipitated independently or with a combination of $MgSO_4 \cdot 1.25H_2O$ or $MgSO_4 \cdot 6H_2O$ at each of the concentration limits for $MgCl_2$, $FeCl_3$ and HCl. Maintaining the concentration of $MgCl_2$ and HCl while varying the concentration of $FeCl_3$ had no effect on the hydrate or hydrates that were formed. An increase in $MgCl_2$ and HCl concentrations had a dehydrating effect on the formation of the hydrates and the effect of HCl was found to be more pronounced.
- The hydrates that were formed did not have a crystalline structure. No conclusive evidence could be drawn on the effect that each factor, $MgCl_2$, $FeCl_3$ and HCl, had on the type of precipitates that were formed.

$ZnCl_2$-HCl-NaCl-H_2O system

- The thermodynamically modelled system showed that an increase in temperature resulted in an increase in the solubility of NaCl. An increase in the concentration of $ZnCl_2$ increased the solubility of NaCl while an increase in the concentration of HCl decreased the solubility of NaCl.
- The statistical analysis of the experimental data showed that $ZnCl_2$ had the most pronounced effect on the solubility of NaCl. Linear models were found to be the most accurate models to describe the systems.
- Experimental linear surface plots showed that:
  - Increasing the temperature did not have a significant effect on the solubility of NaCl;
  - Increasing the concentration of $ZnCl_2$ increased the solubility of NaCl due to the formation of homo-polar bonds which decreases the ionization of the solution;
  - Increasing the concentration of HCl decreased the solubility of NaCl due to the common ion effect.

The results have shown that ion interactions play a crucial role in the solubility of salts in hypersaline brines. However, each ion has a different effect on the solubility of a specific salt and is unique for different systems. The results showed that

thermodynamic modelling can be used as a tool to predict salt solubility trends. However, in order to gain a fundamental understanding of a system, especially complex systems, experimental measurements are necessary. Thus, the experimental measurements in this work have provided a better understanding of how the aqueous chemical environment can be manipulated to develop innovative ways of reinventing extractive metallurgy.

6.2 Recommendations

In-light of the findings presented in this study, the following recommendations are suggested:

- The work covered in this investigation was limited to the thermodynamic conditions and did not take into account the kinetics of the precipitation reactions. In order to gain a full understanding of the system, which can include a realistic mass balance, investigations into the kinetics of the precipitation reactions should be undertaken.

- To fully exploit the power of the process, investigations should be conducted on ways of extracting other valuable metals from the ore that is processed for example, lateritic ores contain large quantities of iron which can be sold as a valuable bi-product, especially in the current expansion of emerging markets.

Appendices

Appendix

A: Experimental solubility calculations

A1.1: $FeCl_3$-$MgCl_2$-HCl-$MgSO_4$-H_20 system

A2.1: $ZnCl_2$-HCl-NaCl-H_20 system

B: XRD patterns

C: Statistical Analysis

C1.1: $FeCl_3$-$MgCl_2$-HCl-$MgSO_4$-H_20 system

C1.2: $ZnCl_2$-HCl-NaCl-H_20 system.

Appendix A: Experimental Results

A1.1: $FeCl_3$-$MgCl_2$-HCl-$MgSO_4$-H_20 system.

Table A1: Raw experimental results for solubility of $MgSO_4$ within factorial Phase 1.

	Experimental Conditions				Conc (mol/l)			Conc (m)		
Experiment #	$FeCl_3$ (m)	$MgCl_2$ (m)	HCL (m)	Density (g/ml)	Fe^{3+}	Mg^{2+}	SO_4^{2-}	Fe^{3+}	Mg^{2+}	SO_4^{2-}
P1.1	0	1	0	1.534	0.00	4.42	3.83	0.00	4.35	3.77
					0.00	4.69	4.05	0.00	4.76	4.11
					0.00	4.74	4.14	0.00	4.84	4.23
P1.2	2	1	0	1.673	2.10	3.25	2.05	2.16	3.34	2.11
					2.14	3.24	2.04	2.21	3.35	2.11
					2.03	3.09	1.93	2.03	3.08	1.92
P1.3	1	1	1.75	1.483	0.96	3.92	2.87	1.09	4.45	3.26
					0.93	3.86	2.86	1.04	4.32	3.20
					0.93	3.86	2.79	1.05	4.32	3.12
P1.4	0	1	6	1.418	0.02	3.67	2.83	0.02	3.69	2.85
					0.00	3.69	2.81	0.00	3.71	2.83
					0.00	3.67	2.81	0.00	3.67	2.81
P1.5	1	3.5	1.75	1.480	1.06	4.06	0.88	1.18	4.51	0.98
					1.06	3.96	0.86	1.17	4.36	0.94
					1.07	3.98	0.86	1.17	4.39	0.94
P1.6	2	1	6	1.490	1.54	2.90	2.09	1.69	3.18	2.30
					1.67	3.14	2.26	1.93	3.63	2.62
					1.63	2.99	2.18	1.84	3.38	2.46
P1.7	2	3.5	3.5	1.456	1.69	3.47	0.85	2.03	4.18	1.02
					1.71	3.48	0.78	2.07	4.21	0.94

					1.67	3.48	0.82	2.01	4.18	0.99
P1.8	1	3.5	0	1.461	1.05	3.94	0.67	1.17	4.37	0.74
					1.06	4.06	0.69	1.19	4.58	0.78
					1.08	4.13	0.70	1.24	4.73	0.81
P1.9	1	3.5	1.75	1.480	1.02	3.84	0.91	1.11	4.16	0.99
					1.16	4.28	1.00	1.34	4.98	1.17
					1.05	3.90	0.91	1.15	4.26	1.00
P1.10	2	6	0	1.570	1.99	4.92	0.03	2.56	6.32	0.04
					1.96	4.79	0.03	2.47	6.03	0.04
					1.87	4.61	0.03	2.26	5.58	0.04
P1.11	1	6	1.75	1.492	1.02	5.50	0.18	1.27	6.88	0.22
					1.11	6.17	0.18	1.53	8.54	0.25
					1.08	5.92	0.17	1.45	7.90	0.23
P1.12	2	3.5	1.75	1.585	1.86	3.33	0.57	1.95	3.50	0.60
					2.01	3.71	0.59	2.25	4.16	0.66
					1.98	3.65	0.58	2.20	4.05	0.65
P1.13	1	3.5	3.5	1.490	1.07	3.96	0.82	1.17	4.31	1.04
					1.10	4.19	0.86	1.23	4.70	1.12
					1.07	4.07	0.87	1.18	4.48	1.11
P1.14	0	6	0	1.399	0.02	6.20	0.07	0.03	7.71	0.09
					0.00	6.53	0.06	0.00	8.42	0.08
					0.00	6.33	0.06	0.00	7.96	0.08
P1.15	1	3.5	1.75	1.480	1.04	3.85	0.92	1.13	4.17	0.99
					1.12	4.13	0.93	1.27	4.69	1.05
					1.06	3.70	0.91	1.13	3.96	0.97
P1.16	0	3.5	3.5	1.398	0.02	4.11	1.13	0.02	4.22	1.16
					0.00	4.28	1.13	0.00	4.45	1.18
					0.00	4.14	1.09	0.00	4.24	1.12
P1.17	0	3.5	1.75	1.388	0.00	4.27	1.03	0.00	4.48	1.08

					0.00	4.38	0.99	0.00	4.64	1.05
					0.00	4.22	1.07	0.00	4.40	1.11
P1.18	0	6	3.5	1.410	0.00	4.64	0.61	0.00	4.86	0.64
					0.00	4.96	0.63	0.00	5.37	0.69
					0.00	4.87	0.64	0.00	5.24	0.69

Table A2: Raw experimental results for solubility of $MgSO_4$ within factorial Phase 2.

	Experimental Conditions				Conc (mol/l)			Conc (m)		
Experiment #	**$FeCl_3$ (m)**	**$MgCl_2$ (m)**	**HCL (m)**	**Density (g/ml)**	**Fe^{3+}**	**Mg^{2+}**	**SO_4^{2-}**	**Fe^{3+}**	**Mg^{2+}**	**SO_4^{2-}**
P2.1	0.5	2.25	0	1.450	0.45	4.20	2.23	0.49	4.56	2.42
					0.43	4.22	2.19	0.46	4.57	2.38
					0.43	4.24	2.22	0.47	4.61	2.42
P2.2	2	6	0	1.570	1.92	4.85	0.04	2.41	6.09	0.05
					1.93	4.78	0.03	2.42	5.97	0.04
					1.82	4.45	0.03	2.13	5.23	0.03
P2.3	2	4.125	1.75	1.585	1.84	3.87	0.44	1.90	4.60	0.53
					1.81	3.74	0.43	1.83	4.35	0.51
					1.83	3.78	0.44	1.86	4.42	0.51
P2.4	2	2.25	0	1.554	2.07	3.80	1.53	2.54	4.64	1.87
					2.12	3.90	1.59	2.66	4.89	1.99
					2.12	3.84	1.59	2.63	4.77	1.97
P2.5	1.25	4.125	1.75	1.507	1.32	4.27	0.69	1.41	5.30	0.86
					1.31	4.21	0.66	1.39	5.18	0.81
					1.30	4.27	0.66	1.39	5.28	0.82
P2.6	0.5	6	0	1.441	0.53	5.24	0.06	0.62	6.12	0.07
					0.51	5.14	0.06	0.59	5.92	0.07

					0.50	5.02	0.06	0.57	5.70	0.07
P2.7	1.25	2.25	1.75	1.501	1.21	3.59	1.51	1.23	4.17	1.76
					1.28	3.76	1.60	1.33	4.52	1.93
					1.27	3.68	1.61	1.31	4.38	1.92
P2.8	1.25	4.125	0	1.485	1.30	4.10	0.32	1.48	4.69	0.37
					1.34	4.26	0.33	1.57	5.00	0.39
					2.38	4.08	0.31	3.39	5.81	0.45
P2.9	0.5	2.25	3.5	1.447	0.53	3.76	1.90	0.49	4.54	2.29
					0.52	3.85	1.92	0.48	4.69	2.35
					0.52	3.78	1.91	0.48	4.58	2.31
P2.10	1.25	4.125	1.75	1.507	1.28	4.22	0.69	1.36	5.18	0.85
					1.27	4.15	0.68	1.33	5.04	0.83
					1.21	3.99	0.69	1.24	4.70	0.81
P2.11	1.25	6	1.75	1.513	1.20	4.66	0.19	1.29	5.77	0.23
					1.19	4.69	0.18	1.28	5.83	0.22
					1.14	4.46	0.19	1.18	5.34	0.23
P2.12	0.5	4.125	1.75	1.435	0.54	4.11	0.72	0.54	4.70	0.82
					0.56	4.27	0.77	0.57	5.00	0.90
					0.51	4.01	0.71	0.50	4.51	0.80
P2.13	2	2.25	3.5	1.460	1.69	3.32	1.42	1.76	4.71	2.02
					1.63	3.15	1.36	1.65	4.31	1.86
					1.64	3.19	1.36	1.66	4.38	1.87
P2.14	1.25	4.125	1.75	1.507	1.32	4.16	0.70	1.40	5.10	0.86
					1.29	4.11	0.69	1.35	4.97	0.84
					1.21	3.91	0.69	1.23	4.57	0.81
P2.15	1.25	4.125	3.5	1.513	1.13	3.75	0.63	1.04	4.52	0.76
					1.15	3.86	0.66	1.07	4.73	0.81
					1.17	3.90	0.66	1.10	4.82	0.82
P2.16	0.5	6	3.5	1.453	0.61	5.30	0.32	0.63	7.41	0.44

					0.51	4.75	0.28	0.50	6.06	0.36
					0.49	4.62	0.28	0.47	5.79	0.35

Table A3: Raw experimental results for solubility of $MgSO_4$ within factorial Phase 3.

	Experimental Conditions				Conc (mol/l)			Conc (m)		
Experiment #	**$FeCl_3$ (m)**	**$MgCl_2$ (m)**	**HCL (m)**	**Density (g/ml)**	**Fe^{3+}**	**Mg^{2+}**	**SO_4^{2-}**	**Fe^{3+}**	**Mg^{2+}**	**SO_4^{2-}**
P3.1	2	3.5	0	1.555	1.74	3.49	0.41	1.87	3.75	0.44
					1.82	3.64	0.43	2.01	4.03	0.47
					1.78	3.56	0.46	1.95	3.89	0.51
P3.2	1.5	6	1.75	1.535	1.45	4.70	0.15	1.59	6.00	0.19
					1.39	4.54	0.15	1.48	5.60	0.18
					1.47	4.80	0.16	1.64	6.23	0.21
P3.3	2	6	0	1.570	1.89	4.66	0.03	2.30	5.69	0.04
					1.84	4.56	0.03	2.20	5.45	0.04
					1.78	4.43	0.03	2.07	5.16	0.04
P3.4	1.5	4.75	1.75	1.532	1.51	4.23	0.35	1.60	5.20	0.42
					1.51	4.18	0.35	1.60	5.12	0.43
					1.44	4.15	0.34	1.50	5.00	0.41
P3.5	1	4.75	1.75	1.485	1.04	4.27	0.41	1.09	5.11	0.49
					1.05	4.24	0.41	1.08	5.06	0.49
					1.04	4.31	0.42	1.09	5.19	0.50
P3.6	1.5	4.75	0	1.517	1.51	4.18	0.10	1.73	4.79	0.11
					1.57	4.29	0.10	1.84	5.04	0.11
					1.52	4.17	0.10	1.75	4.80	0.11
P3.7	1	3.5	0	1.461	1.06	4.00	0.71	1.19	4.49	0.80
					1.06	3.99	0.72	1.19	4.48	0.81

					1.09	4.09	0.74	1.24	4.67	0.84
P3.8	2	4.75	1.75	1.582	1.71	3.73	0.26	1.70	4.25	0.30
					1.71	3.71	0.29	1.70	4.22	0.33
					1.81	3.95	0.28	1.87	4.70	0.34
P3.9	1.5	4.75	1.75	1.532	1.44	4.21	0.32	1.51	5.09	0.39
					1.45	4.25	0.32	1.53	5.19	0.39
					1.43	4.19	0.34	1.50	5.06	0.41
P3.10	1	6	0	1.483	1.00	4.61	0.05	1.14	5.24	0.06
					1.05	4.88	0.05	1.24	5.76	0.06
					1.01	4.69	0.05	1.15	5.37	0.06
P3.11	1.5	3.5	1.75	1.531	1.47	3.78	0.73	1.50	4.44	0.85
					1.37	3.50	0.69	1.34	3.91	0.77
					1.35	3.47	0.67	1.32	3.85	0.74
P3.12	1	6	3.5	1.495	0.98	4.66	0.23	0.97	6.15	0.31
					0.95	4.65	0.25	0.94	6.08	0.33
					1.00	4.73	0.25	0.99	6.31	0.33
P3.13	2	3.5	3.5	1.601	1.66	3.46	0.79	1.49	4.04	0.92
					1.71	3.51	0.76	1.56	4.16	0.90
					1.70	3.47	0.77	1.54	4.09	0.91
P3.14	1.5	4.75	1.75	1.532	1.41	4.15	0.32	1.46	4.96	0.38
					1.42	4.16	0.33	1.48	4.99	0.40
					1.60	4.58	0.32	1.79	6.00	0.41
P3.15	1.5	4.75	3.5	1.536	1.38	4.22	0.50	1.34	5.48	0.65
					1.25	3.89	0.47	1.16	4.72	0.57
					1.23	3.81	0.45	1.13	4.56	0.54
P3.16	1	3.5	3.5	1.490	0.98	3.92	0.93	0.92	4.86	1.15
					0.98	3.91	0.93	0.92	4.85	1.16
					0.96	3.82	0.90	0.89	4.65	1.10

A1.2: $ZnCl_2$-HCl-NaCl-H_20 system.

Table A4: Raw experimental results for the solubility of NaCl at a temperature of 40°C.

	Experimental Conditions			Conc (mol/l)		Conc (m)	
Experiment #	$ZnCl_2$	HCl	Density (g/ml)	NA^+	Zn^{2+}	NA^+	Zn^{2+}
$N1_{40}$	6	0.5	1.536	5.25	2.76	5.94	3.12
$N2_{40}$	3.5	0.375	1.392	4.37	1.84	4.75	2.00
$N3_{40}$	1	0.5	1.218	4.37	0.61	4.84	0.68
$N4_{40}$	6	0.25	1.537	5.25	2.91	6.01	3.34
$N5_{40}$	1	0.25	1.221	4.37	0.61	4.77	0.67
$N6_{40}$	3.5	0.5518	1.390	4.37	1.69	4.69	1.81
$N7_{40}$	3.5	0.375	1.392	4.90	1.96	5.61	2.25
$N8_{40}$	3.5	0.1982	1.393	4.55	1.84	4.95	2.00
$N9_{40}$	3.5	0.375	1.392	4.37	1.90	4.80	2.09
$N10_{40}$	7.0355	0.375	1.593	5.25	3.13	5.89	3.51
$N11_{40}$	0	0.375	1.141	3.76	0.00	3.97	0.00

Table A5: Raw experimental results for the solubility of NaCl at a temperature of 80°C.

	Experimental Conditions			Conc (mol/l)		Conc (m)	
Experiment #	$ZnCl_2$	HCl	Density (g/ml)	NA^+	Zn^{2+}	NA^+	Zn^{2+}
$N1_{80}$	6	0.5	1.536	5.25	3.07	6.06	4.13
$N2_{80}$	3.5	0.375	1.392	4.72	1.87	5.50	2.18
$N3_{80}$	1	0.5	1.218	4.46	0.83	5.32	0.99
$N4_{80}$	6	0.25	1.537	5.33	3.19	6.74	4.03
$N5_{80}$	1	0.25	1.221	4.11	0.67	4.60	0.76
$N6_{80}$	3.5	0.5518	1.390	4.28	1.75	4.80	1.96
$N7_{80}$	3.5	0.375	1.392	4.37	1.81	4.92	2.04
$N8_{80}$	3.5	0.1982	1.393	4.37	1.84	4.90	2.06
$N9_{80}$	3.5	0.375	1.392	4.11	1.78	4.53	1.96
$N10_{80}$	7.0355	0.375	1.593	4.72	3.79	5.06	4.43
$N11_{80}$	0	0.375	1.141	3.58	0.00	3.86	0.00

Table A6: Raw experimental results for the solubility of NaCl at a temperature of 107°C.

	Experimental Conditions			Conc (mol/l)		Conc (m)	
Experiment #	$ZnCl_2$	HCl	Density (g/ml)	NA^+	Zn^{2+}	NA^+	Zn^{2+}
$N1_{107}$	6	0.5	1.536	5.16	4.11	6.24	5.90
$N2_{107}$	3.5	0.375	1.392	5.68	3.21	7.19	4.70
$N3_{107}$	1	0.5	1.218	4.72	0.70	5.67	0.77
$N4_{107}$	6	0.25	1.537	5.25	4.32	5.94	6.41
$N5_{107}$	1	0.25	1.221	4.28	0.83	4.88	0.97
$N6_{107}$	3.5	0.5518	1.390	4.55	2.75	5.25	3.56
$N7_{107}$	3.5	0.375	1.392	4.55	2.69	5.15	3.36
$N8_{107}$	3.5	0.1982	1.393	4.72	2.72	5.39	3.42
$N9_{107}$	3.5	0.375	1.392	4.63	2.72	5.35	3.39
$N10_{107}$	7.0355	0.375	1.593	5.25	4.40	5.31	6.18
$N11_{107}$	0	0.375	1.141	4.11	0.01	4.63	0.01

Sample calculations

$$m_i = \frac{C_i}{\rho - \sum_i^C [C_i \times Mr_i]} \times 1000$$

Where: m_i = concentration of species i ($mol.KgH_20^{-1}$)

C_i = concentration of species i ($mol.L^{-1}$)

ρ = density of solution (g/ml)

Mr_i = molecular weight of species i (g/l)

Appendix B: XRD patterns.

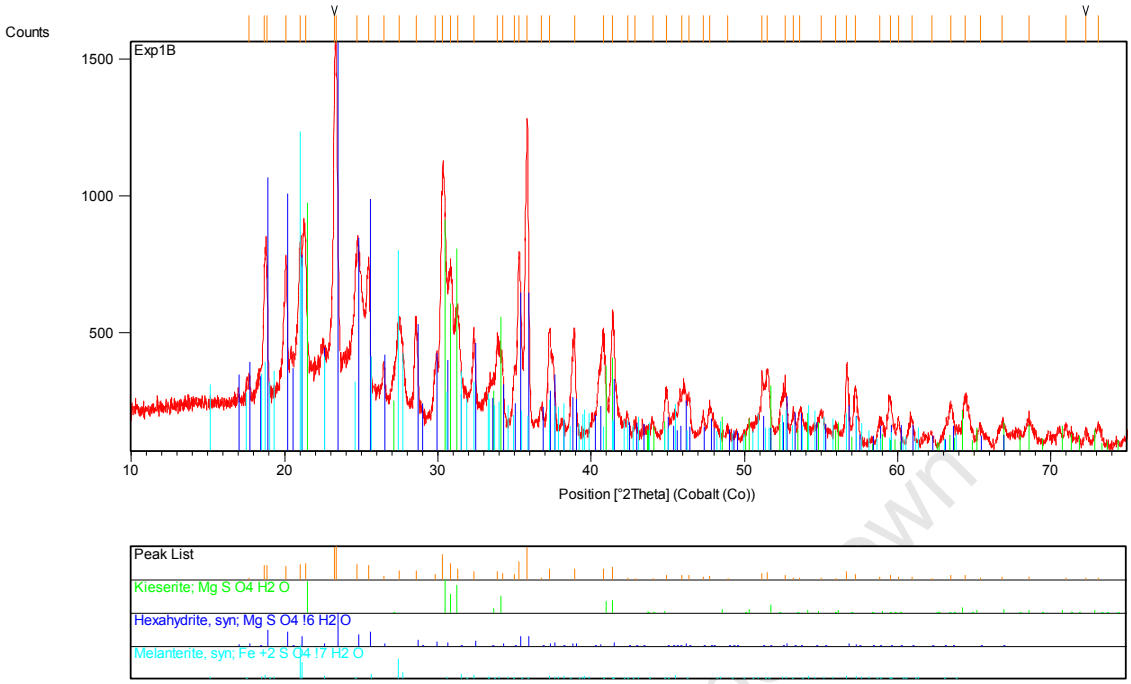

Figure B1: XRD pattern for a 0 m HCl, 0 m $FeCl_3$ and 1 m $MgCl_2$ system to characterise the hydrate/hydrates of $MgSO_4$ at 105°C.

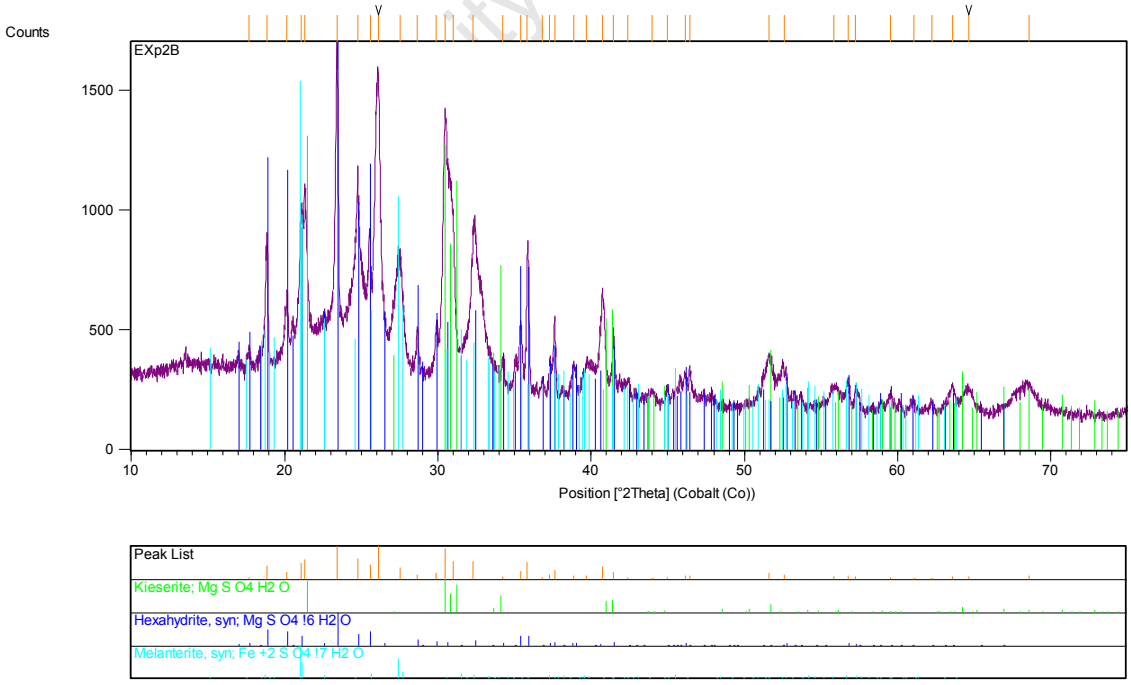

Figure B2: XRD pattern for a 0 m HCl, 2 m $FeCl_3$ and 1m $MgCl_2$ system to characterise the hydrate/hydrates of $MgSO_4$ at 105°C

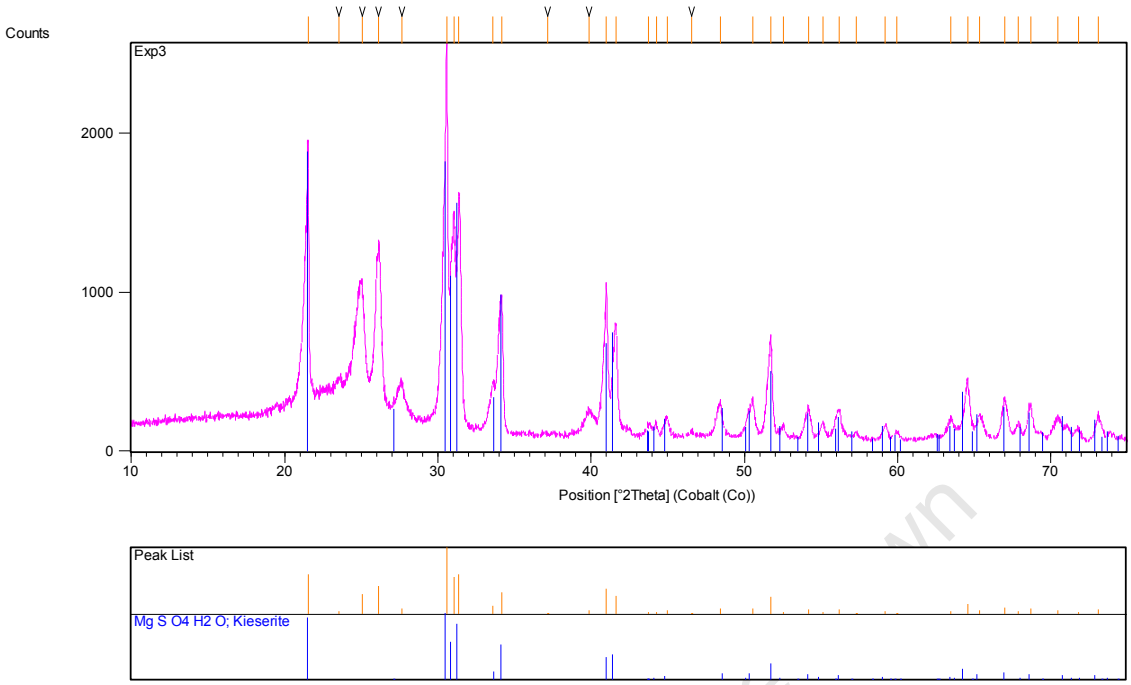

Figure B3: XRD pattern for a 6 m HCl, 0 m $FeCl_3$ and 1 m $MgCl_2$ system to characterise the hydrate/hydrates of $MgSO_4$ at 105°C

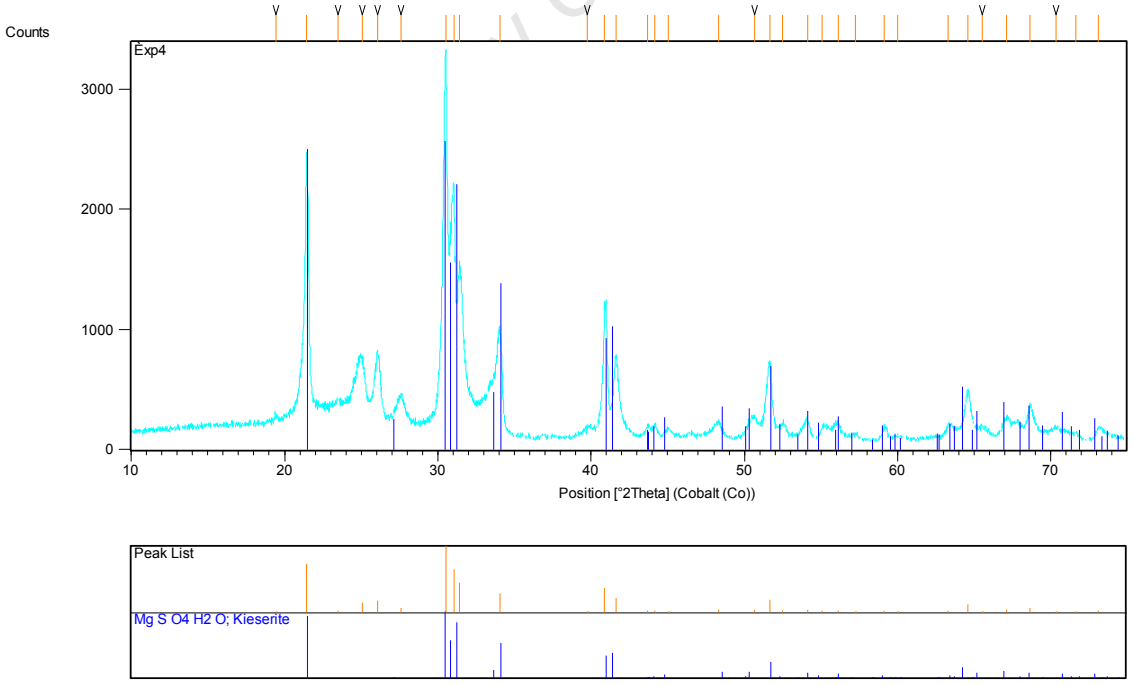

Figure B4: XRD pattern for a 6 m HCl, 2 m $FeCl_3$ and 1 m $MgCl_2$ system to characterise the hydrate/hydrates of $MgSO_4$ at 105°C

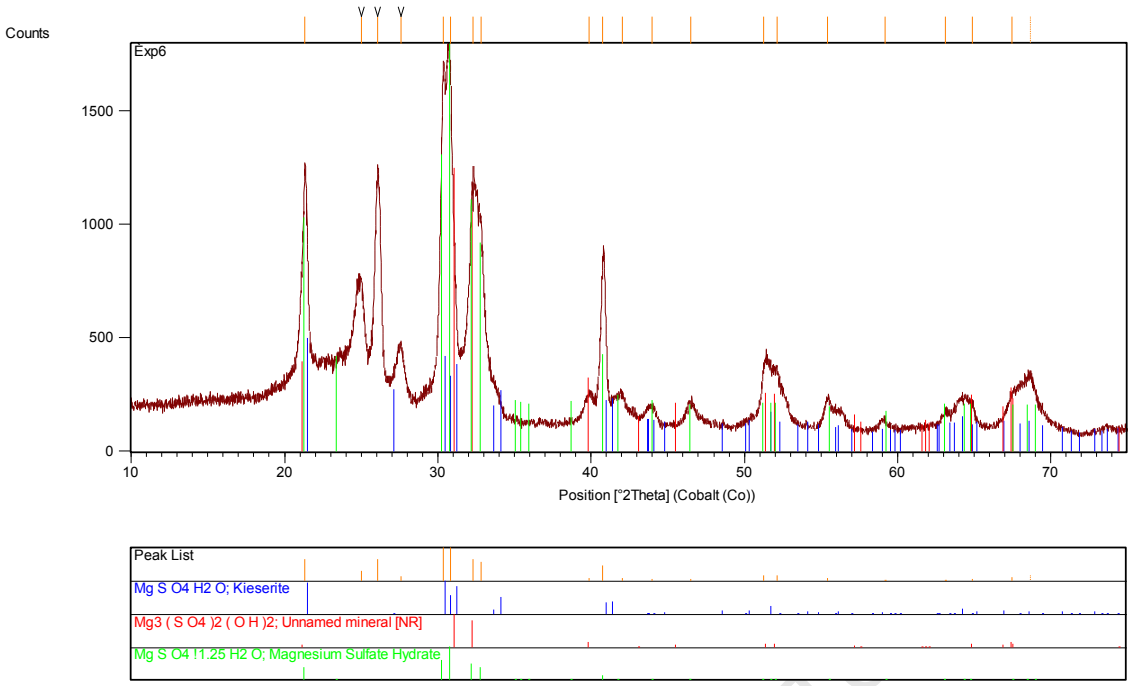

Figure B5: XRD pattern for a 0 m HCl, 2 m $FeCl_3$ and 6 m $MgCl_2$ system to characterise the hydrate/hydrates of $MgSO_4$ at 105°C

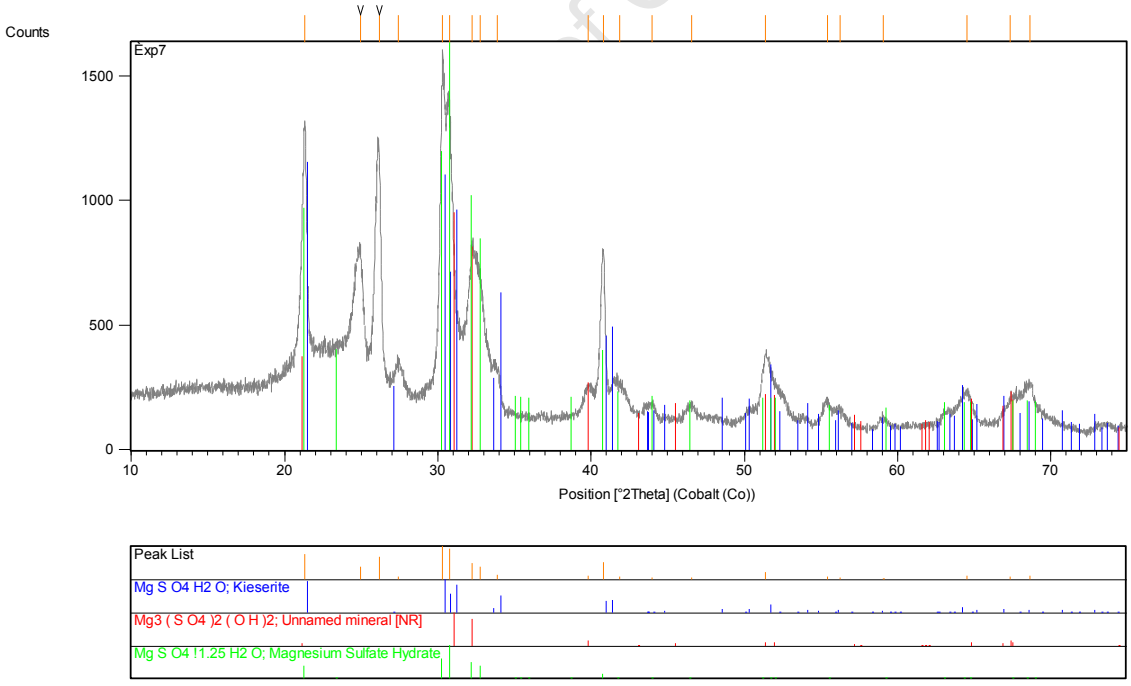

Figure B6: XRD pattern for a 0 m HCl, 0 m $FeCl_3$ and 6 m $MgCl_2$ system to characterise the hydrate/hydrates of $MgSO_4$ at 105°C

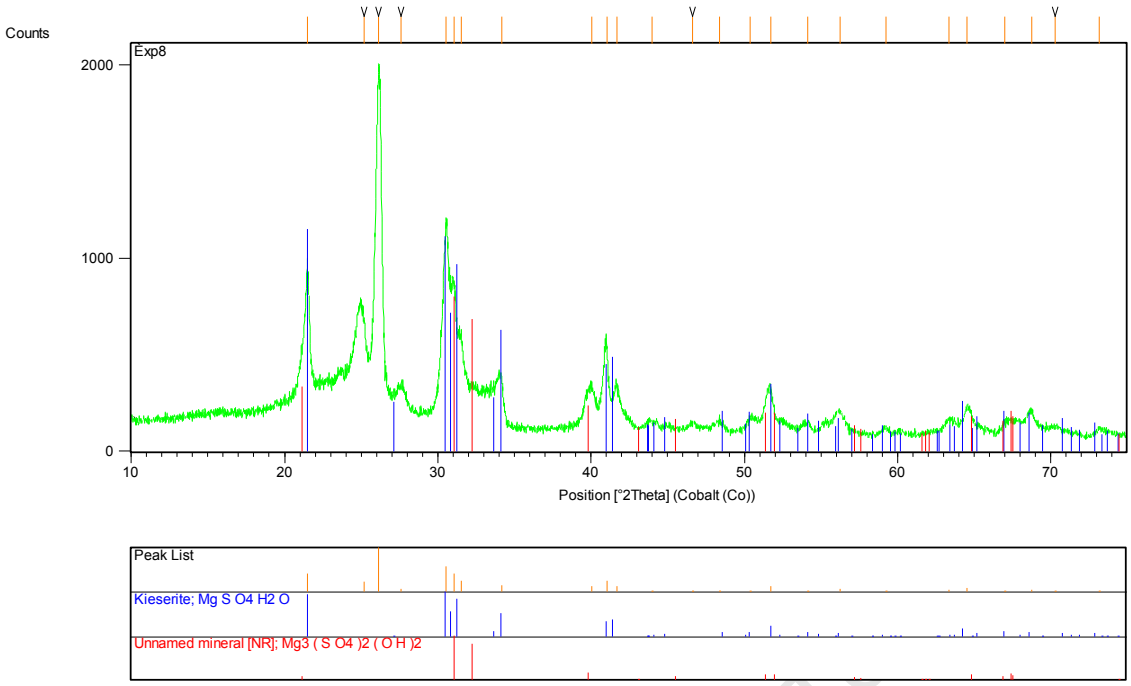

Figure B7:XRD pattern for a 3.5 m HCl, 0 m $FeCl_3$ and 6 m $MgCl_2$ system to characterise the hydrate/hydrates of $MgSO_4$ at 105°C

Appendix C: Statistical Analysis

C1.1: $FeCl_3$-$MgCl_2$-HCl-$MgSO_4$-H_20 system

Model fit summary for Phase 1

Summary (detailed tables shown below)

Source	Sequential p-value	Lack of Fit p-value	Adjusted R-Squared	Predicted R-Squared	
Linear	< 0.0001	0.0084	0.8209	0.6977	
2FI	0.5160	0.0076	0.8132	0.3527	
Quadratic	< 0.0001	0.0768	0.9834	0.9082	Suggested
Cubic	0.0768		0.9982		Aliased

Sequential Model Sum of Squares [Type I]

Source	Sum of Squares	df	Mean Square	F Value	p-value Prob > F	
Mean vs Total	32.85	1	32.85			
Linear vs Mean	17.95	3	5.98	26.98	< 0.0001	
2FI vs Linear	0.56	3	0.19	0.81	0.5160	
Quadratic vs 2FI	2.38	3	0.79	38.47	< 0.0001	Suggested
Cubic vs Quadratic	0.16	6	0.027	12.35	0.0768	Aliased
Residual	4.338E-003	2	2.169E-003			
Total	53.91	18	3.00			

"Sequential Model Sum of Squares [Type I]": Select the highest order polynomial where the additional terms are significant and the model is not aliased.

Lack of Fit Tests

Source	Sum of Squares	df	Mean Square	F Value	p-value Prob > F	
Linear	3.10	12	0.26	119.14	0.0084	
2FI	2.54	9	0.28	130.16	0.0076	
Quadratic	0.16	6	0.027	12.35	0.0768	Suggested
Cubic	0.000	0				Aliased
Pure Error	4.338E-003	2	2.169E-003			

"Lack of Fit Tests": Want the selected model to have insignificant lack-of-fit.

Model Summary Statistics

Source	Std. Dev.	R-Squared	Adjusted R-Squared	Predicted R-Squared	PRESS	
Linear	0.47	0.8525	0.8209	0.6977	6.37	
2FI	0.48	0.8791	0.8132	0.3527	13.63	
Quadratic	0.14	0.9922	0.9834	0.9082	1.93	Suggested
Cubic	0.047	0.9998	0.9982		+	Aliased

+ Case(s) with leverage of 1.0000: PRESS statistic not defined

"Model Summary Statistics": Focus on the model maximizing the "Adjusted R-Squared" and the "Predicted R-Squared".

ANOVA for factorial phase 1

Response 1 MgSO4

ANOVA for Response Surface Quadratic Model

Analysis of variance table [Partial sum of squares - Type III]

Source	Sum of Squares	df	Mean Square	F Value	p-value Prob > F	
Model	20.89	9	2.32	112.56	< 0.0001	
A-FeCl3	*0.16*	*1*	*0.16*	*7.73*	*0.0239*	
B-MgCl2	*2.41*	*1*	*2.41*	*116.77*	*< 0.0001*	
C-HCl	*0.083*	*1*	*0.083*	*4.01*	*0.0801*	
AB0.95	*1*	*0.95*	*45.90*	*0.0001*		
AC0.64	*1*	*0.64*	*30.88*	*0.0005*		
BC0.27	*1*	*0.27*	*13.06*	*0.0068*		
$A^2$3.499E-003	*1*	*3.499E-003*	*0.17*	*0.6912*		
$B^2$1.81	*1*	*1.81*	*87.64*	*< 0.0001*		
$C^2$5.434E-003	*1*	*5.434E-003*	*0.26*	*0.6216*		
Residual	0.16	8	0.021			
Lack of Fit	*0.16*	*6*	*0.027*	*12.35*	*0.0768*	
Pure Error	*4.338E-003*	*2*	*2.169E-003*			
Cor Total	21.06	17				

The Model F-value of 112.56 implies the model is significant. There is only a 0.01% chance that a "Model F-Value" this large could occur due to noise.

Values of "Prob > F" less than 0.0500 indicate model terms are significant. In this case A, B, AB, AC, BC, B^2 are significant model terms. Values greater than 0.1000 indicate the model terms are not significant. If there are many insignificant model terms (not counting those required to support hierarchy),model reduction may improve your model.

The "Lack of Fit F-value" of 12.35 implies there is a 7.68% chance that a "Lack of Fit F-value" this large could occur due to noise. Lack of fit is bad -- we want the model to fit. This relatively low probability (<10%) is troubling.

Std. Dev.	0.14		R-Squared	0.9922
Mean1.35		Adj R-Squared	0.9834	
C.V. %	10.63		Pred R-Squared	0.9082
PRESS	1.93		Adeq Precision	38.201

The "Pred R-Squared" of 0.9082 is in reasonable agreement with the "Adj R-Squared" of 0.9834.

"Adeq Precision" measures the signal to noise ratio. A ratio greater than 4 is desirable. Your ratio of 38.201 indicates an adequate signal. This model can be used to navigate the design space.

Coefficient Factor	Estimate	Standard df	95% CI Error	95% CI Low	High
Intercept	1.07	1	0.064	0.92	1.22
A-FeCl3	-0.14	1	0.050	-0.25	-0.024
B-MgCl2	-1.10	1	0.10	-1.33	-0.86
AB0.43	1	0.064	0.29	0.58	1.39
AC0.36	1	0.065	0.21	0.51	1.32
BC0.45	1	0.12	0.16	0.73	4.62
A^2-0.034	1	0.082	-0.22	0.16	1.40
$B^2$0.83	1	0.088	0.62	1.03	1.71
C^2-0.087	1	0.17	-0.48	0.30	4.65

Final Equation in Terms of Coded Factors:

MgSO4	=
+1.07	
-0.14	* A
-1.10	* B
+0.23	* C
+0.43	* A * B
+0.36	* A * C
+0.45	* B * C
-0.034	* A^2
+0.83	* B^2
-0.087	* C^2

Final Equation in Terms of Actual Factors:

MgSO4	=
+5.61111	
-1.04140	* FeCl3
-1.71938	* MgCl2
-0.19417	* HCl
+0.17392	* FeCl3 * MgCl2
+0.12039	* FeCl3 * HCl
+0.059793	* MgCl2 * HCl
-0.033791	* $FeCl3^2$
+0.13254	* $MgCl2^2$
-9.63542E-003	* HCl^2

Model fit summary for factorial phase 2

***** WARNING: The Cubic Model and higher are Aliased! *****

Summary (detailed tables shown below)

Source	Sequential p-value	Lack of Fit p-value	Adjusted R-Squared	Predicted R-Squared	
Linear	< 0.0001	0.0001	0.8851	0.8174	
2FI	0.9260	0.0001	0.8541	0.2313	
Quadratic	0.0120	0.0003	0.9605	0.3765	Suggested
Cubic	0.0003		1.0000		Aliased

Sequential Model Sum of Squares [Type I]

Source	Sum of Squares	df	Mean Square	F Value	p-value Prob > F	
Mean vs Total	16.43	1	16.43			
Linear vs Mean	8.80	3	2.93	39.51	< 0.0001	
2FI vs Linear	0.043	3	0.014	0.15	0.9260	
Quadratic vs 2FI	0.70	3	0.23	9.07	0.0120	Suggested
Cubic vs Quadratic	0.15	4	0.038	2871.91	0.0003	Aliased
Residual	2.667E-005	2	1.333E-005			
Total	26.13	16	1.63			

"Sequential Model Sum of Squares [Type I]": Select the highest order polynomial where the additional terms are significant and the model is not aliased.

Lack of Fit Tests

Source	Sum of Squares	df	Mean Square	F Value	p-value Prob > F	
Linear	0.89	10	0.089	6683.79	0.0001	
2FI	0.85	7	0.12	9088.69	0.0001	
Quadratic	0.15	4	0.038	2871.91	0.0003	Suggested
Cubic	0.000	0				Aliased
Pure Error	2.667E-005	2	1.333E-005			

"Lack of Fit Tests": Want the selected model to have insignificant lack-of-fit.

Model Summary Statistics

Source	Std. Dev.	R-Squared	Adjusted R-Squared	Predicted R-Squared	PRESS	
Linear	0.27	0.9081	0.8851	0.8174	1.77	
2FI	0.31	0.9125	0.8541	0.2313	7.45	
Quadratic	0.16	0.9842	0.9605	0.3765	6.04	Suggested
Cubic	3.652E-003	1.0000	1.0000		+	Aliased

+ Case(s) with leverage of 1.0000: PRESS statistic not defined

"Model Summary Statistics": Focus on the model maximizing the "Adjusted R-Squared" and the "Predicted R-Squared".

ANOVA for factorial phase 2

Response 1 MgSO4

ANOVA for Response Surface Quadratic Model

Analysis of variance table [Partial sum of squares - Type III]

Source	Sum of Squares	df	Mean Square	F Value	p-value Prob > F	
Model	9.54	9	1.06	41.52	0.0001	
A-FeCl3	*0.079*	*1*	*0.079*	*3.11*	*0.1282*	
B-MgCl2	*5.72*	*1*	*5.72*	*223.85*	*< 0.0001*	
C-hCl	*0.075*	*1*	*0.075*	*2.94*	*0.1371*	
AB0.071	*1*	*0.071*	*2.77*	*0.1469*		
AC3.438E-003	*1*	*3.438E-003*	*0.13*	*0.7262*		
BC0.062	*1*	*0.062*	*2.43*	*0.1698*		
$A^2$8.666E-003	*1*	*8.666E-003*	*0.34*	*0.5814*		
$B^2$0.48	*1*	*0.48*	*18.71*	*0.0050*		
$C^2$1.259E-003	*1*	*1.259E-003*	*0.049*	*0.8316*		
Residual	0.15	6	0.026			
Lack of Fit	*0.15*	*4*	*0.038*	*2871.91*	*0.0003*	
Pure Error	*2.667E-005*	*2*	*1.333E-005*			
Cor Total	9.69	15				

The Model F-value of 41.52 implies the model is significant. There is only a 0.01% chance that a "Model F-Value" this large could occur due to noise.

Values of "Prob > F" less than 0.0500 indicate model terms are significant. In this case B, B^2 are significant model terms. Values greater than 0.1000 indicate the model terms are not significant. If there are many insignificant model terms (not counting those required to support hierarchy), model reduction may improve your model.

The "Lack of Fit F-value" of 2871.91 implies the Lack of Fit is significant. There is only a 0.03% chance that a "Lack of Fit F-value" this large could occur due to noise. Significant lack of fit is bad -- we want the model to fit.

Std. Dev.	0.16	R-Squared	0.9842
Mean1.01	Adj R-Squared	0.9605	
C.V. %	15.77	Pred R-Squared	0.3765
PRESS6.04	Adeq Precision	18.503	

The "Pred R-Squared" of 0.3765 is not as close to the "Adj R-Squared" of 0.9605 as one might normally expect. This may indicate a large block effect or a possible problem with your model and/or data. Things to consider are model reduction, response tranformation, outliers,

"Adeq Precision" measures the signal to noise ratio. A ratio greater than 4 is desirable. Your ratio of 18.503 indicates an adequate signal. This model can be used to navigate the design space.

Coefficient Factor	Estimate	Standard df	95% CI Error	95% CI Low	High
A-FeCl3	-0.11	1	0.062	-0.26	0.042
B-MgCl2	-0.92	1	0.062	-1.07	-0.77
AB0.12	1	0.072	-0.056	0.29	1.40
AC0.026	1	0.072	-0.15	0.20	1.40
BC0.11	1	0.072	-0.064	0.29	1.40
$A^2$0.058	1	0.099	-0.18	0.30	1.52
$B^2$0.43	1	0.099	0.19	0.67	1.52
C^2-0.022	1	0.099	-0.26	0.22	1.52

Final Equation in Terms of Coded Factors:

MgSO4	=
+0.71	
-0.11	* A
-0.92	* B
+0.11	* C
+0.12	* A * B
+0.026	* A * C
+0.11	* B * C
+0.058	* A^2
+0.43	* B^2
-0.022	* C^2

Final Equation in Terms of Actual Factors:

MgSO4	=
+5.75567	
-0.78684	* FeCl3
-1.66383	* MgCl2
-0.080006	* hCl
+0.084874	* FeCl3 * MgCl2
+0.020035	* FeCl3 * hCl
+0.034067	* MgCl2 * hCl
+0.10270	* $FeCl3^2$
+0.12199	* $MgCl2^2$
-7.19061E-003	* hCl^2

Model fit summary for factorial phase 3

***** WARNING: The Cubic Model and higher are Aliased! *****

Summary (detailed tables shown below)

Source	Sequential p-value	Lack of Fit p-value	Adjusted R-Squared	Predicted R-Squared	
Linear	< 0.0001	0.0191	0.9074	0.8376	
2FI	0.2693	0.0202	0.9185	0.5890	
Quadratic	0.0052	0.0840	0.9834	0.8457	Suggested
Cubic	0.0840		0.9979		Aliased

Sequential Model Sum of Squares [Type I]

Source	Sum of Squares	df	Mean Square	F Value	p-value Prob > F	
Mean vs Total	3.48	1	3.48			
Linear vs Mean	1.38	3	0.46	50.02	< 0.0001	
2FI vs Linear	0.037	3	0.012	1.54	0.2693	
Quadratic vs 2FI	0.063	3	0.021	12.77	0.0052	Suggested
Cubic vs Quadratic	9.431E-003	4	2.358E-003	11.14	0.0840	Aliased
Residual	4.231E-004	2	2.116E-004			
Total	4.97	16	0.31			

"Sequential Model Sum of Squares [Type I]": Select the highest order polynomial where the additional terms are significant and the model is not aliased.

Lack of Fit Tests

Source	Sum of Squares	df	Mean Square	F Value	p-value Prob > F	
Linear	0.11	10	0.011	51.88	0.0191	
2FI	0.072	7	0.010	48.84	0.0202	
Quadratic	9.431E-003	4	2.358E-003	11.14	0.0840	Suggested
Cubic	0.000	0				Aliased
Pure Error	4.231E-004	2	2.116E-004			

"Lack of Fit Tests": Want the selected model to have insignificant lack-of-fit.

Model Summary Statistics

Source	Std. Dev.	R-Squared	Adjusted R-Squared	Predicted R-Squared	PRESS	
Linear	0.096	0.9260	0.9074	0.8376	0.24	
2FI	0.090	0.9511	0.9185	0.5890	0.61	
Quadratic	0.041	0.9934	0.9834	0.8457	0.23	Suggested
Cubic	0.015	0.9997	0.9979		+	Aliased

+ Case(s) with leverage of 1.0000: PRESS statistic not defined

"Model Summary Statistics": Focus on the model maximizing the "Adjusted R-Squared" and the "Predicted R-Squared".

ANOVA for factorial phase 3

Response 1 MgSO4

ANOVA for Response Surface Quadratic Model

Analysis of variance table [Partial sum of squares - Type III]

Source	Sum of Squares	df	Mean Square	F Value	p-value Prob > F
Model	1.48	9	0.16	100.02	< 0.0001
A-FeCl3	*0.026*	*1*	*0.026*	*15.95*	*0.0072*
B-MgCl2	*0.63*	*1*	*0.63*	*381.16*	*< 0.0001*
C-hCl	*0.24*	*1*	*0.24*	*148.80*	*< 0.0001*
AB0.037	*1*	*0.037*	*22.46*	*0.0032*	
AC5.966E-003	*1*	*5.966E-003*	*3.63*	*0.1053*	
BC4.216E-004	*1*	*4.216E-004*	*0.26*	*0.6305*	
A^2*3.776E-003*	*1*	*3.776E-003*	*2.30*	*0.1803*	
B^2*0.039*	*1*	*0.039*	*23.72*	*0.0028*	
C^2*1.064E-003*	*1*	*1.064E-003*	*0.65*	*0.4516*	
Residual	9.854E-003	6	1.642E-003		
Lack of Fit	*9.431E-003*	*4*	*2.358E-003*	*11.14*	*0.0840*
Pure Error	*4.231E-004*	*2*	*2.116E-004*		
Cor Total	1.49	15			

The Model F-value of 100.02 implies the model is significant. There is only a 0.01% chance that a "Model F-Value" this large could occur due to noise.

Values of "Prob > F" less than 0.0500 indicate model terms are significant. In this case A, B, C, AB, B^2 are significant model terms. Values greater than 0.1000 indicate the model terms are not significant. If there are many insignificant model terms (not counting those required to support hierarchy), model reduction may improve your model.

The "Lack of Fit F-value" of 11.14 implies there is a 8.40% chance that a "Lack of Fit F-value" this large could occur due to noise. Lack of fit is bad -- we want the model to fit. This relatively low probability (<10%) is troubling.

Std. Dev.	0.041		R-Squared	0.9934
Mean0.47		Adj R-Squared	0.9834	
C.V. %	8.69		Pred R-Squared	0.8457
PRESS	0.23		Adeq Precision	34.843

The "Pred R-Squared" of 0.8457 is in reasonable agreement with the "Adj R-Squared" of 0.9834.

"Adeq Precision" measures the signal to noise ratio. A ratio greater than 4 is desirable.Your ratio of 34.843 indicates an adequate signal. This model can be used to navigate the design space.

Coefficient Factor	Estimate	Standard df	95% CI Error	95% CI Low	High
A-FeCl3	-0.062	1	0.016	-0.10	-0.024
C-hCl	0.19	1	0.016	0.15	0.23
AC0.035	1	0.018	-9.832E-003	0.079	1.40
BC-9.208E-003	1	0.018	-0.054	0.035	1.40
$A^2$0.038	1	0.025	-0.023	0.100	1.52
$B^2$0.12	1	0.025	0.061	0.18	1.52
C^2-0.020	1	0.025	-0.082	0.041	1.52

Final Equation in Terms of Coded Factors:

MgSO4	=
+0.38	
-0.062	* A
-0.31	* B
+0.19	* C
+0.086	* A * B
+0.035	* A * C
-9.208E-003	* B * C
+0.038	* A^2
+0.12	* B^2
-0.020	* C^2

Final Equation in Terms of Actual Factors:

MgSO4	=
+4.68172	
-1.30626	* FeCl3
-1.18808	* MgCl2
+0.092684	* hCl
+0.13781	* FeCl3 * MgCl2
+0.039588	* FeCl3 * hCl
-4.20923E-003	* MgCl2 * hCl
+0.15252	* $FeCl3^2$
+0.078382	* $MgCl2^2$
-6.60938E-003	* hCl^2

C1.2 $ZnCl_2$-HCl-NaCl-H_20 system

Model fit summary at a temperature of 40°C.

***** WARNING: The Cubic Model and higher are Aliased! *****

Summary (detailed tables shown below)

Source	Sequential p-value	Lack of Fit p-value	Adjusted R-Squared	Predicted R-Squared	
Linear	0.0037	0.8317	0.6910	0.5545	Suggested
2FI	0.8604	0.7757	0.6485	0.2760	
Quadratic	0.9426	0.6040	0.5194	-0.1690	
Cubic	0.6040		0.4464		Aliased

Sequential Model Sum of Squares [Type I]

Source	Sum of Squares	df	Mean Square	F Value		p-value Prob > F
Mean vs Total	287.58	1	287.58			
Linear vs Mean	3.18	2	1.59	12.18	0.0037	Suggested
2FI vs Linear	4.951E-003	1	4.951E-003	0.033	0.8604	
Quadratic vs 2FI	0.024	2	0.012	0.060	0.9426	
Cubic vs Quadratic	0.55	3	0.18	0.78	0.6040	.

"Sequential Model Sum of Squares [Type I]": Select the highest order polynomial where the additional terms are significant and the model is not aliased.

Lack of Fit Tests

Source	Sum of Squares	df	Mean Square	F Value	p-value Prob > F	
Linear	0.58	6	0.096	0.41	0.8317	Suggested
2FI	0.57	5	0.11	0.49	0.7757	
Quadratic	0.55	3	0.18	0.78	0.6040	
Cubic	0.000	0				Aliased
Pure Error	0.47	2	0.23			

"Lack of Fit Tests": Want the selected model to have insignificant lack-of-fit.

Model Summary Statistics

Source	Std. Dev.	R-Squared	Adjusted R-Squared	Predicted R-Squared	PRESS	
Linear	0.36	0.7528	0.6910	0.5545	1.88	Suggested
2FI	0.39	0.7540	0.6485	0.2760	3.06	
Quadratic	0.45	0.7597	0.5194	-0.1690	4.95	
Cubic	0.48	0.8893	0.4464		+	Aliased

+ Case(s) with leverage of 1.0000: PRESS statistic not defined

"Model Summary Statistics": Focus on the model maximizing the "Adjusted R-Squared" and the "Predicted R-Squared".

ANOVA for a temperature of 40°C.

ANOVA for Response Surface Linear Model

Analysis of variance table [Partial sum of squares - Type III]

Source	Sum of Squares	df	Mean Square	F Value	p-value Prob > F
Model	3.18	2	1.59	12.18	0.0037
B-HCl	*0.014*	*1*	*0.014*	*0.11*	*0.7536*
Residual	1.05	8	0.13		
Lack of Fit	*0.58*	*6*	*0.096*	*0.41*	*0.8317*
Cor Total	4.23	10			

The Model F-value of 12.18 implies the model is significant. There is only a 0.37% chance that a "Model F-Value" this large could occur due to noise.

Values of "Prob > F" less than 0.0500 indicate model terms are significant. In this case A are significant model terms. Values greater than 0.1000 indicate the model terms are not significant. If there are many insignificant model terms (not counting those required to support hierarchy),model reduction may improve your model.

The "Lack of Fit F-value" of 0.41 implies the Lack of Fit is not significant relative to the pure error. There is a 83.17% chance that a "Lack of Fit F-value" this large could occur due to noise. Non-significant lack of fit is good -- we want the model to fit.

Std. Dev.	0.36		R-Squared	0.7528
Mean5.11		Adj R-Squared	0.6910	
C.V. %	7.07		Pred R-Squared	0.5545
PRESS	1.88		Adeq Precision	9.407

The "Pred R-Squared" of 0.5545 is in reasonable agreement with the "Adj R-Squared" of 0.6910.

"Adeq Precision" measures the signal to noise ratio. A ratio greater than 4 is desirable. Your ratio of 9.407 indicates an adequate signal. This model can be used to navigate the design space.

Factor	Coefficient Estimate	df	Standard Error	95% CI Low	95% CI High
A-ZnCl2	0.63	1	0.13	0.34	0.93
B-HCl	-0.042	1	0.13	-0.34	0.25

Final Equation in Terms of Coded Factors:

NaCl 40	=
+5.11	
+0.63	* A
-0.042	* B

Final Equation in Terms of Actual Factors:

NaCl 40	=
+4.35325	
+0.25247	* ZnCl2
-0.33228	* HCl

Model fit summary at a temperature of 80°C.

Summary (detailed tables shown below)

Source	Sequential p-value	Lack of Fit p-value	Adjusted R-Squared	Predicted R-Squared	
Linear	0.0079	0.2108	0.6273	0.3480	Suggested
2FI	0.1220	0.2514	0.7046	0.2525	
Quadratic	0.4554	0.2161	0.6981	0.0340	
Cubic	0.2161		0.8869		Aliased

Sequential Model Sum of Squares [Type I]

Source	Sum of Squares	df	Mean Square	F Value	p-value Prob > F	
Mean vs Total	253.98	1	253.98			
Linear vs Mean	2.61	2	1.31	9.42	0.0079	Suggested
2FI vs Linear	0.34	1	0.34	3.09	0.1220	
Quadratic vs 2FI	0.21	2	0.10	0.92	0.4554	
Cubic vs Quadratic	0.48	3	0.16	3.78	0.2161	Aliased
Residual	0.084	2	0.042			
Total	257.71	11	23.43			

"Sequential Model Sum of Squares [Type I]": Select the highest order polynomial where the additional terms are significant and the model is not aliased.

Lack of Fit Tests

Source	Sum of Squares	df	Mean Square	F Value	p-value Prob > F	
Linear	1.03	6	0.17	4.06	0.2108	Suggested
2FI	0.69	5	0.14	3.26	0.2514	
Quadratic	0.48	3	0.16	3.78	0.2161	
Cubic	0.000	0				Aliased
Pure Error	0.084	2	0.042			

"Lack of Fit Tests": Want the selected model to have insignificant lack-of-fit.

Model Summary Statistics

Source	Std. Dev.	R-Squared	Adjusted R-Squared	Predicted R-Squared	PRESS	
Linear	0.37	0.7019	0.6273	0.3480	2.43	Suggested
2FI	0.33	0.7932	0.7046	0.2525	2.78	
Quadratic	0.34	0.8490	0.6981	0.0340	3.60	
Cubic	0.21	0.9774	0.8869		+	Aliased

+ Case(s) with leverage of 1.0000: PRESS statistic not defined

ANOVA for a temperature of 80°C.

ANOVA for Response Surface Linear Model
Analysis of variance table [Partial sum of squares - Type III]

Source	Sum of Squares	df	Mean Square	F Value	p-value Prob > F	
Model	2.61	2	1.31	9.42	0.0079	
B-HCl	*1.938E-003*	*1*	*1.938E-003*	*0.014*	*0.9088*	
Residual	1.11	8	0.14			
Lack of Fit	*1.03*	*6*	*0.17*	*4.06*	*0.2108*	
Cor Total	3.72	10				

The Model F-value of 9.42 implies the model is significant. There is only a 0.79% chance that a "Model F-Value" this large could occur due to noise.

Values of "Prob > F" less than 0.0500 indicate model terms are significant. In this case A are significant model terms. Values greater than 0.1000 indicate the model terms are not significant. If there are many insignificant model terms (not counting those required to support hierarchy), model reduction may improve your model.

The "Lack of Fit F-value" of 4.06 implies the Lack of Fit is not significant relative to the pure error. There is a 21.08% chance that a "Lack of Fit F-value" this large could occur due to noise. Non-significant lack of fit is good -- we want the model to fit.

Std. Dev.	0.37		R-Squared	0.7019
Mean4.81		Adj R-Squared	0.6273	
C.V. %	7.75		Pred R-Squared	0.3480
PRESS	2.43		Adeq Precision	8.286

The "Pred R-Squared" of 0.3480 is not as close to the "Adj R-Squared" of 0.6273 as one mightnormally expect. This may indicate a large block effect or a possible problem with your modeland/or data. Things to consider are model reduction, response tranformation, outliers, etc.

"Adeq Precision" measures the signal to noise ratio. A ratio greater than 4 is desirable. Your ratio of 8.286 indicates an adequate signal. This model can be used to navigate the design space.

Factor	Coefficient Estimate	df	Standard Error	95% CI Low	95% CI High
A-ZnCl2	0.57	1	0.13	0.27	0.88
B-HCl	-0.016	1	0.13	-0.32	0.29

Final Equation in Terms of Coded Factors:

NaCl 80	=
+4.80	
+0.57	* A
-0.016	* B

Final Equation in Terms of Actual Factors:

NaCl 80	=
+4.04915	
+0.22913	* ZnCl2
-0.12452	* HCl

Model fit summary at a temperature of 107°C.

Summary (detailed tables shown below)

Source	Sequential p-value	Lack of Fit p-value	Adjusted R-Squared	Predicted R-Squared	
Linear	0.0166	0.3808	0.5512	0.2502	Suggested
2FI	0.4627	0.3541	0.5277	-0.1460	
Quadratic	0.5310	0.2933	0.4868	-0.5684	
Cubic	0.2933		0.7349		Aliased

Sequential Model Sum of Squares [Type I]

Source	Sum of Squares	df	Mean Square	F Value	p-value Prob > F	
Mean vs Total	301.66	1	301.66			
Linear vs Mean	1.66	2	0.83	7.14	0.0166	Suggested
2FI vs Linear	0.074	1	0.074	0.60	0.4627	
Quadratic vs 2FI	0.19	2	0.096	0.72	0.5310	
Cubic vs Quadratic	0.53	3	0.18	2.56	0.2933	Aliased
Residual	0.14	2	0.069			
Total	304.25	11	27.66			

"Sequential Model Sum of Squares [Type I]": Select the highest order polynomial where the additional terms are significant and the model is not aliased.

Lack of Fit Tests

Source	Sum of Squares	df	Mean Square	F Value	p-value Prob > F	
Linear	0.79	6	0.13	1.92	0.3808	Suggested
2FI	0.72	5	0.14	2.09	0.3541	
Quadratic	0.53	3	0.18	2.56	0.2933	
Cubic	0.000	0				Aliased
Pure Error	0.14	2	0.069			

"Lack of Fit Tests": Want the selected model to have insignificant lack-of-fit.

Model Summary Statistics

Source	Std. Dev.	R-Squared	Adjusted R-Squared	Predicted R-Squared	PRESS	
Linear	0.34	0.6409	0.5512	0.2502	1.94	Suggested
2FI	0.35	0.6694	0.5277	-0.1460	2.96	
Quadratic	0.36	0.7434	0.4868	-0.5684	4.05	
Cubic	0.26	0.9470	0.7349		+	Aliased

+ Case(s) with leverage of 1.0000: PRESS statistic not defined

ANOVA for a temperature of 107°C.

ANOVA for Response Surface Linear Model
Analysis of variance table [Partial sum of squares - Type III]

Source	Sum of Squares	df	Mean Square	F Value	p-value Prob > F	
Model	1.66	2	0.83	7.14	0.0166	
B-HCl	*2.996E-003*	*1*	*2.996E-003*	*0.026*	*0.8763*	
Residual	0.93	8	0.12			
Lack of Fit	*0.79*	*6*	*0.13*	*1.92*	*0.3808*	
Pure Error	*0.14*	*2*	*0.069*			
Cor Total	2.58	10				

The Model F-value of 7.14 implies the model is significant. There is only a 1.66% chance that a "Model F-Value" this large could occur due to noise.

Values of "Prob > F" less than 0.0500 indicate model terms are significant. In this case A are significant model terms. Values greater than 0.1000 indicate the model terms are not significant. If there are many insignificant model terms (not counting those required to support hierarchy), model reduction may improve your model.

The "Lack of Fit F-value" of 1.92 implies the Lack of Fit is not significant relative to the pure error. There is a 38.08% chance that a "Lack of Fit F-value" this large could occur due to noise. Non-significant lack of fit is good -- we want the model to fit.

Std. Dev.	0.34		R-Squared	0.6409
Mean5.24		Adj R-Squared	0.5512	
C.V. %	6.50		Pred R-Squared	0.2502
PRESS	1.94		Adeq Precision	7.211

The "Pred R-Squared" of 0.2502 is not as close to the "Adj R-Squared" of 0.5512 as one might normally expect. This may indicate a large block effect or a possible problem with your modeland/or data. Things to consider are model reduction, response tranformation, outliers, etc.

"Adeq Precision" measures the signal to noise ratio. A ratio greater than 4 is desirable. Your ratio of 7.211 indicates an adequate signal. This model can be used to navigate the design space.

Factor	Coefficient Estimate	df	Standard Error	95% CI Low	95% CI High
A-ZnCl2	0.46	1	0.12	0.18	0.73
B-HCl	-0.019	1	0.12	-0.30	0.26

Final Equation in Terms of Coded Factors:

NaCl 107 =
+5.24
+0.46 * A
-0.019 * B

Final Equation in Terms of Actual Factors:

NaCl 107 =
+4.65627
+0.18228 * ZnCl2
-0.15482 * HCl